Molecular Analysis of Lipid Storage and Trafficking

Author:
Zhang, Yuxi

Publication Date:
2014

DOI:
https://doi.org/10.26190/unsworks/2570

Molecular Analysis of Lipid Storage and Trafficking

Yuxi Zhang

UNSW
THE UNIVERSITY OF NEW SOUTH WALES

A thesis submitted for the degree of Doctor of Philosophy,
University of New South Wales

School of Biotechnology and Biomolecular Sciences
University of New South Wales

February 2014

PLEASE TYPE

THE UNIVERSITY OF NEW SOUTH WALES
Thesis/Dissertation Sheet

Surname or Family name: ZHANG

First name:YUXI Other name/s:

Abbreviation for degree as given in the University calendar: PhD

School: Biotechnology and Biomolecular Sciences Faculty: Science

Title: Molecular Analysis of Lipid Storage and Trafficking

Abstract 350 words maximum: (PLEASE TYPE)

Lipid storage and trafficking are essential cellular activities to deliver nutrients and reserve energy for cell growth. The malfunction of either one of these processes could lead to the accumulation of harmful lipids in non-fat tissues and cells. Adipocytes, the master storage depot of fats provides reservoir for energy storage as neutral lipids in the core of lipid droplets. The process of adipogenesis is elegantly regulated under specific physiological condition to favour the development of adipocyte. Seipin has been found as an important protein during adipogenesis and its absence results in lipodystrophy, hypertriglyceridemia, insulin resistance, fatty liver and diabetes. Previous study has shown that PPAR , the master regulator of adipogenesis, may bind to the promoter region of mouse *Seipin* gene. The cloning of the mouse *Seipin* promoter region in a luciferase reporter plasmid showed PPAR promoted the expression of the reporter gene and the co-expression with RXR further increased the expression. Gel shift assay and ChIP qRT-PCR further proved the binding of PPAR to the mouse *Seipin* promoter region. Immunofluorescence study showed PPAR was absent in the nucleus of *Seipin* knockout MEFs during adipogenesis. The addition of PPAR agonist rosiglitazone rescued the differentiation defect and restored the localisation of PPAR to the nucleus. The absence of PPAR might be due to high level of phosphatidic acid (PA) that was detected with PA sensor plasmid. Interesting, the knockdown of *Seipin* in newborn mouse hippocampus neuronal cells greatly influenced the growth of neurons and promoted the formation of supersized lipid droplets under fatty acid loading. The second part of this thesis discovered a novel degradation mechanism of the PI3K/Akt/mTORC1 pathway. The activation of the mTOR complex 1 (mTORC1) pathway under high phospho-Akt level accelerated the degradation of the cholesterol trafficking protein Niemann-Pick C1 (NPC1). This mechanism was observed in several cell lines and the knockdown of the essential component of mTORC1 raptor using siRNA greatly inhibited the degradation of NPC1. Glucose infusion study in rats showed the activation of the PI3K/Akt pathway in the liver cells greatly decreased NPC1 protein level. The degradation of NPC1 by the mTORC1 pathway was hypothesised as a feedback mechanism to shut down the insulin-signalling pathway. Overall, this thesis provided important insights into lipid trafficking and storage.

Declaration relating to disposition of project thesis/dissertation

I hereby grant to the University of New South Wales or its agents the right to archive and to make available my thesis or dissertation in whole or in part in the University libraries in all forms of media, now or here after known, subject to the provisions of the Copyright Act 1968. I retain all property rights, such as patent rights. I also retain the right to use in future works (such as articles or books) all or part of this thesis or dissertation.

I also authorise University Microfilms to use the 350 word abstract of my thesis in Dissertation Abstracts International (this is applicable to doctoral theses only).

Signature

Witness

24/06/14

Date

The University recognises that there may be exceptional circumstances requiring restrictions on copying or conditions on use. Requests for restriction for a period of up to 2 years must be made in writing. Requests for a longer period of restriction may be considered in exceptional circumstances and require the approval of the Dean of Graduate Research.

FOR OFFICE USE ONLY Date of completion of requirements for Award:

THIS SHEET IS TO BE GLUED TO THE INSIDE FRONT COVER OF THE THESIS

Originality Statement

'I hereby declare that this submission is my own work and to the best of my knowledge it contains no materials previously published or written by another person, or substantial proportions of material which have been accepted for the award of any other degree or diploma at UNSW or any other educational institution, except where due acknowledgement is made in the thesis. Any contribution made to the research by others, with whom I have worked at UNSW or elsewhere, is explicitly acknowledged in the thesis. I also declare that the intellectual content of this thesis is the product of my own work, except to the extent that assistance from others in the project's design and conception or in style, presentation and linguistic expression is acknowledged.'

Signature 

Date 24/06/14

Acknowledgements

The past few years of my PhD journey have been tough and windy, filled with confusion and challenges. I even had the feeling that I couldn't finish it. During this journey there are many people whom I would like to say "Thank you" to and it is not easy to finish my PhD without their support.

First of all, to my deeply respected supervisor Robert Yang, thank you so much for giving me the chance to study and learn in your lab. You gave me motivation and inspiration for my research. You provided the best resources that you have got to help me through my journey. Thank you so much for getting me the scholarship and it made my life much easier. Your motivation about research influenced me a lot and now I think research is my life. More importantly, you gave me a lot of freedom in research and provided perfect research and learning environment for everybody in the lab. To the ex- and current lab members, I would like to say thank you to all of you, especially Stephen and Robin. Stephen thanks for your training during my honours and my first year of my PhD. Thanks for all your great ideas about my projects. Robin, thank you so much for all the discussions on the cholesterol project and I don't think I could finish that project without your help and advise. I also want to say thank you to people from the Brown lab and Dawes lab, thanks for all the chemicals, plasmids and equipment that I borrowed.

Last of all, I would like to thank my family. Here, I really want to say a big thank you to my fiancée Helen. Thank you for your support and I'm sorry for not spending enough time with you in the past few years. I'm looking forward to our wedding and our new stage of life.

Yuxi Zhang

Abstract

Lipid storage and trafficking are essential cellular activities to deliver nutrients and reserve energy for cell growth. The malfunction of either one of these processes could lead to the accumulation of harmful lipids in non-fat tissues and cells. This thesis reports a novel transcriptional regulation of mouse *Seipin* by the master regulator of adipogenesis PPARγ. This helps the understanding of how *Seipin* is regulated during adipogenesis, which is the fundamental step in lipid storage. Moreover, Seipin deficiency not only affects the balance of lipids in cells, it also affects neurite growth as observed in *Seipin* knockdown newborn mouse hippocampus neuronal cells. Adipocytes, the master storage depot of fats provides reservoir for energy storage as neutral lipids in the core of lipid droplets. The process of adipogenesis is elegantly regulated under specific physiological condition to favour the development of adipocyte. Seipin has been found as an important protein during adipogenesis and its absence results in lipodystrophy, hypertriglyceridemia, insulin resistance, fatty liver and diabetes. Previous study has shown that PPARγ, the master regulator of adipogenesis, may bind to the promoter region of mouse *Seipin* gene. The cloning of the mouse *Seipin* promoter region in a luciferase reporter plasmid showed PPARγ promoted the expression of the reporter gene and the co-expression with RXRα further increased the expression. Gel shift assay and ChIP qRT-PCR further proved the binding of PPARγ to the mouse *Seipin* promoter region. Immunofluorescence study showed PPARγ was absent in the nucleus of *Seipin* knockout MEFs during adipogenesis. The addition of PPARγ agonist rosiglitazone rescued the differentiation defect and restored the localisation of PPARγ to the nucleus. The absence of PPARγ might be due to high level of phosphatidic acid (PA) that was detected with PA sensor plasmid. Interesting, the knockdown of *Seipin* in newborn mouse hippocampus neuronal cells greatly influenced

the growth of neurons and promoted the formation of supersized lipid droplets under fatty acid loading.

The observation of cholesterol accumulation in NPC1 deficient cancer cell lines helps to identify a novel NPC1 protein degradation mechanism that is triggered by the PI3K/Akt/mTORC1 pathway. The activation of the mTOR complex 1 (mTORC1) pathway under high phospho-Akt level accelerated the degradation of the cholesterol trafficking protein Niemann-Pick C1 (NPC1). The knockdown of the essential component of mTORC1 Raptor using siRNA greatly inhibited the degradation of NPC1. Glucose infusion study in rats showed the activation of the PI3K/Akt pathway in the liver cells greatly decreased NPC1 protein level. The degradation of NPC1 by the mTORC1 pathway was hypothesised as a feedback mechanism to shut down the insulin-signalling pathway. The knowledge of NPC1 degradation and the mechanism controlling this process may give more insights into both cholesterol trafficking and cancer growth as the NPC1 deficient cancer cells are more resistant to chemotherapeutic drugs.

Abbreviations

12-kDa FK506-binding protein	FKBP12
3-hydroxy-3-methyl-glutaryl-CoA reductase	HMG-CoAR
4E-binding protein 1	4E-BP1
5’ untranslated region	5’ UTR
Acyl-CoA:cholesterol acyltransferase	ACAT
Adipocyte differentiation-related protein	ADRP
Adipose triglyceride lipase	ATGL
ATP-bind cassette, sub family A1	ABCA1
Bicinchonicic acid	BCA
Bovine Serum Albumin	BSA
DEP domain containing mTOR-interacting protein	DEPTOR
Diacylglycerols	DAGs
DNA-binding domain	DBD
Dulbecco’s Modified Eagle Medium	DMEM
Endoplasmic reticulum	ER
Endoplasmic reticulum-associated degradation	ERAD
Ethylenediaminetetraccetic acid	EDTA
Fat-specific of 27 kDa	FSP27
Fetal Bovin Serum	FBS
Forkhead box protein O1	FoxO1
Growth factor receptor-bound protein 10	Grb10
GTPase-activating protein	GAP
Hormone sensitive lipase	HSL
Human papillomavirus	HPV

Insulin receptor substrate	IRS
Isobutylmethylxanthine	IBMX
Late endosomes/lysosomes	LE/LY
Ligand-binding domain	LBD
Low-density lipoprotein	LDL
Low-density lipoprotein receptor	LDLR
Lysosome-associated membrane protein 1	Lamp1
Mammalian lethal with sec-13 protein 8	mLST8
Mammalian stress-activated map kinase-interacting protein 1	mSin1
Mannose 6-phosphate receptor	M6PR
Mechanistic target of rapamycin	mTOR
Monoacylglycerols	MAGs
Monoglycerol lipase	MGL
mTOR complex 1	mTORC1
mTOR complex 2	mTORC2
Neonatal Calf Serum	NCS
Niemann-Pick C	NPC
Peroxisome-proliferator activated receptor	PPAR
Phosphatase and tensin homologue	PTEN
Phosphatidic acid	PA
Phosphatidylcholine	PC
Phosphatidylethanolamine	PE
Phosphatidylinositol	PI
Phosphatidylinositol (3,4,5) trisphosphate	PIP_3
Phosphatidylinositol (4,5) biphosphate	PIP_2

Phosphatidylserine	PS
Phosphoinositide-3-kinase	PI3K
Plasma membrane	PM
Pleckstrin Homologue	PH
PPAR-responsive regulatory elements	PPREs
Prolin-rich Akt substrate 40 kDa	PRAS40
Protein kinase B	PKB
Protein kinase C	PKC
Protein observed with rictor 1	Protor1
Quantitative RT-PCR	qRT-PCR
Rapamycin-insensitive companion of mTOR	Rictor
Ras homologue enriched in brain	Rheb
Regulatory-associated protein of mammalian target of rapamycin	Raptor
Retinoid X receptor	RXR
RNA interference	RNAi
S6 kinase 1	S6K1
Serum and glucocorticoid-induced protein kinase 1	SGK1
Site 1 protease	S1P
Site 2 protease	S2P
SREBP- cleavage-activating protein	Scap
Standard error mean	SEM
Sterol responsive element binding protein	SREBP
Sterol-sensing domain	SSD
Tail-interacting protein of 47 kDa	TIP47
Thiazolidinedione	TZD

Trancriptional start site	TSS
Trans Golgi network	TGN
Transactivation domain	AF2
Triacyglycerols	TAGs
Tuberous sclerosis 1 and 2	TSC 1/2
Wax ester synthase/diacylglycerol acyltransferase	WS/DGAT

Table of Contents

List of Tables

List of Figures

1. Chapter 1: Introduction

Diseases associated with lipid storage are rapidly increasing in developed countries. The balancing of metabolic energy is important for life and the storage of lipids like sterols and fatty acids as neutral lipids in lipid droplets of white adipocytes is essential for cells to prevent lipotoxicity at the cellular level. Excess lipid storage beyond the capacity of white adipose tissue is associated with dyslipidemia and the development of type 2 diabetes results in insulin resistance. Lipid droplets are found in all eukaryotic cells and in some prokaryotic cells. It was initially thought that lipid droplets are inert lipid storage organelles, but recent studies showed they are also involved in intracellular vesicle trafficking, temporal protein storage, viral replication and protein degradation[1-6]. These suggested lipid droplets are playing important roles in cells to maintain normal cellular activity. The understanding of lipid droplet metabolism, biosynthesis and interactions with other cellular organelles may lead to more insights into the cure of lipid storage diseases. Also, the mysterious protein Seipin was studied to understand how adipogenesis is regulated. Impaired cholesterol trafficking is one of the most studied areas of lipid storage diseases. Niemann-Pick type C (NPC) disease, an autosomal recessive disorder, characterised by accumulation of free cholesterols in late endosomes and lysosomes, patients with NPC disease develop progressive neurodegeneration and hepatosplenomegaly[7]. This thesis discovered a novel mechanism of the protein degradation of NPC1, an important protein of the cholesterol trafficking pathway.

1.1 Lipid Droplets

Lipid droplets are intracellular and cytoplasmic structures that are responsible for the storage of neutral lipids. They are found in yeast, plants, bacteria and mammals[8-10]. In mammalian cells, they are most abundant in the adipocytes for energy storage, and steroidogenic cells for hormone production. However, they could also be found in non-adipocytes. These non-adipogenic lipid droplets are thought to be responsible for temporal lipids storage, which are used for β-oxidation, membrane biogenesis and protein lipidation[11].

1.1.1 Lipid droplet Morphology

Comparing to membrane-bound organelles found in eukaryotic cells, lipid droplets are surrounded by a monolayer of phospholipids and the core is consisted of neutral lipids[12]. Figure 1.1 shows the monolayer morphology of lipid droplets. The most abundant neutral lipids found in lipid droplets are triacylglycerols and sterol esters, but other endogenous neutral lipids like free cholesterol, retinol ester and xenobiotic hydrophobic compounds are also present in lipid droplets. Proteins have also been found on lipid droplets and they are bound through hydrophobic or electrostatic interactions[13]. The most well known proteins associated with lipid droplets are the PAT (Perilipin, Adipophilin and TIP47-related protein domain) family of proteins[14].

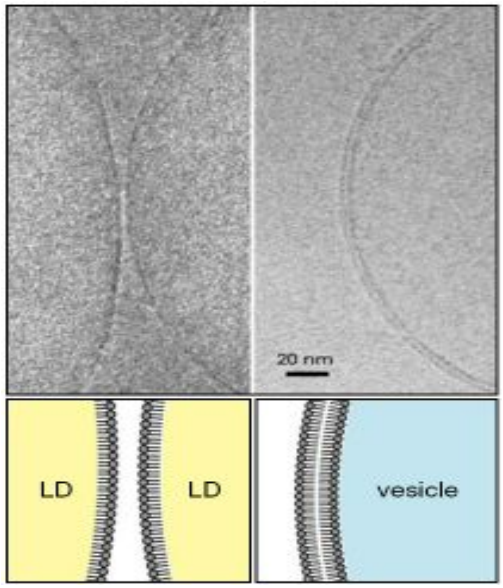

Figure 1.1 Cryoelectron microscopy of lipid droplets. (Figure adapted from Fujimoto *et al.*, 2008). The figure on the left shows the phospholipid monolayer of lipid droplets. In contrast, the figure on the right shows the phospholipid bilayer structure of a membrane vesicle.

1.1.2 Lipid Droplet Function

The major role of lipid droplets is to store neutral lipids and these neutral lipids can be released from the lipid core for energy metabolism, membrane phospholipid biosynthesis and steroid biosynthesis[15]. The hydrolysis of triacylglycerols (TAGs) would lead to the release of diacylglycerols (DAGs) and free fatty acids from the lipid cores. The released DAGs can be used for the synthesis of phospholipids via the phospholipid biosynthetic pathway, and the free fatty acids can be used for energy supply. In addition, free fatty acids may act as ligands that can influence gene expression by binding to nuclear receptors, such as the peroxisome-proliferator activated receptor (PPAR) family. However excess free fatty acids can disrupt phospholipid membrane integrity, alter lipid signalling pathway and induce apoptosis[16]. Therefore, one of the important roles of lipid droplets is to regulate the

availability of substrates, such as free fatty acids, for energy metabolism and cellular signalling.

Studies have shown that lipid droplets are not the only sites of energy reservoir, but they may also facilitate other cellular activities. As mentioned before, they are involved in signalling, intracellular vesicle trafficking, temporal protein storage, protein degradation and more. One of the studies conducted by Cermelli *et al.* showed that histones H2A, H2Av, and H2B were found to be attached to lipid droplets from *Drosophila* embryos [17]. They also used biochemistry, genetics, real-time imaging, and cell biology to study the interaction; they confirmed that about 50% of certain embryonic histones are physically attached to lipid droplets, a localisation conserved in other fly species. Another important finding was the histones attached on lipid droplets are transferred to nuclei during development. These findings revealed that lipid droplets are no longer inert organelles just for storing energy, but they are also playing important roles in different cellular activities.

1.1.3 Lipid Droplet Formation

The formation of lipid droplets from the endoplasmic reticulum (ER) is the well-believed model. In this model, neutral lipids like triacylglycerols and sterol esters are accumulated between the leaflets of the ER membrane until certain sizes. They are then suggested to bud from the ER membrane to form independent organelles that are wrapped around by a monolayer of phospholipids and some specific proteins [9, 15, 18]. Figure 1.2 and 1.3A show this model.

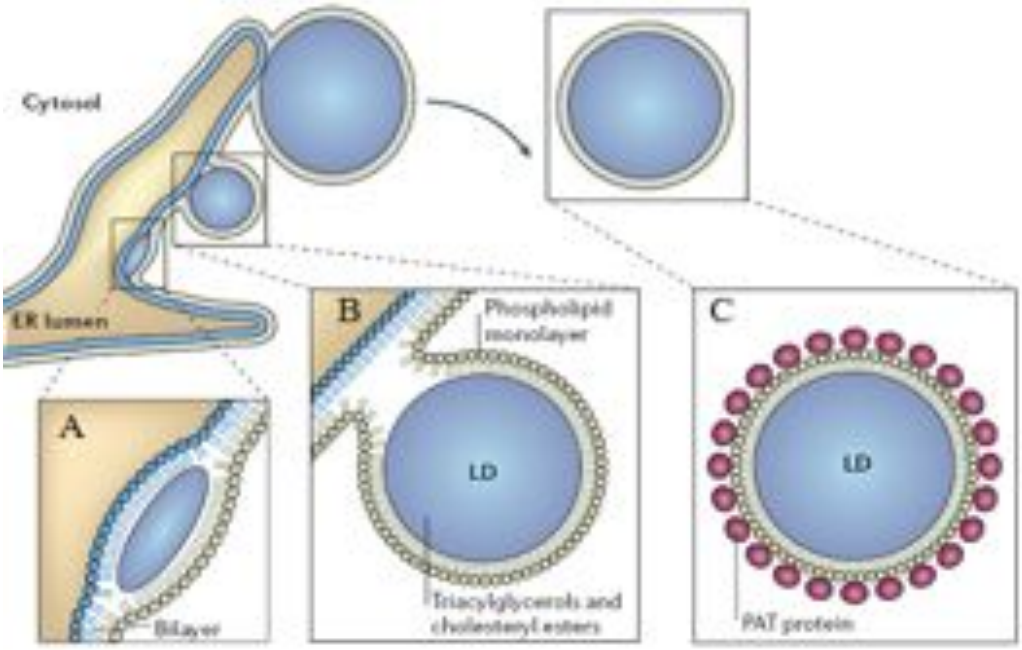

Figure 1.2 Model for lipid droplet formation. (Figure adapted from Martin and Parton, 2006). In this model, (A) neutral lipids are accumulated between the two leaflets of the ER membrane and they will form the core of lipid droplets. (B) When the neutral lipids have reached to certain size, they are suggested to bud from the ER while a monolayer of phospholipids and specific proteins wrap around the lipid core to form the (C) mature lipid droplets.

However, alternative mechanisms have been proposed. One of the alternative models hypothesised that the lipid core of neutral lipids are detached from the ER membrane together with the cytoplasmic and lumenal leaflets of the membrane to form the mature lipid droplets (Figure 1.3B). One important aspect of this model is it explained the presence of ER integral membrane in lipid droplets as membrane "tab" that was observed by electron microscopy [18].

Another hypothesis was observed in bacteria. The enzyme wax ester synthase/diacylglcerol acyltransferase (WS/DGAT) is responsible for the synthesis of traiacylglycerols and it localises in the plasma membrane and cytosol. In this model, the lipid esters are thought to be synthesised near the cytoplasmic domain of the enzyme.

As shown in Figure 1.3C, the lipid esters are synthesised on the surface of cytoplasmic membrane as an oleogenous emulsive layer. As more and more lipid esters are accumulated, phospholipids are acquired to form the mature lipid droplets [18].

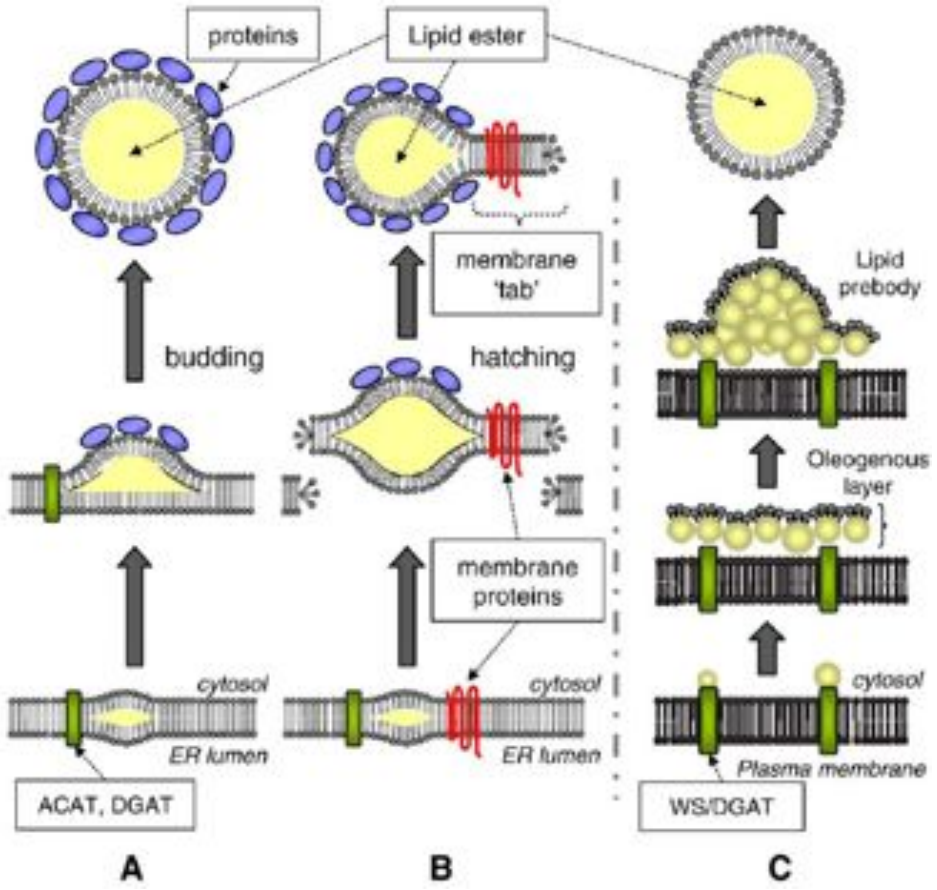

Figure 1.3 Hypothetical models of lipid droplet formation. (Figure adapted from Ohsaki *et al.*, 2008). **A** is the most popular model of lipid droplet biogenesis. As explained in Figure 1-2, lipid esters are accumulated between the leaflets of the ER membrane and the mature lipid droplets are budded from the ER. **B** represents the alternative mechanism where the lipid droplets are formed by a process called "hatching". In this model, the lipid cores are detached from the ER membrane together with the cytoplasmic the lumenal membranes of the ER to form the mature lipid droplets. Also, the membrane "tab" consisted of the mature lipid droplets explained the presence of ER integral membrane proteins on lipid droplets. **C** represents another model of lipid droplet formation in bacteria. In this model, the transmembrane protein wax ester synthase/diacylglycerol acyltransferase (WS/DGAT) synthesise the lipid esters triacylglycerols. The accumulation of the lipid esters along the cytoplasmic membrane surface will lead to the formation of the oleogenous emulsive layer and the lipid prebodies. Phospholipids are acquired during this process to form the phospholipid monolayer of the mature lipid droplets.

1.1.4 Hydrolysis of Lipid Droplet

Hydrolysis of lipid droplets is essential for normal lipid regulation and it is favoured by adipose triglyceride lipase (ATGL) and hormone-sensitive lipase (HSL). During lipid droplet hydrolysis, the insoluble triacylglycerols are converted to soluble fatty acids and monoacylglycerols (MAGs) directly at the surface of lipid droplets. Before the identification of ATGL, HSL was thought as the rate-limiting enzyme that is responsible for the hydrolysis of lipid droplets. The triacylglycerols stored in lipid droplets are hydrolysed for energy supply when is demanded. Observations made in HSL knockout mice revealed that there is another enzyme that is responsible in this process and ATGL was found to be the rate-limiting enzyme. ATGL is predominantly expressed in white adipose tissues in mammals[19]. It is involved in the breakdown of TAG to DAG and fatty acid. The DAG is then hydrolysed to monoacylglycerol and fatty acid by HSL. The final step is the generation of glycerol and fatty acid by monoglycerol lipase (MGL)[20]. Therefore, these enzymes are essential when energetic substrates are required and they are regulated under tight hormonal regulation[21].

1.1.5 Growth of Lipid Droplets

The growth of pre-existing lipid droplets is still a controversial topic and several hypothesis have been postulated[11]. Figure 1.4 shows five possible ways for a pre-existing lipid droplet to grow larger. First, large size lipid droplets may be formed by mutual fusion of pre-existing lipid droplets. Bostrom *et. al.* showed that it may be facilitated by a mechanism similar to vesicular fusion due to the presence of SNARE proteins in lipid droplets[22]. The finding of fat-specific of 27 kDa (FSP27) -mediated atypical lipid droplet fusion showed small donor lipid droplets fuse into large acceptor

lipid droplets and this fusion event is dependent on the difference in the internal pressures of contacting lipid droplets[23]. Importantly, the finding of homotypic lipid droplet fusion by Parton and colleagues revealed that there are three types of lipid droplet growth in adipocytes[24]. The first type of growth does not involve other lipid droplets. The second type is similar to the FSP27-mediated atypic fusion and the last one is the homotypic fusion of lipid droplets, which occurs in 15 min. In our previous study, we also observed the homotypic lipid droplet fusion[25]. Lipid droplet may remain in contact with the ER membrane and additional lipid esters are obtained from the ER. This hypothesis was came from the study conducted by Robenek *et. al.* who showed the association of lipid droplets with the cytosolic surface of the adipophilin-enriched ER membrane[11]. Third, the pre-existing lipid droplet may be transiently connected to the ER membrane and they may undergo a cycle of fusion and fission for the lipid transfer. Alternatively, the supply of lipid esters may be transported by soluble carrier proteins from the ER to the lipid droplets. Finally, the lipid esters may be synthesised by specific enzymes located on the surface of lipid droplets[26-29].

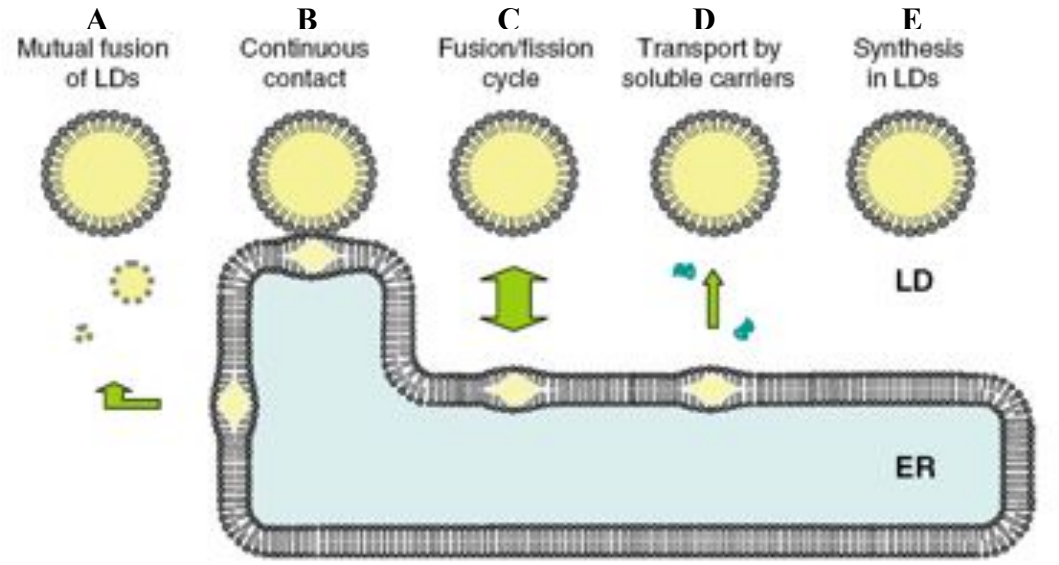

Figure 1.4 Hypothetical mechanisms of lipid droplet growth. (Figure adapted from Fujimoto *et al.*, 2008). **A**. Larger size lipid droplets may be formed by mutual fusion of pre-existing lipid droplets. **B**. Pre-existing lipid droplets may remain in contact with the ER membrane and additional lipid esters may be transferred from the ER to the pre-existing lipid droplets. **C**. The pre-existing lipid droplet may be transiently connected to the ER membrane and they may undergo a cycle of fusion and fission for the lipid transfer. **D**. The supply of lipid esters may be carried by soluble carrier proteins from the ER to the lipid droplets. **E**. The lipid esters may be synthesised by specific enzymes of the lipid droplets.

1.1.6 Size of lipid droplets

Lipid droplet-associated proteins may regulate the size of mature lipid droplets. Different studies have shown that mutation of some lipid droplet-associated proteins could generate irregular lipid accumulation or the reverse[30-33]. Study conducted by Fei *et al*. showed that the mutation of *Fld1,* yeast orthologue of human *BSCL2*, which encodes a protein of unknown function called SEIPIN[34-36] could lead to the formation of supersized lipid droplets in *fld1*Δ cells [30]. Seipin is a transmembrane protein, which localises to the ER. In human, mutations of the *Seipin* gene leads to near-complete absence of adipose tissue and patients with this rare autosomal recessive disorder will have severe hypertriglyceridemia, insulin resistance, fatty liver and

diabetes due to ectopic lipid accumulation in non-adipose tissues [35]. Recent studies in yeast, fly and mammalian cells showed the level of Seipin/Fld1 inversely correlates with TAG storage. This suggests that Seipin may control the size of lipid droplet through the regulation of TAG synthesis[37-39]. A more recent finding showed that another protein called fat-specific protein of 27 kDa (FSP27) regulates the size of lipid droplets. The ablation of FSP27 could lead to rapid lipolysis and it was also observed that *FSP27*-deficient mice could tolerate diet-induced obesity and insulin resistance[40]. Another study conducted by Guo *et al.* using RNAi (RNA interference) showed that 1.5% (227 genes) of the genome of *Drosophlia* S2 cells are functioning in lipid droplet formation and regulation. They also showed that the mutation of genes encoding for enzymes in the phosphatidylcholine biosynthetic pathway could lead to supersized lipid droplet formation[31]. However, the molecular mechanism behind this irregular lipid droplet formation resulting from the mutation of the phospholipid biosynthetic enzymes is still not clear.

1.1.7 Proteins of lipid droplets

Lipid droplets were initially thought as inert organelle without any function except for energy storage. However, proteomic studies on lipid droplets in the past few years completely overthrew this point of view. The PAT family, perilipin, adipocyte differentiation-related protein (adipophilin) and TIP47 (tail-interacting protein of 47 kDa) are proved to localise on the surface of lipid droplets. Moreover, other proteins like FSP27, histones, caveolin, Rab18 and more proteins have been identified. These proteins are proved to interact with lipid droplets and facilitate some regulation mechanisms that are still not well understood[17, 23, 41-45].

PAT family proteins localise to lipid droplet surface. The PAT family protein named after perilipin, adipophilin (also called ADRP) and TIP47 have been shown to localise to the droplet surface by immunofluorescence microscopy[43]. Robenek *et. al.* used the combination of freeze-fracture electron microscopy and immunoglod labeling successfully showed that the PAT family proteins were distributing throughout the lipid droplet surface, core and integral components of the phospholipid monolayer membrane[43]. Perilipin is found in adipocytes and steroidogenic cells and adipophilin is found in preadipocytes, these two proteins cover most of the surface of lipid droplets to protect the core lipids from hydrolysis by HSL. However, during lipolysis perilipin is phosphorylated by protein kinase A and lipid droplets are accessible by lipases[44]. The TIP47 protein was identified in a yeast two-hybrid screen using the cytosolic domain of the cation-dependent mannose 6-phosphate receptor (M6PR) as a bait to screen an expression library from human Jurkat cells[45]. Analysis of the amino acid sequence showed that TIP47 is highly similar to the sequences of perilipin (43% identity) and ADRP (60% identity, 80% similarity). It was found that the cellular distribution of TIP47 is dependent upon the storage of neutral lipids [45]. Recent study showed TIP47 is involved in the biogenesis of lipid droplets[46].

The other protein called caveolin has been shown to localise on lipid droplets[4, 47, 48]. Caveolins form the structural framework of caveolae (small invaginations of the plasma membrane). It facilitates signal transduction, cholesterol transport, and endocytosis[4]. The association of caveolins with lipid droplets was hypothesised to maintain cellular cholesterol balance and facilitate intracellular signalling[4, 48]. Other study conducted by Martin *et al.* found that GFP tagged Rab18 localized to lipid droplets and immunoelectron microscopy showed its direct association with the surface of the

phospholipid monolayer[41]. Because the Rab family of proteins are important in vesicular trafficking through cycles of GTP binding and hydrolysis, the association of Rab proteins with lipid droplets might suggest lipid droplets can distribute themselves via the interaction with Rab18 to other cellular compartments for energy supply. They also suggested that the recruitment of Rab18 to lipid droplets is depending on the metabolic state of individual lipid droplet. However, the overall mechanism is not well understood. Recent study of Rab18 showed that it interacts with the Hepatitis C virus non-structural protein NS5A and this promote the physical interaction between Hepatitis C virus and lipid droplets[49].

1.1.8 Phospholipids

Biosynthesis of phospholipids is the fundamental process that produces lipid droplets in all cell types. In mammalian cell membranes, there are more than 1000 different phospholipids which are formed by different combination of fatty acyl chains and polar head groups[50]. The most abundant phospholipids in mammalian cell membranes are phosphatidylcholine (PC), phosphatidylethanolamine (PE), phosphatidylinositol (PI), and phosphatidylserine (PS). PC constitutes about 40 to 50% of total phospholipids and it is the most abundant phospholipids found in mammalian cell membranes. PE constitutes about 20 to 50% of total phospholipids and it is the second most abundant phospholipids. Depending on the cell type and tissue, the percentage of different phospholipids varies[50]. Deletion of genes involve in PC synthesis in *Drosophila* S2 and yeast showed supersized lipid droplet formation[25, 31]. The cylindrical shape of PC provides the ability to stabilise lipid droplet from fusion. Lipid analysis in supersized lipid droplet mutant showed increased level of the fusogenic phospholipid

PA. Therefore, the balance between PC and PA plays a big role in controlling the size of lipid droplets. Specifically, the propensity of membrane fusion is correlated with the effective spontaneous curvature of a particular lipid. The effective spontaneous curvature of a lipid is determined by its molecular structure and how it interacts with the other lipids in the membranes. For instance, the phospholipid PC has a spontaneous curvature of zero and a cylindrical shape. In contrast, the phospholipid PA has a negative spontaneous curvature (monolayer with surface bulging in the direction of the hydrocarbon chains) and a conical shape. Study showed that the negative spontaneous curvature and conical shape promotes membrane fusion[51]. However, it is still not clear how this process is regulated.

1.2 Adipogenesis

Mature adipocytes contain unilocular lipid droplets and they are the major depots for energy storage. The development of adipocytes from mesenchymal stem cells involves complicated gene activation and regulation[52]. There are two main steps in adipogenesis. During the determination phase, preadipocytes are developed from mesenchymal stem cells. Then preadipocytes are differentiated to mature adipocytes in the terminal differentiation phase. In the terminal differentiation phase, CEBPβ and CEBPδ are first expressed[53] and lead to the expression of PPARγ. The activation of PPARγ promotes the expression of its target genes and results in lipid uptake, glycerol uptake, lipid storage and inhibits lipolysis[54]. In addition, the sterol responsive element binding protein 1c (SREBP1c) increases the activation of PPARγ through the production of PPARγ ligands[55]. The finding of endogenous ligands of PPARγ is a continuing challenge in the field of adipogenesis. Recent discovery of increased level of

lysophosphatidic acid could increase the activity of PPARγ have shed some light on the finding of endogenous PPARγ agonist. Study also speculated that PA may act as PPARγ antagonist, but more evidence is needed to confirm this hypothesis.

1.2.1 PPARγ

PPARγ belongs to the nuclear receptor superfamily of ligand-inducible transcription factors[56]. There are two other members of this family, PPARα and PPARβ/δ. PPARγ is known as the master regulator of adipogenesis, the activation of PPARγ in fibroblast leads to the differentiation of adipocytes[57]. PPARγ is highly expressed in white adipose tissue and brown adipose tissue. It is not only the master regulator of adipogenesis, but it also regulates lipid metabolism and insulin sensitivity[54]. The finding of thiazolidinedione (TZD) as PPARγ agonist leads to its use in the treatment of type II diabetes[58]. The binding of PPARγ to PPAR-responsive regulatory elements (PPREs) requires the formation of heterodimers with retinoid X receptor (RXR). The binding of the heterodimers controls the expression of genes involved in adipogenesis, lipid metabolism, inflammation, cell proliferation, apoptosis and maintenance of metabolic homeostasis[54, 59]. Moreover, it also controls the secretion of adiponectin, resistin, leptin and tumor necrosis factor-α[60-63]. As mentioned above, the finding of endogenous PPARγ is underway. It is known that lipids like oleic, linoleic and linolenic acids bind to PPARγ and lipid metabolites like prostaglandin J2, 8S-hydroxyeicosatetraenoic acid and oxidised phospholipids also bind to PPARγ[64-66]. PPARγ contains three major domains, a N-terminal transactivation domain (AF1), a highly conserved DNA-binding domain (DBD) and a C-terminal ligand-binding domain (LBD) with transactivation domain (AF2). The binding of ligands to PPARγ induces

conformational changes and the recruitment of specific cofactors is ligand dependent[67]. Alternative splicing and differential promoter usage results in two PPARγ isoforms: PPARγ1 and PPARγ2[54]. PPARγ2 is specifically expressed in adipose tissue under physiological conditions whereas PPARγ1 is expressed in many tissues. PPARγ not only regulates adipogenesis, it also maintains mature adipocytes[67]. Furthermore, patients with heterozygous mutations of *PPARγ* have been characterised with partial lipodystrophy, insulin resistance and dyslipidemia[68].

1.3 Seipin

The human *Berardinelli-Seip congenital lipodystrophy 2* (*BSCL2*) encodes the mysterious protein Seipin with unknown function. It has been shown recently that Seipin may regulate both lipid droplet dynamics and adipogenesis[30, 35, 36, 69-71]. Fld1, the yeast orthologue of mammalian Seipin, was found in two independent screens of the yeast deletion library[30, 36]. The deletion of *fld1* was found to have supersized lipid droplets. 30% of the mutant had the supersized lipid phenotype while the other 60% had clustering of small size lipid droplets. The human mutant *BSCL2* was identified linking to Berardinelli-Seip congenital lipodystrophy type 2, an autosomal recessive disorder[69]. Loss of function mutation of *BSCL2* leads to the most severe form of congenital generalised lipodystrophy (CGL), which is characterised by an almost complete loss of adipose tissue, early onset of diabetes, hypertriglyceridemia and fatty liver[35, 72]. Additionally, dominant gain of function mutations of *BSCL2* was found to cause mental retardation in Seipin deficient patients, this Seipin related neurological disorder was termed seipinopathies[73]. The deficiency of Seipin also leads to supersized lipid droplet formation in the salivary glands in drosophila[38].

Therefore, Seipin is a well-conserved protein in regulating dynamics of lipid droplets and adipogenesis.

1.3.1 Structure of Seipin

Seipin is an ER membrane protein and its localisation to the ER was confirmed in several studies[30, 37, 70, 74]. Seipin has two transmembrane domains with both N and C termini facing the cytoplasm and a large luminal loop[75, 76] (Figure 1.5). However, it lacks any functional domains, which makes it hard to predict its function. The human *SEIPIN* encodes two isoforms, 398 and 462 amino acids in length, due to alternative translation initiation sites. The longer isoform has an additional of 64 amino acids at its N terminus. The human *BSCL2* gene has three transcripts: 1.6 kb, 1.8 kb and 2.2 kb. The 1.8 kb transcript is exclusively expressed in the brain and testis and the other two transcripts are ubiquitously expressed. Both 1.8 and 2.2 kb transcripts can encode the 398 and 462 amino acid isoforms. However, the 1.6 kb transcript can only encode the 398 amino acid isoform. The central region of *SEIPIN* is well conserved in its orthologue in terms of secondary structure but both N and C termini are diverged. Yeast *fld1* has only 12 amino acids at its N terminus and 11 amino acids at the C terminus. The overexpression of the full length or the truncated Seipin without the cytoplasmic tails can rescue the lipid droplet defect in yeast Fld1 mutant cells[30]. This indicates that the main function of Seipin is conserved through evolution. Recent study conducted by Wang *et al.* showed the formation of Fld1/Ldb16 complex in yeast may resemble the structure of human Seipin and the deletion of LDB16/YCL005W caused supersized lipid droplet formation, altered phospholipid metabolism and impaired lipid droplet protein distribution[77]. These phenotypes are similar to the deletion of FLD1.

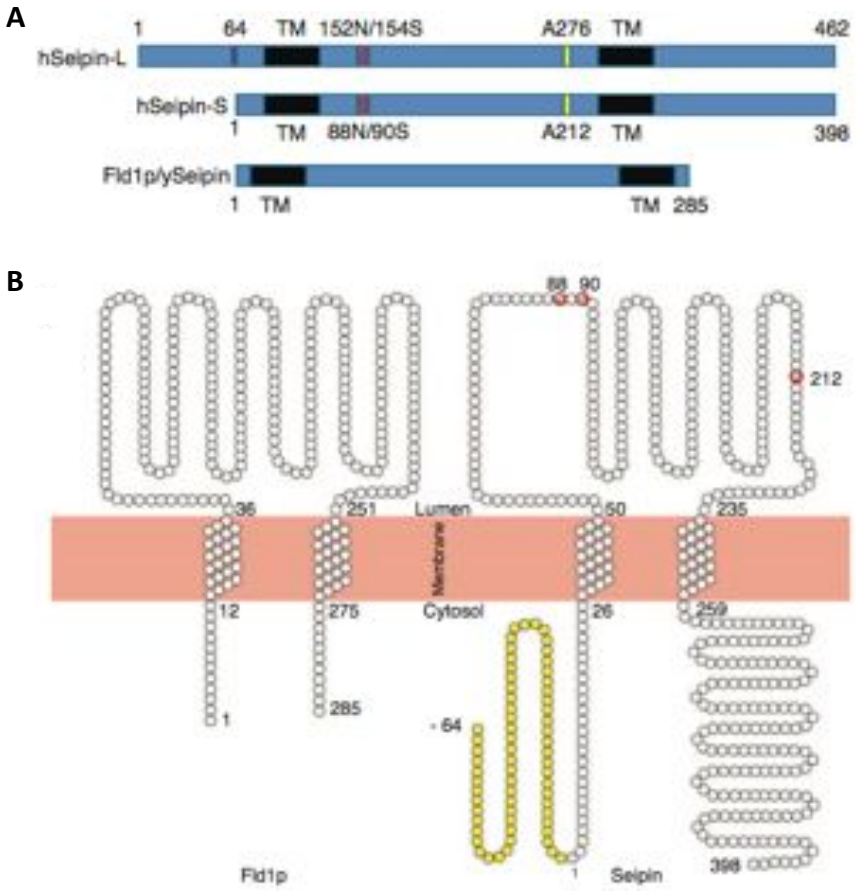

Figure 1.5 Domains and topology of human seipin and yeast orthologue Fld1. Figure adapted from Fei *et al.*, 2011. A. Schematic diagram of yeast Fld1 and human long (hSeipin-L) and short (hSeipin-S) Seipin isoforms. Residues for glycosylation mutants (88,90/152,154) and the lipodystrophic mis-sense mutant (212/276) are indicated. TM, transmembrane domain. B. Membrane topology of yeast Fld1 and human Seipin. The disease-assocaited mutants are marked in red.

1.3.2 Congenital generalised lipodystrophy

Congenital generalised lipodystrophy (CGL) is a rare human genetic disease. There are four types of CGL identified. CGL1 is caused by mutations in the 1-acylglycerol-3-phosphate-O-acyl transferase 2 (*AGPAT2*). AGPAT2 catalyses the formation of phosphatidic acid (PA) from 1-acylglycerol-3-phosphate (LPA). The dysfunction of AGPAT2 impairs PA synthesis resulting in impairment of TAG synthesis in adipose

tissue. CGL2 is caused by the mutation of *BSCL2/SEIPIN* and it is the most severe form of lipodystrophy, which is characterised by almost complete lost of adipose tissue[34]. However, its function is still unknown and it remains the most mysterious lipodystrophic protein. CGL3 and CGL4 are due to the mutations in caveolin-1 (*CAV1*) and cavin (*PTRF*), both of which are essential for caveolae formation[78, 79]. Caveolae are important in adipocyte function and they are densely located on the adipocyte plasma membrane. The lack of caveolae disrupts adipocyte signalling and lipid uptake[80].

1.3.3 Seipin function

The function of Seipin is still a mystery. shRNA study in both 3T3-L1 cells and C3H10T1/2 pluripotent stem cells showed Seipin was more likely involved in the conversion of preadipocytes to adipocytes during terminal differentiation, because the terminal differentiation marker gene *cebpa, pparg and srebp* were greatly attenuated. Importantly, the addition of PPARγ agonist pioglitazone could rescue the adipogenesis defect[70, 81]. Overexpression of diacylglycerol acyltransferase (DGAT) in *Seipin* knockout flies rescued the lipid droplet phenotype[38], suggesting that seipin may involve in the process of TAG synthesis. Moreover, fat accumulation in *Seipin* knockout mouse was greatly reduced and adipogenesis was severely affected[72]. The defect of adipogenesis may be due to the accumulation of PA in the *Seipin* knockout cells. PA is the essential substrate in the synthesis of major phospholipids and TAG. The mutations in *Lipin1* also give rise to severe generalised lipodystrophy[82, 83]. The accumulation of PA in Lipin1 deficient mice, AGPAT2 knockdown cells and liver of *Agpat2*$^{-/-}$ mice suggests that PA may inhibit adipogenesis. Recent study showed cyclic

phosphatidic acid (CPA) serves as naturally occurring PPARγ antagonist[84], so it is possible that the accumulation of PA in *Seipin* knockout cells may act as PPARγ antagonist and inhibit adipogenesis. The addition of PPARγ agonist pioglitazone rescued impaired adipogenesis in *Seipin* knockdown 3T3-L1 cells[70] leads to the hypothesis that Seipin may work at the level of PA to TAG synthesis.

As mentioned above that PA is a cone shaped fusogenic phospholipid that promotes lipid droplet fusion. The deletion of *Seipin* leads to the accumulation of PA and it is possible that high level of PA on the monolayer of lipid droplets may promote fusion resulting in the supersized lipid droplet phenotype observed in Seipin deficient cells. The increase of PA may also enhance DAG synthesis by lipin1 and therefore TAG. The ER localisation of Seipin also suggests that it may involve in the synthesis of TAG. The absence of any putative functional domain of Seipin makes it hard to predict its function. Although it has been shown that Seipin can form a homo-oligomer of about 9 subunits[85], it is more urgent to identify enzyme(s) that could physically and/or functionally interact with seipin.

1.4 PI3K/Akt/mTOR pathway

The response to insulin of adipocytes significantly increase glucose uptake. The discovery of the phosphoinositide-3-kinase (PI3K) / Akt pathway has led to the identification of components and mechanism of insulin signalling pathway. The downstream target mechanistic target of rapamycin (mTOR) is a complex network that regulates protein and lipid synthesis, energy metabolism and cell survival[86].

1.4.4 PI3K/Akt pathway

The production of phosphatidylinositol (3,4,5) trisphosphate (PIP_3) by PI3K is one of the hyperactivated signal observed in a wide range of cancers, such as ovarian, breast, lung, and prostate[87-96]. The most common phenotype of these cancer cells is the over activated PI3K pathway, especially elevated Akt activity and the mutation of Phosphatase and tensin homologue (PTEN). The consequent activation of targets downstream of PIP_3 triggers a series of cellular responses, such as proliferation, cell growth, apoptosis and motility. These processes are hugely affected in cancer cells to favour cell growth and inhibit apoptosis. Moreover, cancer cells tend to switch to glucose-dependent metabolism and it is relied on the insulin PI3K pathway[97]. Figure 1.5 shows a schematic diagram of the PI3K pathway. When ligand like insulin binds to the insulin receptor on the plasma membrane, this recruits and activates PI3K on the plasma membrane. PI3K then converts phosphatidylinositol (4,5) biphosphate (PIP_2) to PIP_3. Akt is then translocated to the plasma membrane and interacted with PIP_3 via its PH domain. Akt is phosphorylated at two residues Thr308 and Ser473 by PDK1 and mTORC2, respectively[86, 98]. The mutation of PTEN observed in wide range of cancer cells led to over activated PI3K signalling due to the inability of PTEN to inhibit the conversion of PIP_2 to PIP_3. Constitutively activation of the PI3K pathway in *Pten* heterozygous mice showed high incidence of prostate, breast and liver cancers[99, 100]. Another important downstream target of the PI3K pathway is Akt. The mutation of Akt usually leads to imbalance proliferation, apoptosis and growth. Akt is also known as protein kinase B (PKB), which is a serine/threonine kinase. There are three members of the Akt family, Akt1, Akt2 and Akt3. They are ubiquitously expressed, but isoform specific function has been identified. Akt1 is involved in cell survival[101, 102]. Akt2

plays a role in glucose homeostasis[102, 103] and Akt3 is more likely involved in brain development[104]. The phosphorylation of Akt at Thr308 by PDK1 is necessary and sufficient for Akt activation. Moreover, mTORC2 phosphorylates Akt at Ser473 for maximal activation[105, 106].

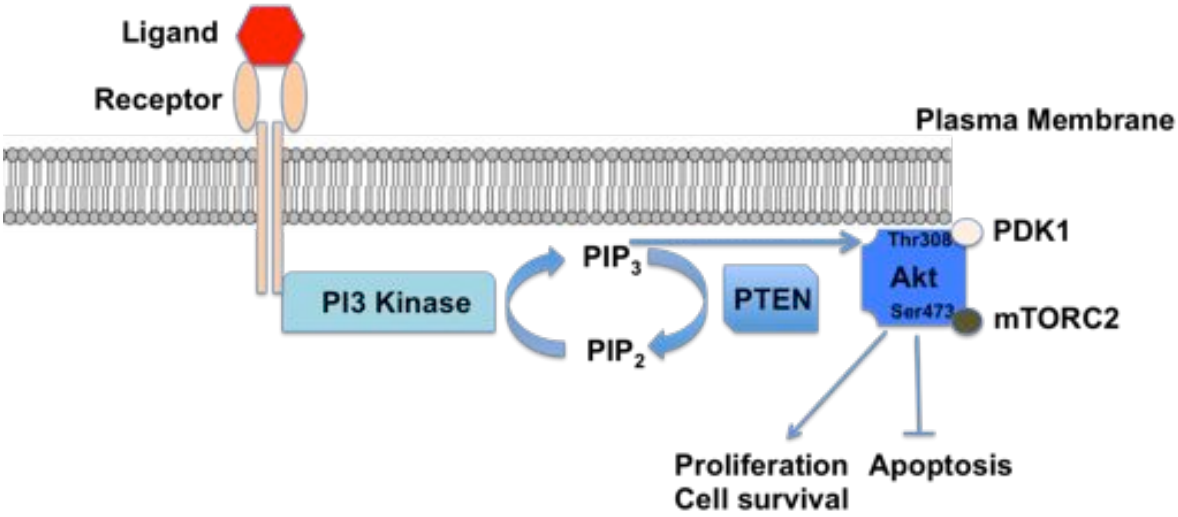

Figure 1.6 Schematic diagram of the PI3K pathway. Ligand like insulin binds to the insulin receptor on the plasma membrane; the binding recruits and activates PI3K on the plasma membrane. PI3K then converts phosphatidylinositol (4,5) biphosphate (PIP_2) to phosphatidylinositol (3,4,5) trisphosphate (PIP_3). Akt is then translocated to the plasma membrane and interacted with PIP_3 via its PH domain. Akt is phosphorylated at two residues, Thr308 and Ser473 by PDK1 and mTORC2, respectively. Activated Akt then phosphorylates downstream targets and plays roles in proliferation, cell survival, apoptosis and more.

1.4.5 mTOR pathway

The discovery of mTOR as the physical target of rapamycin has helped us to understand more about how cells respond and adapt to diverse environmental changes. There are two complexes that contain the mTOR serine/threonine protein kinase. mTOR complex 1 (mTORC1) and mTOR complex 2 (mTORC2) both share the catalytic mTOR subunit and the mammalian lethal with sec-13 protein 8 (mLST8)[107, 108]. As shown in Figure 1.6, mTORC1 also comprises DEP domain containing mTOR-interacting protein

(DEPTOR), regulatory-associated protein of mammalian target of rapamycin (raptor) and proline-rich Akt substrate 40 kDa (PRAS40)[109-111]. In contrast, the mTORC2 comprises rapamycin-insensitive companion of mTOR (rictor), mammalian stress-activated map kinase-interacting protein 1 (mSin1) and protein observed with rictor 1 (protor1)[108, 112, 113].

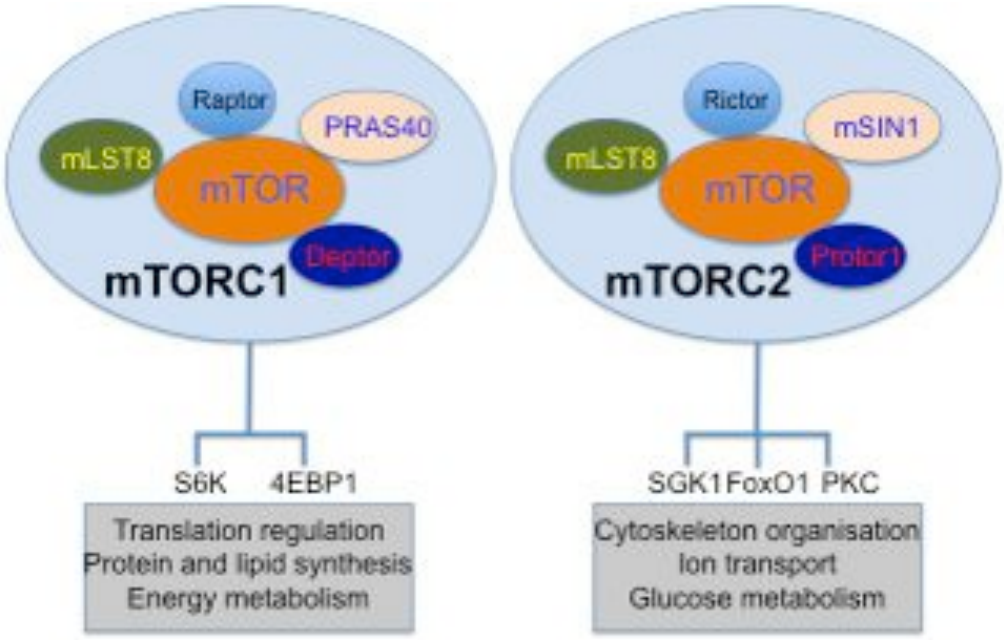

Figure 1.7 Mechanistic target of rapamycin complexes. Mammalian target of rapamycin (mTOR) pathway controls cellular activities through the action of mTOR complex 1 (mTORC1) and mTORC2. mTORC1 and mTORC2 shares the catalytic mTOR subunit and the mammalian lethal with sec-13 protein 8 (mLST8). In comparison, mTORC1 also contains DEP domain containing mTOR-interacting protein (DEPTOR), regulatory-associated protein of mammalian target of rapamycin (raptor) and proline-rich Akt substrate 40 kDa (PRAS40). The activation of mTORC1 phosphorylates its downstream targets S6K and 4EBP1, this controls translation regulation, protein and lipid synthesis and energy metabolism. In contrast, mTORC2 comprises of rapamycin-insensitive companion of mTOR (rictor), mammalian stress-activated map kinas-interacting protein (mSin1) and protein observed with rictor 1 (protor1). mTORC2 controls cytoskeleton organisation, ion transport and glucose metabolism through the activity of SGK1, FoxO1 and PKC respectively.

The binding of rapamycin with the intracellular 12-kDa FK506-binding protein (FKBP12) inhibits mTORC1 assembly. Because FKBP12 does not interact with mTORC2, it was originally thought that rapamycin has no effect on mTORC2

assembly. Sarbassove *et al.* showed prolong rapamycin treatment inhibited mTORC2 assembly, but this inhibitory effect was only specific to certain cell types[114]. There is much less known about the mTORC2 pathway. Studies showed that mTORC2 is required for maximal Akt activation[106]. It activates serum and glucocorticoid-induced protein kinase 1 (SGK1) to control ion transport. It also controls forkhead box protein O1 (FoxO1) for regulating adipogenesis and glucose metabolism[115, 116]. Moreover, it activates protein kinase C-α (PKC) for cytoskeletal organisation[108].

The mTORC1 pathway controls cellular activity through the balancing of environmental inputs like growth factors, stress, energy level, oxygen and amino acids. The activation of mTORC1 by the stimulation of these factors regulates protein and lipid synthesis, lysosome biogenesis, autophagy and energy metabolism[86]. The major downstream targets of mTORC1 are S6 kinase 1 (S6K1) and translational regulators eukaryotic translation initiation factor 4E-binding protein 1 (4E-BP1). Both enzymes are important in the controlling of translation initiation[117]. mTORC1 directly phosphorylates S6K1 at the Thr389 and leads to conformational change of S6K1. This allows the docking of PDK1 to phosphorylates S6K1 at the Thr229 for final activation[118]. The activation of S6K1 regulates translation initiation factors for protein synthesis and it also mediates ribosome biogenesis[119]. Also, mTORC1 regulates translation initiation through the phosphorylation of 4E-BP1. Translation initiation requires the assembly of pre-initiation complex, which contains eIF4A, eIF4E, eIF4G and ribosomes. As the eIF4E inhibitor, 4E-BP1 prevents the interaction of eIF4G with eIF4E. The phosphorylation of 4E-BP1 by mTORC1 allows the binding eIF4E to eIF4G and leads to the binding of these translational initiation factors to the 5’ end of an mRNA[117, 120].

mTORC1 also involves in the regulation of lipid synthesis. The phosphorylation of S6K1 controls the sterol regulatory element-binding proteins (SREBPs)[121]. SREBPs remain in its inactive state on the ER and respond to insulin and sterol depletion. There are three isoforms of SREBPs, SREBP1a, SREBP-1c and SREBP-2 and they are the gene products of SREBP1 and 2[122]. The inactive SREBPs form a complex with the sterol-sensing protein SREBP cleavage-activating protein (Scap). Condition like low cholesterol level transfers the complex to the Golgi with the aid of COPII vesicles. The N terminus of SREBPs is released by Golgi-localised Site-1 protease (S1P) and Site-2 protease (S2P). The cleaved N terminus then enters the nucleus and activates genes involved in cholesterol biosynthesis[123]. mTORC1 also regulates insulin signalling via S6K1. The activation of the PI3K pathway by insulin results in mTOR activation. Studies showed that the phosphorylation of S6K1 by mTORC1 favours the inhibition of the insulin-signalling pathway through Grb10, which blocks the binding of insulin receptor substrate (IRS) to insulin receptors on the plasma membrane[124, 125]. Overall, the mTOR pathway regulates major cellular processes to balance environmental inputs and outputs.

1.5 Cholesterol Trafficking

Cholesterol can be produced via *de novo* synthesis in the ER and exogenous cholesterol can be delivered to cells through the receptor-mediated lipoprotein uptake. Cholesterol is an essential lipid of mammalian cells; the defect of cholesterol trafficking would lead to imbalance cholesterol homeostasis. Figure 1.7 shows a diagram of the cholesterol trafficking pathway.

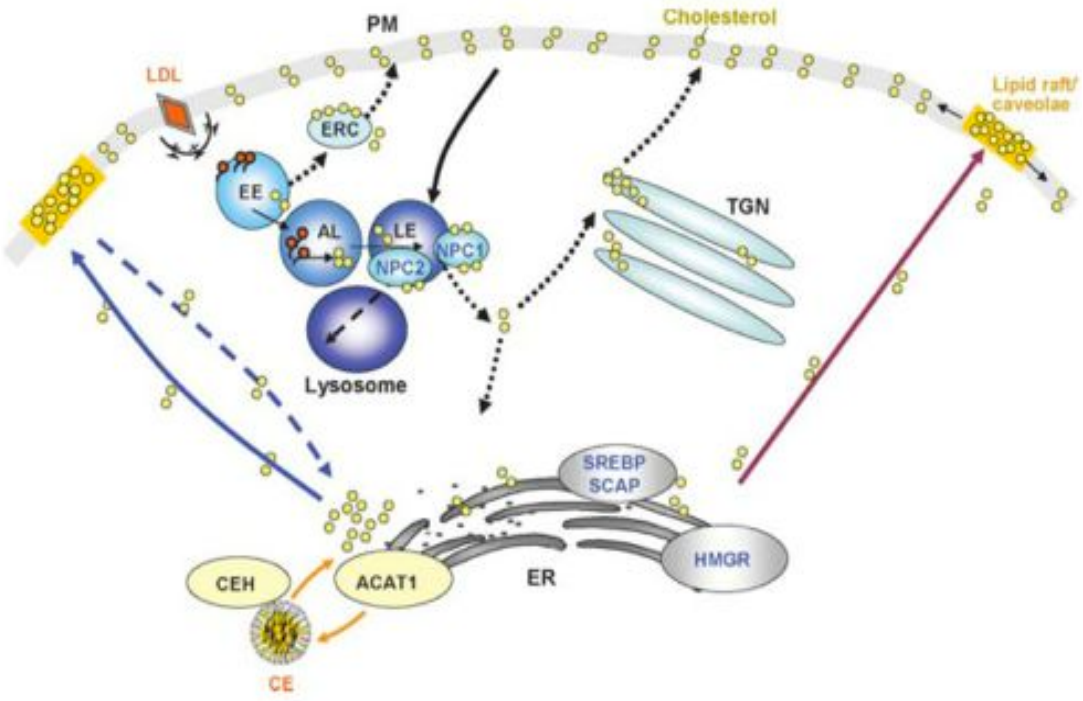

Figure 1.8 Cholesterol Trafficking in mammalian cells. (Figure adapted from Chang *et al.* 2006). Cholesterol is obtained in two major pools in mammalian cells: cholesterol derived in low-density lipoprotein (LDL) and *de novo* synthesis of cholesterol in the endoplamic reticulum (ER). Niemann-Pick C1 and C2 (NPC1 and NPC2) proteins facilitates the trafficking of LDL-derived free cholesterol in the late endosomes lysosomes (LE/LY). The translocation of cholesterol may involve both vesicular and non-vesicular mechanism to organells such as the ER and the plasma membrane (PM) through the trans-Golgi network (TGN). The dotted lines represent the mechanisms that are now well understood. The cholesterol sensing protein sterol regulatory element binding (SREBP) and HMG-CoA reductase (HMGR) in the ER detects the level of cholesterol and facilitates the production of cholesterol. Acyl-coenzyme A:cholesterol acyltransferase 1 (ACAT1) helps to package free cholesterol into cholesterol esters in lipid droplets to prevent lipotoxicity.

Cholesterol is transported as cholesterol esters in low-density lipoprotein (LDL). LDL binds to the LDL receptor on the plasma membrane and the LDL is then endocytosed via the clathrin-mediated pathway. The release of free cholesterol is facilitated by acidic hydrolase that is localised in the late endosomes/lysosomes (LE/LY)[126]. The LDL-derived free cholesterol is then effluxed from the LE/LY to other organelles, such as the plasma membrane and the ER, via the concerted action of Niemann-Pick C1 (NPC1)

and Niemann-Pick C2 (NPC2)[127, 128]. The free cholesterol can then be delivered to the plasma membrane and the ER via the trans Golgi network (TGN). However, the exact mechanism of intracellular transport of cholesterol from the LE/LY to the other organelle is still not fully understood. The amount of cholesterol delivered to the ER facilitates the regulation of cholesterol synthesis and uptake from LDL. The SREBP pathway in the ER controls this feedback regulation. When cholesterol is high in the ER, the SREBP pathway shuts down the expression of the genes responsible for cholesterol synthesis and uptake[122]. The accumulation of cholesterol in the ER also promotes the synthesis of cholesterol esters in the ER by ACAT1 and storing them in lipid droplets to lower lipid toxicity[129]. One of the main focuses of this thesis is the NPC1 protein, which facilitates the trafficking of cholesterol out of LE/LY with the aid of NPC2. NPC1 contains 13 transmembrane domains, three large luminal loops, six cytosolic loops and a C-terminal cytoplasmic tail (Figure 1.8) [130]. The mutation of either NPC1 or NPC2 causes lipid storage and trafficking disorder that is characterised by the intracellular accumulation of LDL-derived free cholesterol within the LE/LY in cells of liver, spleen and brain[129]. There is no cure for NPC disease, although the administration of steroid hormone allopregnanolone to young NPC1 mice delayed the neurodegeration[131]. The understanding of how NPC1 works in the cholesterol trafficking pathway may help to develop cures for patients with cholesterol trafficking diseases.

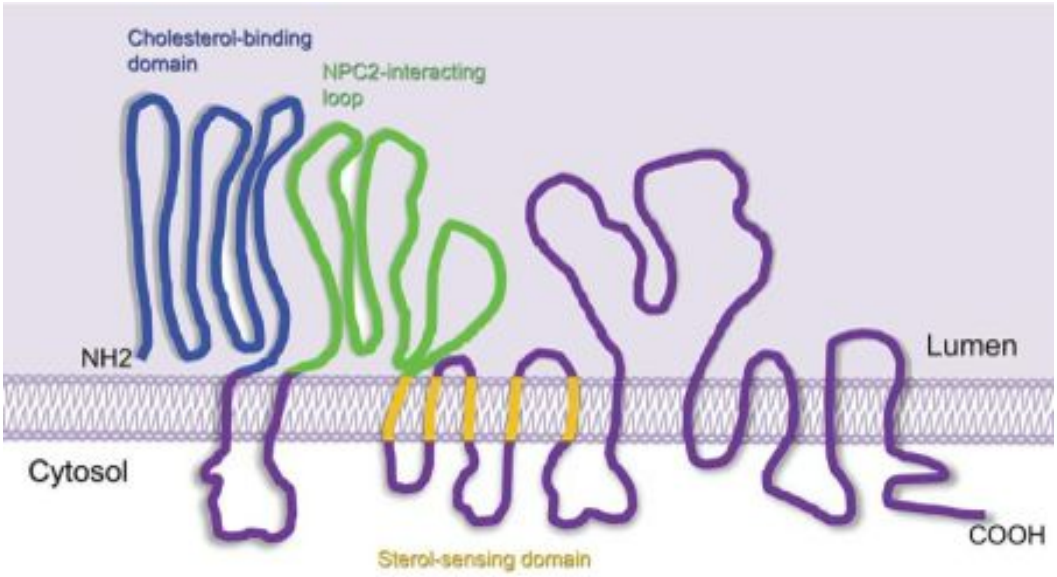

Figure 1.9 Membrane topology of NPC1. (Figure adapted from Yang and Du, 2013). NPC1 contains 13 transmembrane domains, three large luminal loops, six cytosolic loops and a C-terminal cytoplamsmic tail. The N-terminus is the cholesterol-binding domain and is shown in blue. The second luminal loop contains the NPC2-interactin domain and is shown in green. The sterol-sensing domain is between transmembrane domains 3 to 7 and is shown in yellow.

1.6 Aims

1. Cholesterol trafficking plays a big role in cellular homeostasis and the protein NPC1 is essential in this process. The observation of free cholesterol accumulated in human papillomavirus (HPV) negative cervical cancer cells C33A has led to the hypothesis that NPC1 might be absent. Also, the extremely high Akt activity was only observed in HPV negative C33A cells but no in HPV negative cervical cancer cells. The main aim of this part of the thesis was to investigate why NPC1 was absent in this HPV negative cervical cancer cells comparing to HPV positive cervical cancer cells, which did not have free cholesterol accumulation phenotype.

2. Seipin, a mysterious protein of interest with unknown biological function. The transcription factor that controls the expression of the mouse and human SEIPIN gene *BSCL2* was investigated. Previous published ChIP data suggested PPARγ was bound to the promoter region of *BSCL2*. The main aim was to confirm if PPARγ actual binds to the potential site and promote the expression of the seipin gene.

3. Seipin is involved in adipogenesis and the absence of Seipin results in lipodystrophy and seipinopathy in patients. The role of Seipin was investigated during adipogenesis and its relationship with PPARγ was also examined. Because *Seipin* has very high expression in brains, the function of Seipin was also investigated in newborn mouse hippocampus neuronal cells by knockdown studies.

2. Chapter 2. MATERIALS AND METHODS

2.1 General Materials and Methods

All the general materials and siRNAs used in this study are listed in **Table 1-1**.

Table 1-1. Materials used in this study

Materials	**Supplier/Description**
RFP antibody	Abcam
β actin antibody	Abcam
Perilipin antibody	Abcam
Acetic Acid Glacial	Ajax FineChem
Ethylenediaminetetraacetic Acid (EDTA)	Ajax FineChem
Methanol	Ajax FineChem
N-Hexane	Ajax FineChem
Potassium Chloride	Ajax FineChem
Chloroform	Ajax FineChem
Ethanol Absolute	Ajax FineChem
Diethyl Ether	Ajax FineChem
Tris (Hydroxymethyl) Aminomethane	Ajax FineChem
Sodium Hydroxide	Ajax FineChem
Sodium Chloride	Ajax FineChem
Hydrochloric Acid	Ajax FineChem
Isopropanol	Ajax FineChem
Phospholipid Internal Standard Mix	Avanti Polar Lipids

mTOR antibody	Cell Signaling
Phospho-mTOR S2448 antibody	Cell Signaling
S6K antibody	Cell Signaling
Phospho-S6K T389 antibody	Cell Signaling
Akt antibody	Cell Signaling
Phospho-Akt T308 antibody	Cell Signaling
Phospho-Akt S473 antibody	Cell Signaling
KAPA SYBR® FAST qPCR Kits	KapaBiosystems
Dynabeads® Magnetic Beads	Life Technologies
Dulbecco's Modified Eagle Medium (DEME)	Life Technologies
RPMI 164 Medium, GlutaMAX	Life Technologies
Fetal Bovine Serum (FBS)	Life Technologies
Neonatal Calf Serum (NCS)	Life Technologies
Penicillin-Streptomycin (10,000U/mL)	Life Technologies
OPTI-MEM	Life Technologies
TrypLE™ Express	Life Technologies
D-PBS	Life Technologies
ProLong® Antifade Gold Reagent	Life Technologies
Alexa Fluor Antibodies	Life Technologies
TRIzol® TM Reagent	Life Technologies
Lipofectamine RNAiMAX® Reagent	Life Technologies
SuperScript® VILO™ cDNA Synthesis Kit	Life Technologies
BODIPY 493/503	Life Technologies
PCR purelink purification kit	Life Technologies

Plasmid Mini-Prep Kit	Life Technologies
Puromycin	Life Technologies
DECP treated water – DNA/RNAse free	Life Technologies
Gibco® MEM Non-Essential Amino Acids	Life Technologies
TLC Silica Gel Glass Plates	Merck
TLC aluminium sheet	Merck
Oleic acid [1- ^{14}C]	MP Biomedicals
Restriction Enzymes	New England Biolabs
KOD Hot Start DNA polymerase	Novagen
Bacteriological Peptone	Oxoid
Rosglitazone	Sigma-Aldrich
Human Rictor siRNA	Sigma-Aldrich 5'-3'GACACUACAACAAGUGGCA[dT][dT]
Human Raptor siRNA	Sigma-Aldrich 5'-3' CUAGUCUGUUUCGAAAUUU[dT][dT]
Mouse Seipin siRNA	Sigma-Aldrich
Bovine Serum Albumin (BSA)	Sigma-Aldrich
Oleic Acid > 99% GC	Sigma-Aldrich
Insulin Solution 10mg/mL	Sigma-Aldrich
3-Isobutyl-1methylxanthine ≥99% (HPLC)	Sigma-Aldrich
Dexamethasone	Sigma-Aldrich
Bicinchoninic Acid (BCA) Kit	Sigma-Aldrich
Iodine	Sigma-Aldrich
Triacylglycerol Standard (TLC)	Sigma-Aldrich

Sterol Ester Standard (TLC)	Sigma-Aldrich
Cholesterol Standard (TLC)	Sigma-Aldrich
Doxycycline	Sigma-Aldrich
Ampicillin	Sigma-Aldrich
Kanamycin	Sigma-Aldrich
Rat liver tissue	Provided by Nigel Turner UNSW

2.2 General Buffers

All buffers used in this study were prepared with MilliQ water (MilliQ system, Millipore NSW) and sterilised either by filtration through a 0.22μm filter or by autoclaving for 15 min at 121°C. pH calibration was carried out using HCl and NaOH.

2.3 Quantitative RT-PCR (qRT-PCR) Primers

qRT-PCR primers were designed using the online software, Primer 3.0 based on the cDNA sequences obtained from http://www.ncbi.nlm.nih.gov/gene (NCBI).

All the qRT-PCR primers used in this study are listed in Table 1-2.

Table 1-2. qRT-PCR Primers used in this study

Primer (qRT-PCR)	**Sequence**
ABCA1	5’ – GCTGCCTCCTCCACAA 3’ - GCTTTGCTGACCCGCTCCTGGATC
GAPDH	5’ – CCACTCCTCCACCTTTGAC 3’ - ACCCTGTTGCTGTAGCCA

HMG-COA	5’ – TACCATGTCAGGGGTACGTC 3’ - CAAGCCTAGAGACATAATCATC
LDLR	5’ – TGACAATGTCTCACCAAGCTCTG 3’ – CTCACGCTACTGGGCTTCTTCT
NPC1	5’ – CAATGACAACTGCACCATCC 3’ – GTGTCATTCAGGCAGTTGGTGAC
SREBP1c	5’ – CGGAGCCATGGATTGCAC 3’ – CAGTGACTTCCCTGGCCTA
SREBP2	5’ – CCCTGGGAGACATCGACGA 3’ – CGTTGCACTGAAGGGTCCA
ChIP DR1	5’ – GTGTGTCCAACACCTCCGGA 3’ – ATGACTGCTTTAGGTGTCTC
ChIP Positive Control	5’ – GAATTCCAGCAGGAATCAGG 3’ – GCCAAAGAGACAGAGGGCG
ChIP Negative Control	5’ – ACCAAAACCCACAAATTCCA 3’ – CTGCTCCTGCTGTCTCTCCT
36B4	5’ – CCCACTTACTGAAAAGGTCA 3’ - TTAGTCGAAGAGACCGAATC
aP2	5’ – ACATGAAAGAAGTGGGAGTG 3’ - GGTTATGATGCTCTTCACCT
BSCL2 (mouse)	5’ – GACCAGATCAAAGGA 3’ – AAGGATGGTGCAGAAGAGC
BSCL2 (human)	5’ – CTCCTGCTATTTGGCTTTGC 3’ – GCTGAGGAAGGTGAAGTTGC
CEBPA	5’ – CAAGAACAGCAACGAGTACC 3’ – TTGACCAAGGAGCTCTCAG
Pref-1	5’ – TCTGCGAAATAGACGTTCGGGCTT

	3’- CCCTAACCCATGCGAGAACGATGGC
Caspase3	5’ – ACTTCCATAAGAGCACTGCA 3’ – ACCATGGCTTAGAATCACAC

2.4 RNA Extraction and cDNA Synthesis

Total RNA was extracting using Trizol™ reagent. Mammalian cells were grown in 6-well plate. Cell monolayer was rinsed with ice cold PBS once and cells were lysed directly in each well by adding 1 mL of Trizol™. After 5 minutes of incubation, cell lysate was passed several times through a pipette. 200µL of chloroform was added to each sample and vortexed for 15 seconds. The mixture was then incubated at room temperature for 3 minutes. Samples were then subjected to centrifugation at 12,000 × g for 15 minutes at 4°C. The upper aqueous phase was then transferred to new tube. RNA was then precipitated from the aqueous phase by adding 500µL of isopropyl alcohol. After 15 minutes incubation at room temperature, sample was spun at 12,000 × g for 10 minutes at 4°C. The RNA precipitate might not be visible. The RNA precipitate was washed with 1mL 75% ethanol and subjected to centrifugation at 7,500 × g for 5 minutes at 4°C. The washing step was repeated once. The RNA pellet was air-dried for 10 minutes and then dissolved in DEPC treated water. Two micrograms of RNA were used for cDNA synthesis using the Superscript VILO cDNA synthesis kit.

2.5 qRT-PCR

All the qRT-PCR primers used in this study were listed in Table 1-2. qRT-PCR was performed using KAPA SYBR® FAST qPCR Kits. qRT-PCR samples were held at 95°C for 3 minutes then followed by 40 cylces of denaturation at 95°C for 5 seconds, annealing at 60°C for 20 seconds and extension at 72°C for 30 seconds. The mRNA

expression levels were normalised against the housekeeping gene and compared to the control samples.

2.6 Mammalian Cell Culture

Most of the cell lines were grown in Dulbecco's Modified Eagle Medium (DMEM), except the prostate cancer cell lines, were grown in RPMI 1640 medium. All media were supplemented with 10% Fetal Bovine Serum (FBS) and 1% penicillin/Streptomycin (P/S). Cells were incubated at 37°C with 5% CO_2 where the media were refreshed every two days. Mouse embryonic fibroblasts (MEFs) were grown in DMEM supplemented with heat-inactivated FBS, non-essential amino acids and 1% P/S.

2.6.1 Adipocyte Differentiation

MEFs were grown in DMEM containing 10% heat-inactivated FBS and 1% Penicillin/Streptomycin. Adipocyte differentiation was induced two days post confluence with insulin (10μg/mL), dexamethasone (1μM), isobutylmethylxanthine (IBMX) (0.5mM) and rosiglitazone (1μM). The medium was then changed every two days to DMEM/FBS/P/S supplemented with insulin (10μg/mL) and rosiglitazone (1μM) until the end of differentiation.

2.6.2 Fatty Acid Supplementation

Mammalian Cells were supplemented with oleate-coupled BSA to stimulate neutral lipid biosynthesis. To couple oleate to BSA, 20mM of sodium oleate was mixed with 5% BSA at a molar ratio of approximately 8:1. Oleate-coupled BSA was added to

culture medium at a ratio of 1.5mL of oleate-coupled BSA to 16mL of medium. The final concentration of oleate was 400μM. The mixture was then filtered through a 0.22μm filter. Cells were incubated with oleate for 14 hours.

2.6.3 Plasmid Transfection

Transient Plasmid Transfection was carried out using Lipofectamine LTX. Briefly, cell culture medium was changed to DMEM/FBS without antibiotics at least 6 hours prior to transfection. Lipofectamine LTX and plasmid DNA were diluted in OPTI-MEM in separate tubes then mixed and incubated for 5 minutes before adding to the cell culture. The amount of DNA and LTX used were depending on the size of the dishes used. The transfection medium was changed 6 hours after transfection to DMEM/FBS/P/S. Cells were harvested 24 hours after transfection.

Table 1-3. Plasmids used and primer sequences of designed constructs

Akt-HA (wild type)	Gift from Prof. David James, Garvan Institute
Myr-Akt-HA (wild type)	
Myr-Akt-HA* (constitutively active)	
Myc-WT-Akt	Gift from Prof. Andrew Brown, UNSW
Myc-DN-Akt	
Myc-CA-Akt	
NPC1-mCherry	Gift from Dr. Robin Du, UNSW
pMT3-PPARG	F - 5'-ATCGAGCGGCCGCGCTGTTATGGGTGAAACTC R 5'-ATCGACTCGAGCTAATACAAGTCCTTGTAGATCTC
pMT3-RXRA	F - 5'-ATCGAGCGGCCGCGCAGACATGGACACCAAAC R - 3'- ATCGACTCGAGCTAGGTGGCTTGATGTGGTG
mRFP-PASS (PA Sensor)	Gift from Dr. Guangwei Du, UTHSC

Seipin DR1 luciferase plasmid (500bp mouse)	F - 5'-CGATCGCTAGCCTCTGTGTGTGTCCAACACC R - 3'-ATCAGCTCGAGACATGCTTTGGAGACCAATC
Seipin DR1 luciferase plasmid (2.5kb human)	F- 5'- CGATCGCTAGCCATATTGAGAACGCCGGTTG R-3'- ATCAGCTCGAGACTTCCTGACGAGCCTCTGTTG

2.6.4 siRNA Transfection

Transient siRNA Transfection was carried out using Lipofectamine RNAiMAX. Like the plasmid transfection, medium was changed to DMEM/FBS without antibiotics at least 6 hours prior to transfection. The transfection mixture was prepared by diluting siRNA and RNAiMAX in OPTI-MEM in separate tubes. After 5 minutes incubation, the diluted siRNA and RNAiMAX were mixed and incubated for 20 minutes before adding to the cell culture. Depends on the purpose of the experiments, cells were harvested either 24 or 48 hours after transfection.

2.6.5 Insulin Treatment

Mammalian cells were grown to desired cell confluence and starved overnight in starvation medium, which contained 0.2% fatty acid free BSA and antibiotics. Cells were then incubated with insulin. The length of the treatment and the final concentration of insulin added were depending on the design of each experiment.

2.6.6 Drug Treatment

Mammalian cells were grown to desired cell confluence. Depends on the design of the experiment, starvation was not necessary for some experiments. If starvation was required it was carried out using 0.2% BSA starvation medium. MG132 (50μM), LY294002 (25μM), MK2206 (1μM), Rapamycin (0.1μM), PF-4708671 (0.16μM) and

Cycloheximide (35μM) were used in this study. The length of each treatment is stated in the result section.

2.7 Protein Analysis

2.7.1 SDS-PAGE and Western Blotting

All the buffers used are listed in Table 1-4.

Table 1-4. Buffers used for Western Blotting

Buffer	Recipe
Lysis Buffer	10mM Tris pH 7.4, 100mM NaCl, 1% SDS
SDS-PAGE Gel Running Buffer	3g Tris-base, 14.4g Glycine, 10% SDS in 1L of MilliQ water
Wet Transfer Buffer	3g Tris-base, 1.4g Glycine and 200mL methanol in 1L of MilliQ water
Ponceau Red C Stain	0.5g Ponceau C and 25 mL Acetic Acid in 1L water
Tris Buffered Saline-Tween 20 (TBS-T)	2.42g Tris-base pH7.6, 8.78g NaCl and 0.05% Tween 20.

Cell Lysis – Cells were washed twice with ice cold PBS before lysis. Lysis buffer containing with protease and phosphatase inhibitors was added. Cell lysate was scraped off from tissue culture dish and passed through a 22 gauge needle 15 times and vortexed at low speed for 10 minutes. Protein concentration was determined using BCA

assay kit. The amount of proteins in each samples were normalised to 5μg/μL for SDS-PAGE.

SDS-PAGE – Normalised protein lysates were mixed with 2 times protein loading buffer and heated at 70°C for 10 minutes on a heat block. Heated samples were then loaded onto SDS-PAGE gel. SDS-PAGE was run at 200 V for 30 minutes for commercial pre-cast gels or 160 V for 60 minutes for home made gels. After running, proteins from the gels were transferred to nitrocellulose membrane by wet transfer system at 100V for 60 minutes

Western Blotting – After wet transferred, membranes were stained with Ponceau Red C to confirm proteins were successfully transferred to nitrocellulose membranes. Once confirmed, the stain was rinsed off with TBS-T. The membranes were then blocked with 5% BSA in TBS-T for 60 minutes at room temperature. For most of the experiments performed in this study, membranes were incubated with primary antibody overnight at 4°C in 5% BSA/TBS-T. After primary antibody incubation, membranes were washed with TBS-T 3 times 5 minutes each. Membranes were then incubated with secondary antibody in 5% BSA/TBS-T for 60 minutes at room temperature, followed by 3 washes with TBS-T. Proteins were detected using the enhance chemiluminesscence (ECL) detection kit. Protein bands were visualised using the BioRad ChemiDoc XRS+ imager.

2.8 Lipid Analysis

2.8.1 Neutral Lipid Extraction

Mammalian cells were grown in 100mm dishes to 80 – 90% confluence. Cells were washed twice with ice cold PBS. Cells were trypsinised and cell counting was

performed to determine the number of cells in each sample. The amount of cells in each sample was normalised so each sample contained the same number of cells. 2mL of methanol was added to each sample and mixed thoroughly. 2mL of hexane was then added and the mixture was vortexed for 30 seconds and centrifuged at 1,000 ×g for 5 minutes. The top layer was transferred to glass vial and vacuum dried.

2.8.2 Phospholipid Extraction

The extraction protocol was based on the Folch's protocol with some modifications. All the organic solvents and water used were mass spectrometry grade. Mammalian cells were grown in 100mm dishes to 80 – 90% confluence. Cells were washed with ice cold PBS and cells were scraped off from dishes and cell number was determined. Same amount of cells from each sample was transferred to glass tubes and centrifuged at 3,000 ×g for 5 minutes. Supernatant was discarded and 20μM internal standard was added to each sample. Cell lysis was carried out by adding 1.2mL of $CHCl_3$/MeOH (1:1), 0.4mL $CHCl_3$ and 0.64mL 1% $HClO_4$. The mixture was vortexed for 1 minute then subjected to centrifugation at 4,500 ×g for 15 minutes at 4°C. The upper aqueous phase was discarded with glass tips and 0.8mL of 1% $HClO_4$ was added to each sample. Samples were mixed by vortexing and centrifuged again at 4,500 ×g for 10 minutes. The upper aqueous phase was discarded and this washing step was repeated 2 more times. After the last washing step, the bottom organic phase from each sample was transferred to glass vial with glass tips and they were vacuum dried.

2.8.3 Thin Layer Chromatography (TLC)

Silica Gel 60 F254 TLC plates were used to run the neutral lipid samples. Running Tank was equilibrated with hexane/diethyl ether/acetic acid (85:15:1), with cholesterol

ester and triacylglycerol as standard. Lipids were visualised by staining the TLC plates with iodine. Image of the plate was obtained by scanning it using EPSON PERFECTION 4490 PHOTO scanner.

2.9 Microscopy

2.9.1 Sample Fixation and Staining

Mammalian cells grown on coverslips were washed with PBS three times then fixed with 4% paraformaldehyde for 15 minutes at room temperature. Fixed cells were washed with PBS three times then incubated with 1mL of 1.5mg/mL glycine for 10 minutes at room temperature. Cells were washed three times with PBS.

Lipid droplet staining – Mammalian lipid droplets were stained with freshly prepared 2μg/mL BODIPY 493/503 in 150mM NaCl for 10 minutes. Stained cells were then washed with PBS three times 5 minutes each. Coverslips were then mounted onto slides using ProLong® Antifade Gold Reagent. Slides were sealed with nail polish.

Filipin Staining – Free cholesterol in mammalian cells were stained with 50μg/mL filipin in PBS for 60 minutes at room temperature. Cells were washed three times 5 minutes each with PBS and then mounted onto slides using ProLong® Antifade Gold reagent. Slides were sealed with nail polish.

2.9.2 Fluorescence Microscopy

Images were obtained using Leica TCS SP5 CW STED confocal laser scanning microscope equipped with multiple visible laser lines: Diode laser, Argon-ion laser, diode pumped solid state laser and Helium-Neon laser. Another microscope used was the Olympus Fluoview FV1000 confocal microscope that features 405, 476, 488, 512 543 and 633 excitation laser lines.

2.9.3 Immunofluorescence

Cells grown on coverslips were fixed and permeabilised with 0.1% saponin in PBS for 30 minutes at room temperature. Cells were then blocked with blocking buffer which contained 0.3% BSA and 0.05% saponin for 60 minutes at room temperature. Primary antibody was then diluted in blocking buffer and incubated with cells for 60 minutes at room temperature. Cells were then washed with 3% BSA/PBS three times 5 minutes each. Cells were then incubated with secondary Alexa Fluor antibody in blocking buffer for 60 minutes at room temperature, followed by three times washing with 3% BSA/PBS for 5 minutes each. The coverslips were then mounted onto slides with ProLong® Antifade Gold reagent. Fluorescence images were captured using either the Leica or Olympus confocal microscopes.

2.10 Luciferase Assay

Cells were grown as triplicate in 24-well plate and transfected with dedicated plasmids. After 24 hours of transfection, cells were washed with PBS twice. The assay was done using the Promega Dual-Luciferase® Reporter Assay System. Briefly, washed cells were lysed with the provided passive lysis buffer and incubated for 30 min on a orbital

shaker. 20µL of cell each cell lysate was pipetted into 96-well plate with clear bottom. The luciferase signal was measured with luminometer.

2.11 Electrophoretic mobility shift assay (Gel shift assay)

Table 1-5. Oligos designed for the gel shift assay

Forward-DR1 oligo	CACTGAACTTAAGAACCCATG
Reverse-DR1 oligo	CATGGGTTCTTAAGTTCAGTG
Mutant Forward-DR1 oligo	CACACAAGATAAGAACCCATG
Mutant Reverse-DR1 oligo	CATGGGTTCTTATCTTGTGTG

2.11.1 Preparation of Nuclear Extract

Cells transfected with dedicated plasmids were washed with ice cold PBS and cells were scraped in 5mL PBS/plate. Cells were pellet at 800g for 5 min at 4°C. The pellet was then resuspended in 10X pellet volume of BufferA (10mM HEPESpH 7.9, 10mM KCl, 1.5mM $MgCl_2$, 50µL 1M DTT and 1X protease inhibitor tablet) and incubated for 15 min at 4°C. The mixture was then vortexed thoroughly for 25 min and lysis was checked under microscope with trypan blue. The mixture was pelleted at 10,000g for 2 min at 4°C. The pellet was then resuspended in 2X pellet volume of BufferC (20mM HEPES pH 7.9, 25% glycerol, 420mM NaCl, 1.5mM $MgCl_2$, 0.2mM EDTA, 50µL 1M DTT and 1X protease inhibitor tablet) and incubated on ice for 30 min with flick mixing every 10 min. The mixture was then spun at 21,000g for 5 min at 4°C and supernatant was retained and flash freeze in liquid nitrogen and transferred to -80°C or use straight away.

2.11.2 Preparation of Radiolabelled Probe

1µL of 100ng/µL of the forward-DR1 or mutant forward-DR1 were mixed with 3µL of water and polynucleotide kinase buffer. 4µL of [γ-^{32}P]-ATP (40µCi) and 1µL of T_4 polynucleotide kinase were added and mixed y pipetting. The mixtures were incubated at 37°C in heat block with a beaker covering the tube for 30 min. During the incubation time, 3.7µL of 100ng/µL reverse-DR1 or mutant reverse-DR1 were mixed with 4µL of 10X TNE (100mM Tris-HCl pH8.0, 500mM NaCl and 10mM EDTA pH8.0) and 32.3µL of milliQ water. After 30 min of incubation, the reverse-DR1 oligos were combined with the forwards and boil at 100°C in a heat block for 1 min and the heat block was then switched off. The oligos were left in the heat block overnight to allow the annealing of the oligos with gradual cooling.

2.11.3 Purification of Radiolabelled Probe

The annealed oligos were transferred to washed purification tubes and spun in 15mL falcon tube for 2 min. The purification column was discarded and flow-through was retained. The purified probes were stored at -20°C.

2.11.4 Gel Shift

The non-denaturing gel was prepared with 7.5mL of 40% acrylamide, 2.5mL 10X TBE, 39mL milliQ water, 0.2mL 25% APS and 50µL TEMED. The sample buffer contained 1.5µL of 1mg/mL dIdC, 1.5µL of 10mM DTT, 1µL of 1mg/mL BSA, 3µL 10X gel shift buffer (100mM HEPES pH7.8, 500mM KCl, 500mM $MgCl_2$, 10mM EDTA, 50% glycerol), 17µL milliQ water and the radiolabelled probe. For the preparation of different samples, 1µL of antibody or water as control was added to 3µL of nuclear extract. The mixture was incubated for 5 min and then added to the sample buffer.

Marker dye was prepared as follow: 5µL of 0.05% bromophenol blue (55bp dsDNA), 5µL of 0.05% Xylene-cyanol FF (250bp dsDNA) and 10µL formamide. Each sample was loaded onto the gel and run for 2 hours at 250V. After running, the gel were tried using flat-bed dryer for 30 min. The dired gel was then assembled into imaging cassette with freshly blanked phosphor screen. The film was incubated for 24 hours. The image was then read using phosphor imager.

2.12 ChIP qRT-PCR

2.12.1 Cell Preparation

12 150mm plates of MEFs were grown in high glucose DMED with desired supplements. 3.5mL of 10% Fixing buffer (70mM HEPES-KOH pH 7.5, 140mM NaCl, 1.4mM EDTA, 0.7mM EGTA and 1.5mL formaldehyde) was added to each plate and incubated at room temperature for 10 min. 2.2mL of 2M glycin was added to quench formaldehyde and incubated for 10 min at room temperature. The cells were then washed with 10mL ice cold PBS and cells were scraped from plates in 5mL ice cold PBS. Collected cells were passed through an 18G needle to break up cells and then transferred in siliconised falcon tubes. Cells were spun at 3200g for 15 min at 4°C and 1mL of supernatant was transferred to eppendorf tube and spun at 8000g for 1 min to remove excess supernatant. The pellet was then frozed at -80°C.

2.12.2 Immunoprecipitation

Dynabeads were blocked in 0.25mL of PBS + 0.5% (w/v) BSA (100uL beads per $7X10^7$ cells). 14µL of antibody was added per 100µL beads and incubated at 4°C for more than

4 hours. The conjugated beads were washed with 1mL block solution twice and resuspended in 10µL of block solution. Cell pellets were resuspended in 10mL LB1 (50mM HEPES-KOH pH 7.5, 140mM NaCl, 1mM EDTA, 10% glycerol, 0.5% Igepal CA630, 0.25% Triton X-100 and protease inhibitor tablet) and incubated for 10 min at 4°C on roller. The mixture was then spun at 2000g for 5 min at 4°C and supernatant was discarded. The cell pellet was resuspended in 3mL LB3 (10mM Tris-Cl pH 8.0, 100mM NaCl, 1mM EDTA, 0.5mM EGTA, 0.1% NaDOC, 0.5% N-laurylsarcosine and protease inhibitor tablet) and split into 6 500µL aliquots in polystyrene falcon tubes and sonicated using the bioruptor on high setting (30 seconds on, 30 seconds off and total sonication time 10 min). The sonicates were collected by centrifugation at 800g for 30 seconds and were combined in 3 Eppendorf tubes (1mL each). Debris was removed by centrifugation at 20,000g for 5 min at 4°C and the supernatant was combined in 15mL falcon tubes. 300µL of 10% Triton X-100 was then added. 200µL of sonicate was removed and retained as an input sample. 100µL of blocked dynabeads was added to each sample and incubated overnight at 4°C with gentle rocking. The samples were then place on magnet for more than 1 min and supernatant was removed. Beads were then resuspended in1mL RIPA buffer (50mM HEPES-KOH pH 7.5, 500mM LiCl, 1mM EDTA, 1% Igepal CA630 and 0.7% NaDOC) and transferred to a 1.5mL Eppendorf tube. The eppendorf tube was then placed on magnet to remove supernatant. The beads were washed with 1mL RIPA buffer 6 times and the beads were finally washed with TBS buffer (20mM Tris-Cl pH 7.6 and 150mM NaCl) in screw-cap tubes. Finally, 200µL of elution buffer (50mM Tris-Cl pH 8.0, 10mM EDTA and 1% SDS) was added to each sample and reverse crosslinking was done by incubating at 65°C overnight in screw-cap tubes in hybridisation oven.

2.12.3 ChIP qRT-PCR

After crosslinking, 200µL of TE buffer with 4µL of 20mg/mL proteinase K and 8µL of 1mg/mL RNase A were added to each sample and incubated for 1 hour at 55°C. The DNA was then purified with standard phenol/chloroform extraction and ethanol precipitation protocols. qRT-PCR was run using the purified DNA as template.

2.13 Statistical Analysis

All the data obtained in this thesis was analysed in GraphPad Prism 6. The sample errors were measured using the standard error mean (SEM). Statistical significance was obtained either by one-way ANOVA or two-way ANOVA.

3. Chapter 3: Involvement of the PI3K/Akt/mTORC1 Pathway in NPC1 Degradation

3.1 Background

Cholesterol is an essential lipid that can be obtained through dietary absorption and endogenous biosynthesis. It plays a number of important roles in membrane synthesis and assists in the formation of membrane microdomains called lipid rafts for membrane trafficking and signalling. Furthermore, it serves as precursor for the biosynthesis of steroid hormones, bile acids and vitamin D in specialised tissues and cells. Therefore, any malfunction of cholesterol homeostasis will affect many physiological processes.

Niemann-Pick type C (NPC) proteins, NPC1 and NPC2, facilitate the trafficking of low-density lipoprotein (LDL)-derived cholesterol from late endosomes/lysosomes (LE/LY) to other organelles, such as the endoplasmic reticulum (ER) and plasma membrane. The mutation of either one of the NPC proteins will lead to the rare autosomal recessive lipid storage disease called Niemann-Pick type C disease, which causes accumulation of unesterified cholesterol and other lipids, such as sphingolipids, in the LE/LY[132, 133]. Progressive neurodegeneration, lung dysfunction and hepatosplenomegaly are the major causes of premature death in NPC patients[134, 135]. Approximately 95 % of NPC disease is caused by the mutations in the *NPC1* gene, and the rest are due to the mutation of the *NPC2* gene[136]. Because LDL-derived cholesterol cannot be transported to other organelles such as the ER in NPC deficient cell, the cell senses low level of cholesterol. This will increase the expression of genes responsible for cholesterol synthesis and uptake through the activation of the lipogenic transcription factor sterol regulatory element-binding protein (SREBP) despite the

accumulation of cholesterol in the LE/LY. It has been proposed that NPC1 and NPC2 work in tandem to export LDL-derived cholesterol from the LE/LY in a "hand off" model, where cholesterol is passed from NPC2 to NPC1 and then exported out from LE/LY[137, 138].

There are over 200 disease-causing mutations have been identified in the *NPC1* gene so far. The most prevalent I1061T mutation of the *NPC1* gene inhibits the correct folding of the protein and targets it for endoplasmic reticulum-associated degradation (ERAD). Chemical chaperon treatment helps the folding of the mutant protein and prevents the degradation of the mutant NPC1 [139]. I1061T mutation may not be the only mutation that leads to the low stability of the protein. Other mutations may also target NPC1 for abnormal degradation. However, how NPC1 is targeted for degradation is still not clear and it is necessary to understand how this process is regulated.

3.2 Human Papillomavirus positive cervical cancer cell accumulates huge amount of unesterified cholesterol

This study was first initiated by the discovery of huge amount of unesterified/free cholesterol accumulated in a cervical cancer cell line called C33A using filipin staining (Figure 3.1). There are two types of cervical cancer cells, the Human Papillomavirus (HPV) negative and HPV positive. Although certain amount of free cholesterol was detected with filipin staining in HPV positive cervical cancer cell SiHa, the amount of free cholesterol detected in HPV negative C33A cells was enormous.

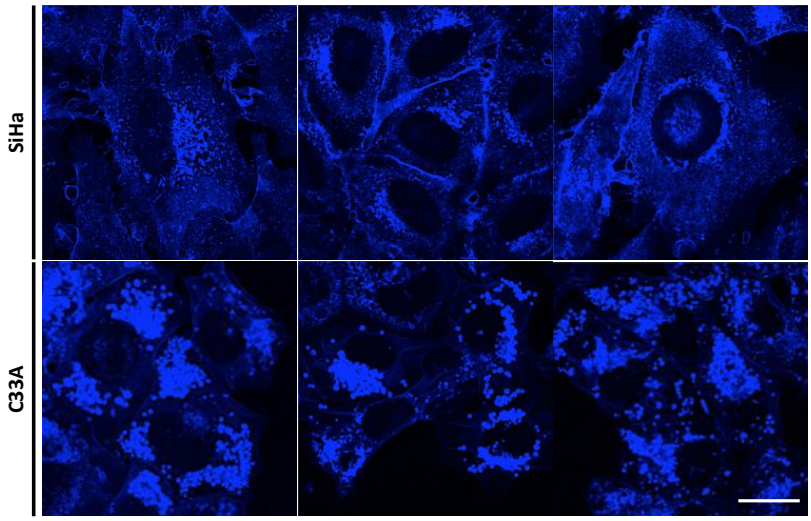

Figure 3.1 Filipin fluorescent staining of free cholesterol in SiHa and C33A cells. Free cholesterol in both SiHa and C33A cells was stained with filipin. Huge amount of free cholesterol was observed accumulating in HPV negative C33A cells. HPV positive SiHa cells were observed with less free cholesterol accumulation. Bar = 10μm.

In normal cells, high level of free cholesterol is toxic and cells tend to package them as cholesterol esters in lipid droplets by Acyl-CoA:cholesterol acyltransferase (ACAT). Figure 3.2 shows that there were less numbers of lipid droplets in the C33A cells and their sizes were bigger compared to the SiHa cells. In contrast, SiHa cells had evenly distributed smaller sized lipid droplets. The neutral lipids in both C33A and SiHa cells were then extracted and subjected to thin layer chromatography. Figure 3.3 shows there were more cholesterol esters accumulated in the C33A cells. The huge amount of cholesterol esters found in the C33A cells is likely a protective mechanism that the cell employed to lower the toxicity of high level of free cholesterol accumulation. In contrast, SiHa cells had much less cholesterol esters. Densitometry of the band intensities of the cholesterol esters of both SiHa and C33A cells showed there was over 200% increase of cholesterol esters in the C33A cells (Figure 3.3). Similarly, another neutral lipid triacylglycerol was also increased by about 50% in band intensity.

Interestingly, there were some extra neutral lipid bands observed on the C33A TLC plate. However, the identities of those bands were unknown given no proper standards available.

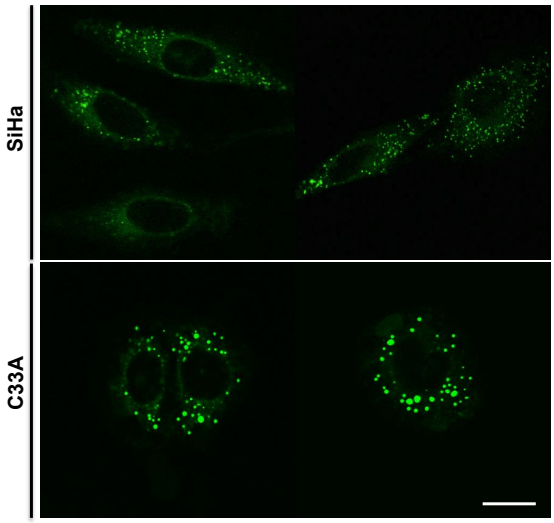

Figure 3.2 Lipid droplets of SiHa and C33A cells. SiHa and C33A cells were stained with BODIPY 493/503 and C33A cells were observed with larger size lipid droplets comparing to evenly distributed smaller lipid droplets in SiHa cells. Bar = 20μm.

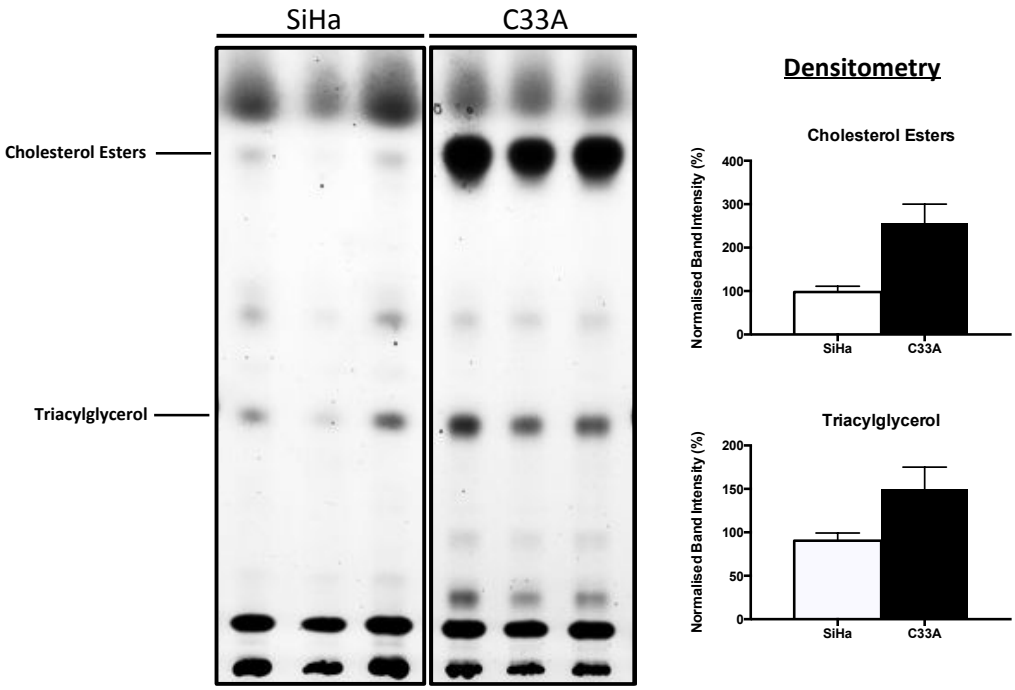

Figure 3.3 Thin layer chromatography of neutral lipids from C33A and SiHa cells. C33A cells had more than 200% increased of cholesterol esters and approximately 50% increased of triacylglycerol accumulated comparing to SiHa cells.

By measuring the cholesterol contents of the cell lysates of C33A and SiHa cells, it was confirmed that there were significantly more free cholesterol accumulated in the C33A cells (Figure 3.4). However, the total cholesterol content was quite similar between the two cell lines.

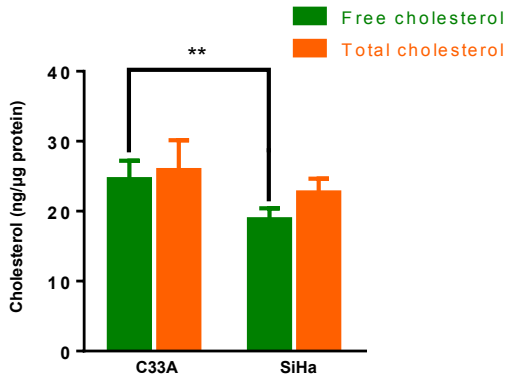

Figure 3.4 Free cholesterol and total cholesterol level in C33A and SiHa cells. There were significantly more free cholesterol accumulated in the C33A cells comparing to the SiHa cells. However, the amount of total cholesterol was similar in both cells. n = 3, **p < 0.001.

3.3 The high level of free cholesterol observed in C33A cells was accumulated in the late endosomal/lysosomal compartment

Enormous amount of free cholesterol was observed accumulating in C33A cells. The next step was to find out where the free cholesterol accumulates. After LDL enters cells via the receptor-mediated endocytosis, free cholesterol was then released from cholesterol esters of endocytosed LDLs by lysosomal acid lipase. The released free cholesterol might be accumulated in the lysosomal compartment at which the cholesterol esters are hydrolysed to free cholesterol. With the aid of the late endosomal/lysosomal marker Lysosome-associated membrane protein 1 (Lamp1), the free cholesterol accumulated in the C33A cell was most likely localised in the late endosomes/lysosomes. Figure 3.5 shows the immunofluorescence signal of Lamp1 and

filipin fluorescence staining of free cholesterol in C33A and SiHa cells. HeLa cell is another HPV positive cervical cancer cell line. Similar to SiHa cell, HeLa cell had much less free cholesterol accumulation. Lysosomes revealed by the Lamp1 signal were enlarged in the C33A cells whereas in the other two cell lines, lysosomes were represented as small and evenly distributed punctate structures in the other two cell lines.

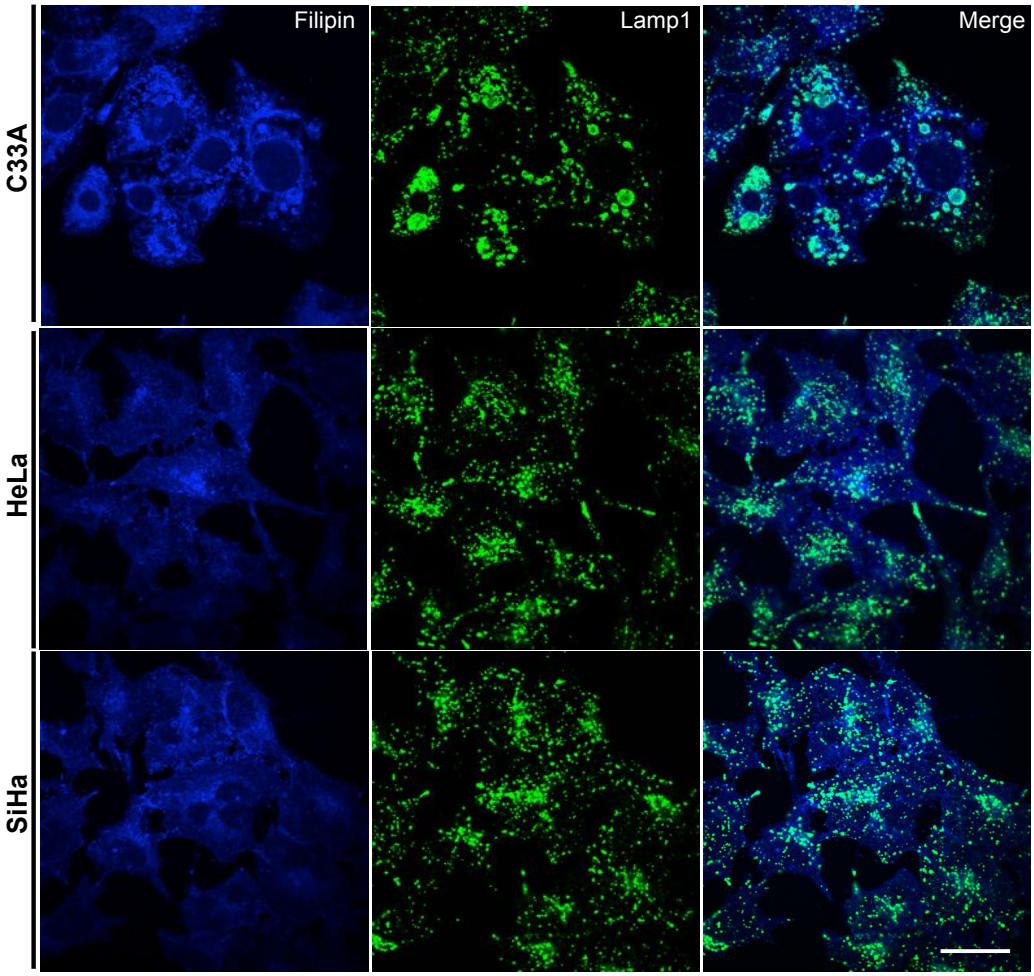

Figure 3.5 Co-localisation study of filipin stained free cholesterol and immunofluorescence of Lysosomal-associated membrane protein 1 (Lamp1) in cervical cancer cells. HPV negative C33A cells had larger amount of free cholesterol accumulated in the lysosomal compartment, whereas the HPV positive HeLa and SiHa cells accumulated much less free cholesterol. The lysosomal compartments of the C33A cells were enlarged comparing to more evenly distributed punctate structures in both HeLa and SiHa cells. Bar = 10μm.

3.4 Accumulation of free cholesterol in C33A cells is due to NPC1 deficiency

The free cholesterol accumulation phenotype of C33A cells was similar to cells with deficient NPC1 protein. In order to check if NPC1 was present in the C33A cells, Western blot was done to examine the NPC1 protein level. Figure 3.6A shows that NPC1 protein level in C33A cells was greatly reduced. This may explain why there were enormous amount of free cholesterol accumulated in the C33A cells. NPC1 is responsible for the export of LDL-derived free cholesterol from the late endosome/lysosome compartment to other organelles. The deficiency of NPC1 would lead to the accumulation of free cholesterol in the LE/LY as observed in the C33A cells. The reduced level of NPC1 in the C33A cells might be due to two possibilities, decreased gene expression or abnormal protein degradation.

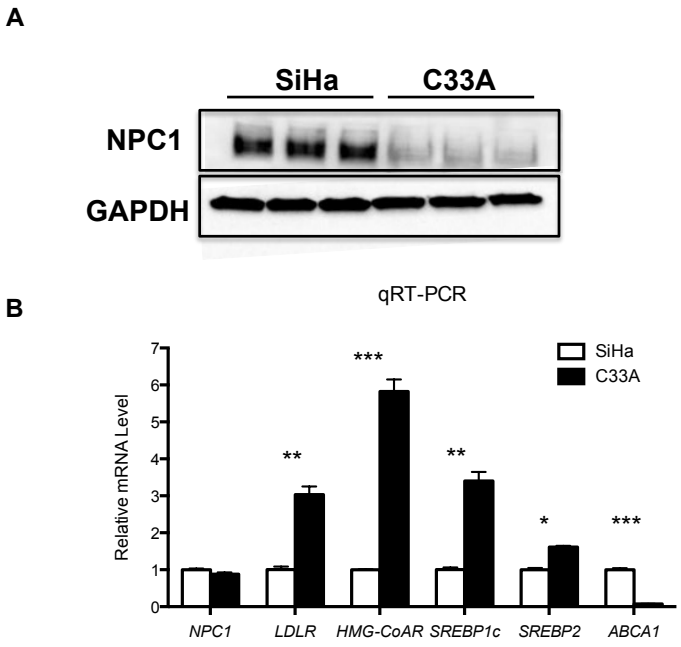

Figure 3.6 Western blot and qRT-PCR of SiHa and C33A cells. Western blot shows that NPC1 was almost abolished in the C33A cells but the mRNA level of NPC1 was similar to the SiHa cells. A. Western blot of NPC1 and GAPDH in SiHa and C33A cells. B. mRNA level of *NPC1, LDL Receptor* (*LDLR*), *3-hydroxy-3-methyl-glutaryl-CoA reductase* (*HMG-COAR*), *sterol regulatory element-binding protein 1c* (*SREBP1c*), *sterol regulatory element-binding protein* (*SREBP2*) and *ATP-Binding Cassette, Sub-Family A1* (*ABCA1*) in SiHa and C33A was measured by qRT-PCR. n = 3, * $p < 0.01$ ** $p < 0.001$ *** $p < 0.0001$.

To check the mRNA level of the *NPC1* gene, total RNA was extracted from both SiHa and C33A cells, and quantitative RT-PCR (qRT-PCR) was performed. Figure 3.6B shows that the mRNA level of *NPC1* in both cancer cells were comparable and there was no significant changed of the *NPC1* transcription level. NPC1 deficiency causes accumulation of free cholesterol in the LE/LY and inhibits the export of cholesterol to other organelles like the ER. Low cholesterol level activates the sterol regulatory element-binding protein (SREBP) pathway. This subsequently up-regulates the expression of low-density lipoprotein receptor (*LDLR*) for LDL uptake and 3-hydroxy-3-methyl-glutaryl-CoA redutase (*HMG-CoAR*) for endogenous cholesterol biosynthesis. Figure 3.6B shows that the expression of *LDLR, HMG-CoAR, SREBP1c* and *SREBP2* were highly upregulated in the C33A cell. The ATP-Binding Cassette, Sub-Family A1 (*ABCA1*), which responsible for cholesterol efflux was significantly down regulated. The increase of cholesterol uptake and synthesis and decrease of cholesterol efflux worsens the accumulation of free cholesterol in the C33A cells.

3.5 NPC1 is targeted for proteasome degradation

Quantitative RT-PCR showed the transcription of *NPC1* was comparable to the SiHa cell, this pointed to another possibility of increased NPC1 degradation in the C33A cell. In mammalian cells, there are two major pathways for protein degradation, the ubiquitin-proteasome degradation pathway and the lysosomal proteolysis pathway. The first experiment was to treat the cancer cells with proteasome inhibitor MG132, because it has been shown that NPC1 could be degraded via the ubiquitin proteasome degradation pathway[139]. Figure 3.7B shows that the treatment of C33A cells with MG132 dramatically rescued the NPC1 protein from degradation. The treatment was

also been able to stablise NPC1 from proteasome degradation in SiHa cells. Filipin staining of C33A cells treated with MG132 showed reduced free cholesterol accumulation (Figure 3.7C). However, it did not fully rescue the cholesterol accumulation phenotype. Degradation of NPC1 might be due to misfolding of the protein. To test this, chemical chaperon, glycerol was added to the growth medium (Figure 3.7A). NPC1 was partially rescued after the treatment, but it is not comparable to the extent of the MG132 treatment.

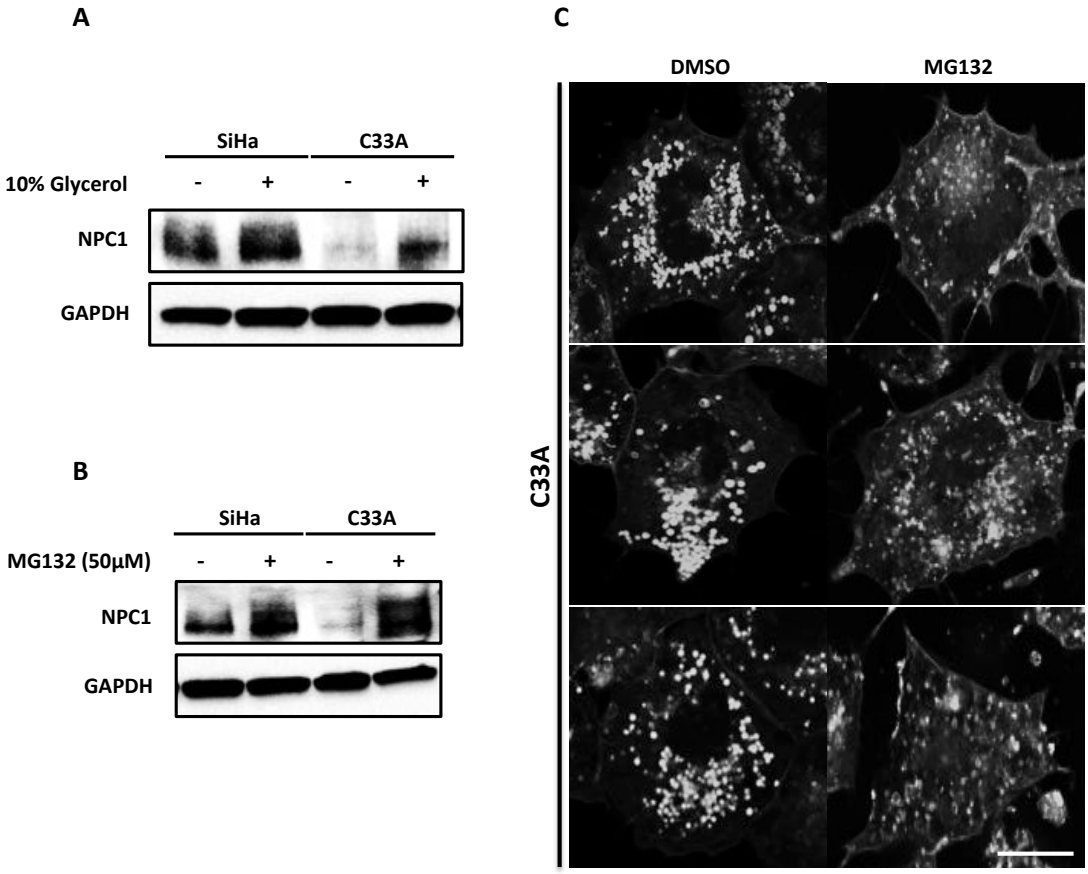

Figure 3.7 Chemical chaperon and MG132 treatment rescued NPC1 from degradation. The absence of NPC1 in C33A cells may be due to the continuous degradation of the protein via the ubiquitin proteasome degradation pathway. A. SiHa and C33A cells were treated for 24 hours in 10% glycerol, which act as chemical chaperon, cell lysates were subjected to Western blot for NPC1 analysis. B. SiHa and C33A cells were treated with proteasome inhibitor MG132 for 24 hours, the NPC1 level was dramatically rescued by the MG132 treatment. There was also NPC1 rescuing effect observed in the SiHa cells after the treatment. C. C33A cells treated with DMSO and MG132 were fixed and stained with filipin to check the accumulation of free cholesterol. Although the treatment of MG132 did not fully rescue the cholesterol accumulation phenotype, the amount of free cholesterol accumulated were decreased in the MG132 treated C33A cells. Bar = 10μm.

3.6 NPC1 deficiency correlates with high level of phospho-Akt

Akt is a serine/threonine kinase that phosphorylates proteins; it is involved in metabolism, apoptosis and proliferation. High P-Akt level in cancer cells promote proliferation and increase cell survival. Figure 3.8 shows that Akt phosphorylated at serine residue 473 was highly enriched in the C33A cell. Figure 3.9 shows the negative correlation between NPC1 protein level and P-Akt level. SiHa and HeLa cells had relatively low P-Akt level and the NPC1 protein level was normal. However, the P-Akt level was high in the C33A cells and the NPC1 protein level decreased by about 50% according to the densitometry study shown in Figure 3.9. The same trend was also observed in prostate cancer cell lines, PC3 and LNCaP. Figure 3.10A shows high P-Akt level detected in the LNCaP cell was correlated with lower NPC1 protein level. Similar to the C33A cell, LNCaP cell also displayed the NPC1 phenotype, which had higher free cholesterol accumulation (Figure 3.10B). These data suggested that there might be a link between Akt signalling and NPC1 turnover. To find out if Akt is involved in the degradation of NPC1, several experiments were designed to test this hypothesis.

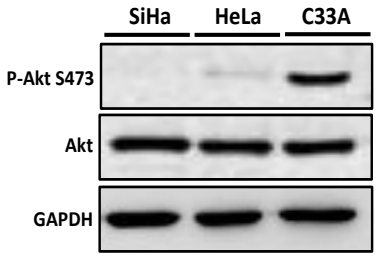

Figure 3.8 Phospho-Akt level in cervical cancer cells. Cell lysates of SiHa, HeLa and C33A cells were subjected to Western for P-Akt S473 analysis.

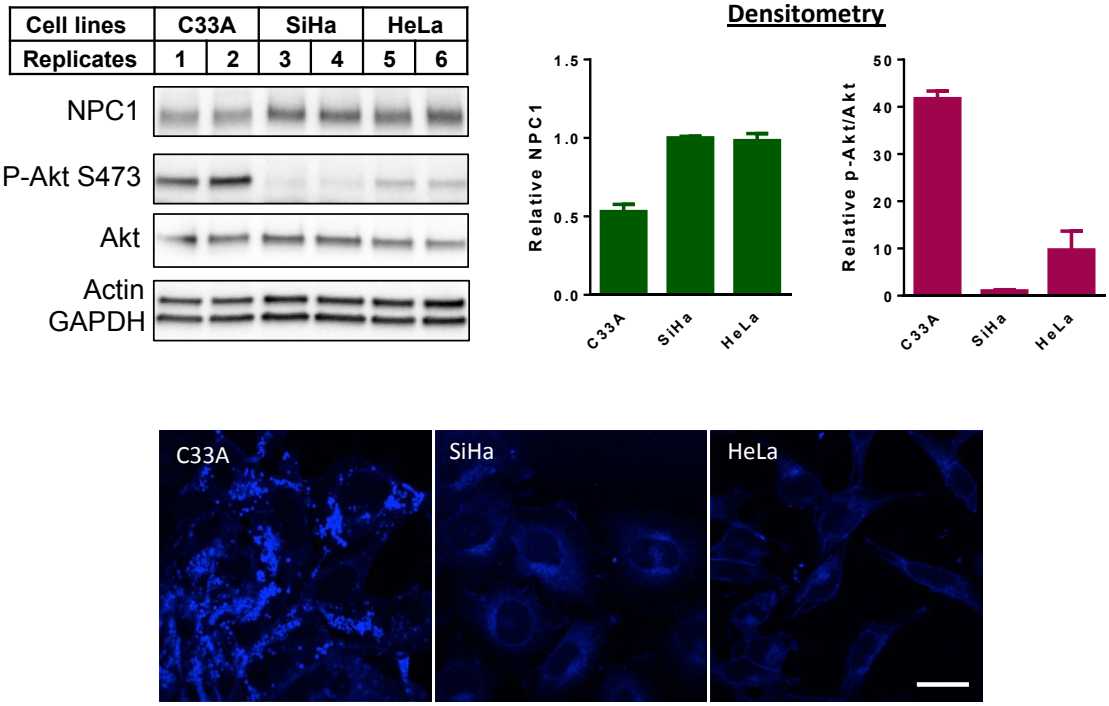

Figure 3.10 High Phospho-Akt level cells may correlate with low NPC1 level in C33A cells. Western blot clearly shows that the NPC1 level of C33A cells was about 50% lower than the SiHa and HeLa cells. The high level of P-Akt negatively correlates with the NPC1 level in the C33A cells. The filipin staining confirmed the NPC1 cholesterol accumulation phenotype. Bar =20µm.

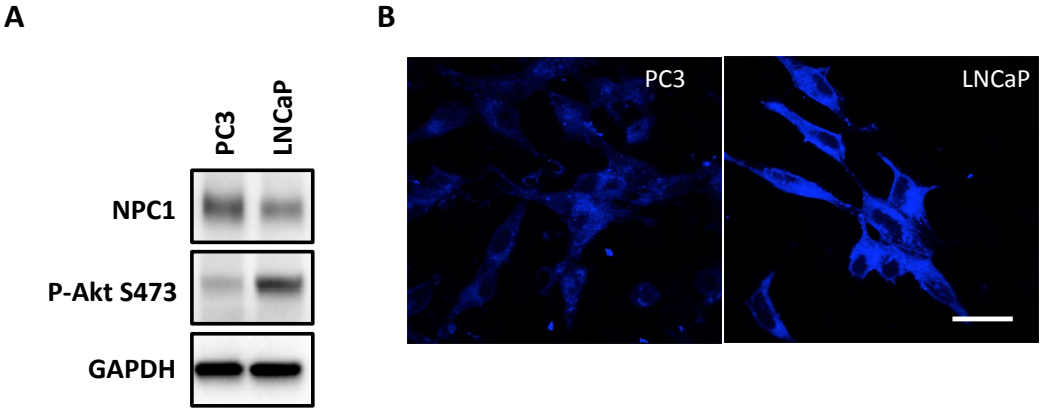

Figure 3.9 NPC1 protein level in prostate cancer cells. A. Western blot shows the NPC1 level in LNCaP was lower than the PC3 cells and this correlates with much higher P-Akt S473 level in the former cells. B. Filipin staining shows the LNCaP cells had high level of free cholesterol accumulated. Bar = 20µm.

3.7 Wortmannin treatment rescued NPC1 from degradation

Akt is phosphorylated via the PI3K pathway upon the activation of the receptor tyrosine kinase, e.g. the activation of PI3K through the binding of insulin to the insulin receptor. Inhibition of the PI3K pathway in C33A cells should decrease Akt phosphorylation and if NPC1 is targeted for degradation when phospho-Akt (P-Akt) level is high, NPC1 should be rescued. Wortmannin directly inhibits PI3 kinase and PI3 kinase, which is an upstream effector of Akt phosphorylation. As expected, wortmannin treatment lowered Akt phosphorylation in C33A cells but drastically increased NPC1 expression (Figure 3.11A). SiHa cells had no detectable P-Akt and there was no obvious increase of NPC1 observed. Filipin staining in Figure 3.11B shows there was less free cholesterol accumulated in the C33A cells after wortmannin treatment. These data indicated that the PI3K/Akt pathway may be involved in the degradation of NPC1.

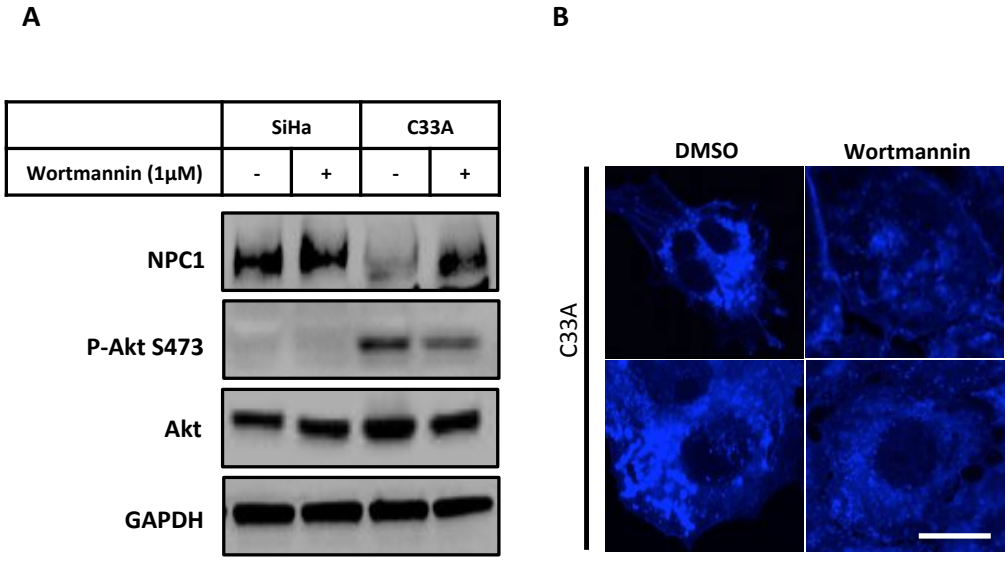

Figure 3.11 Inhibition of the phosphoinositide 3-kinase (PI3K) pathway rescued NPC1 protein in C33A cells. A. PI3K inhibitor wortmannin was used to inhibit the phosphorylation of Akt in both SiHa and C33A cells. The treatment of SiHa cells with wortmannin did not have much effect to the phospho-Akt level and there was not change to the NPC1 protein level. The treatment of C33A cells with wortmannin greatly rescued the NPC1 protein level. B. Filipin staining shows there were less free cholesterol accumulated after wortmannin treatment.

3.8 Specific Akt inhibitor abolished Akt phosphorylation and rescued NPC1

Next, direct inhibition of Akt phosphorylation by a specific inhibitor MK2206 was tested. MK2206 specifically inhibit Akt phosphorylation, if Akt is involved in the degradation of NPC1, a more effective rescuing effect should be observed. Figure 3.12 clearly shows that MK2206 completely abolished Akt phosphorylation at serine 473 and there was more NPC1 observed than the treatment with LY294002, which was also a PI3 kinase inhibitor. This further confirmed Akt is involved in the degradation of NPC1.

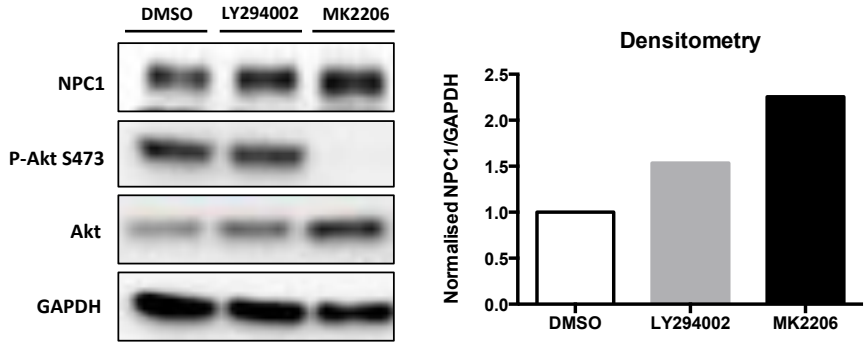

Figure 3.12 Inhibition of Akt phosphorylation by specific Akt inhibitor MK2206 stablised NPC1 from degradation. C33A cells were treated with PI3K inhibitor LY294002 and Akt inhibitor MK2206 overnight and cell lysates were subjected to Western blot for NPC1 analysis.

3.9 Insulin treatment stimulated the degradation of NPC1

As observed in cervical and prostate cancer cells the increased P-Akt level has lead to the degradation of NPC1. As shown in Figure 3.11 and 3.12, the inhibition of the PI3K pathway or direct inhibition of Akt phosphorylation rescued NPC1 from degradation. If the degradation of NPC1 is regulated by P-Akt, the stimulation of Akt phosphorylation by activating the PI3K pathway upon insulin treatment would also lead to the degradation of NPC1. Insulin sensitive HEK293E cells were used to conduct this

experiment due to its high insulin sensitivity. Before insulin stimulation, cells were starved overnight to make sure the insulin pathway was not activated and NPC1 was at a stable state. After 2 hours of insulin stimulation, the level of NPC1 decreased to 80% of the level observed at time 0 (Figure 3.13). The level of NPC1 decreased to 50% of the original level after 8 hours of insulin treatment. In contrast, when Akt inhibitor MK2206 was added together with insulin, Akt phosphorylation was inhibited and the NPC1 level was increasing over the period of the treatment. This clearly shows that P-Akt can accelerate NPC1 degradation.

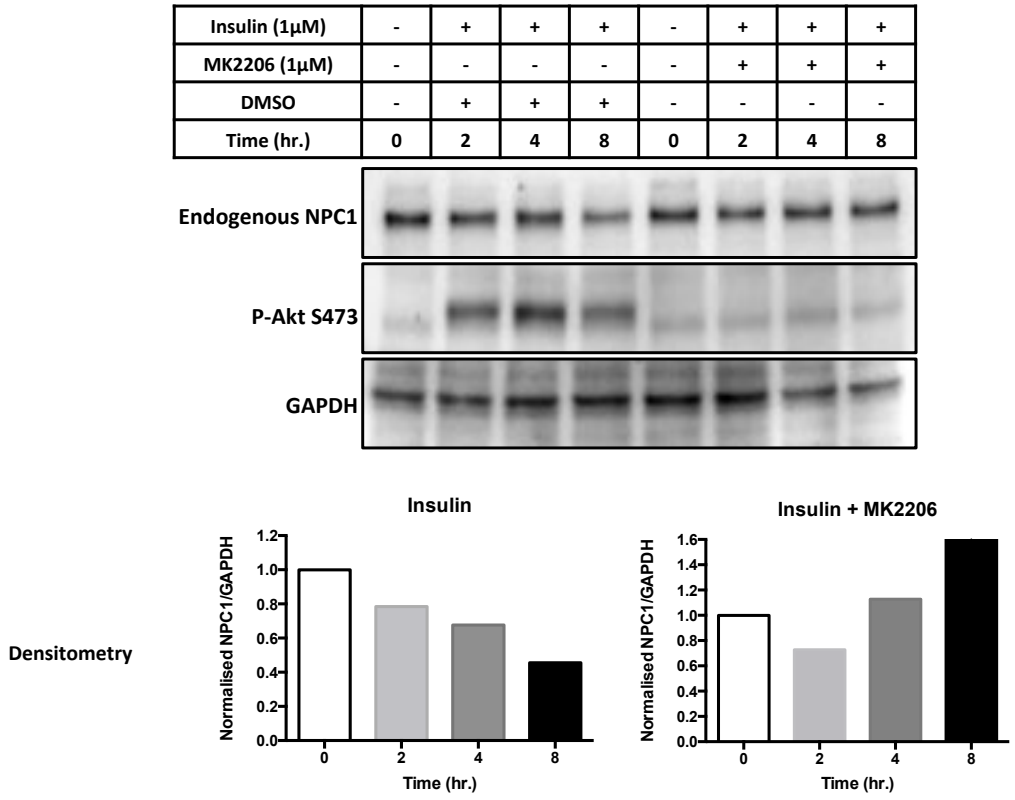

Figure 3.13 Insulin treatment of HEK293E cells stimulates Akt phosphorylation and leads to the degradation of NPC1. HEK293E cells were starved overnight in starvation medium. Akt phosphorylation was stimulated at time 0 with insulin and cells were harvest at 0, 2, 4 and 8 hours after the addition of insulin. MK2206 was added together with insulin one set of cells. Inhibition of Akt phosphorylation by MK2206 did not lead to the degradation of NPC1. However, NPC1 level was gradually decreased over the treatment. Densitometry shows that cells treated with insulin alone has lead to 50% loss of NPC1 after 8 hours of treatment. On the other hand, the NPC1 level was increased in the insulin and MK2206 treated cells.

3.10 Overexpression of constitutively active Akt promoted NPC1 degradation

Constitutively active Akt construct was transfected into SiHa cell that had low level of P-Akt and high level of NPC1. Overexpression of constitutively active Akt should promote NPC1 degradation and less NPC1 protein should be seen on the Western blot. The constitutively active Akt used was tagged with a myristolation signal sequence, which target the tagged protein to the plasma membrane for activation. To make the Akt constitutively active, the Pleckstrin Homology (PH) domain was deleted. As the control, wild type Akt with and without the myristolation signal sequence were also transfected into SiHa cells (Figure 3.14C). After 24 hours of transfection, both Akt and Myr-Akt transfected cells had low level of P-Akt S473. The constitutively active Myr-Akt* transfected cells had high level of P-Akt S473 and the NPC1 protein was dramatically decreased (Figure 3.14A). Filipin staining also showed a higher level of free cholesterol accumulated in the cell (Figure 3.14B).

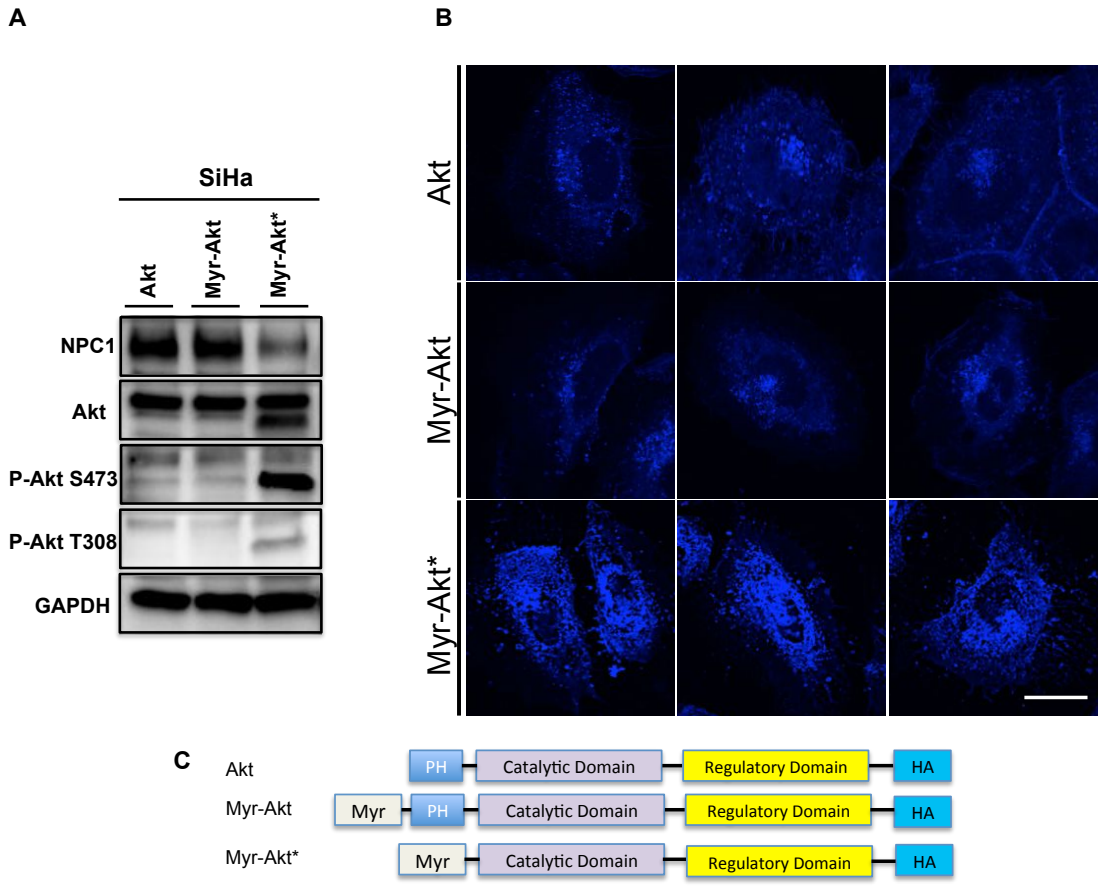

Figure 3.14 Overexpression of constitutively active Akt in SiHa cells accelerates NPC1 degradation and free cholesterol accumulation. A. Overexpression of constitutively active Myr-Akt* in SiHa cell promoted Akt phosphorylation at serine 473 and lead to the degradation of the NPC1 protein. The Pleckstrin Homology (PH) domain of the constitutively active Myr-Akt* was deleted, two bands could be seen on the total Akt blot. The lower band was corresponded to the Myr-Akt*. B. Filipin staining of constitutively active Akt transfected SiHa cell showed higher level of free cholesterol was accumulated. C. Three Akt constructs were overexpressed in SiHa. Wild type Akt (Akt), wild type Akt with the myristoylation sequence (Myr-Akt) and the constitutively active Akt mutant, which has the PH domain and the regulatory domain deleted (Myr-Akt*). Bar = 10μm.

3.11 Overexpression of dominant negative Akt in C33A cells rescued NPC1 from degradation

As shown above in Figure 3.14, the overexpression of constitutively active Akt construct in SiHa cells accelerated the degradation of NPC1. It was expected that the transfection of a dominant negative Akt construct in C33A cells should have an opposite effect. Figure 3.15 clearly shows that the transfection of a dominant negative form of Akt in C33A cells protected NPC1 from degradation. Although the level of P-Akt was not completely abolished, the rescuing effect was obvious. However, the transfection of the constitutively active Akt did not further enhance the degradation of NPC1. This could be due to the already high level of P-Akt in the C33A cell and this high level of P-Akt has already reached the limit of triggering NPC1 degradation.

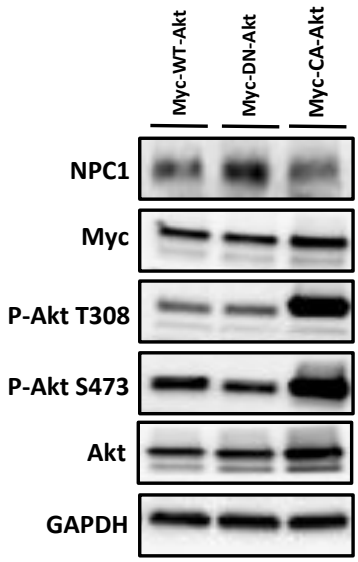

Figure 3.15 Overexpression of dominant negative form of Akt rescued NPC1 protein from degradation in C33A cell. Three overexpression Akt constructs, wild type (Myc- WT-Akt), dominant negative (Myc-DN-Akt) and constitutively active (Myc-CA-Akt), were transfected into C33A cells for 24 hours. Cell lysates were subjected to Western blot for NPC1 analysis. Dominant negative Akt reduced the level of P-Akt S473 and protected NPC1 from degradation.

3.12 Overexpression of constitutively active Akt in HEK293E cell also accelerated NPC1 degradation

Figure 3.13 shows the stimulation of Akt phosphorylation upon insulin treatment lead to the degradation of NPC1. Figure 3.15 shows the overexpression of constitutively active Akt in the SiHa cell increased NPC1 degradation. Also, Figure 3.15 shows the overexpression of dominant negative Akt could rescue NPC1 from degradation. To further confirm that the observation made in the human cervical cancer cells was not limited in just one cell type, constitutively active Akt was transfected into human embryonic kidney HEK293E cells. Figure 3.16A shows the level of NPC1 degradation was dependent on the level of Akt phosphorylation. To make sure the transfection of the Akt construct did not affect the expression of *NPC1*, quantitative RT-PCR was performed. Figure 3.16B shows there was no significant change in terms of *NPC1* gene expression when constitutively active Akt was overexpressed. These data indicated that the decreased NPC1 level upon Akt activation was due to the degradation of the protein.

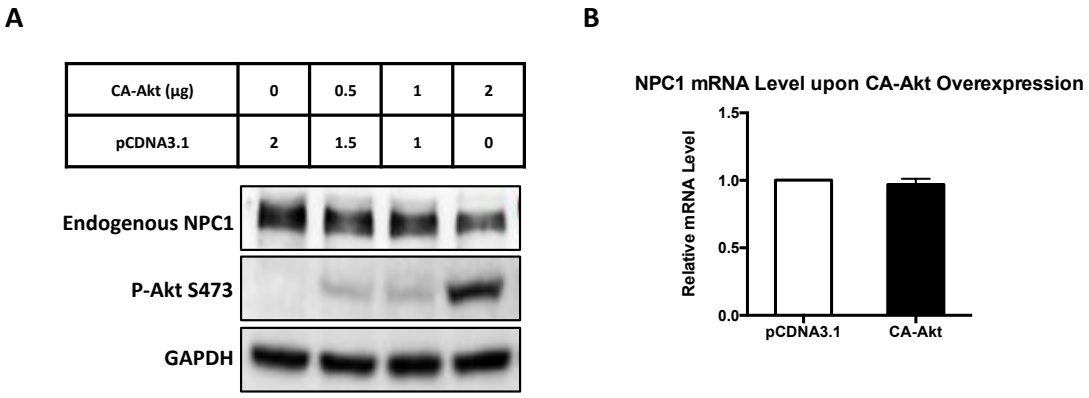

Figure 3.16 Overexpression of CA-Akt construct in HEK293E decreases endogenous NPC1. The overexpression of constitutively active Akt (CA-Akt) construct does not affect the NPC1 mRNA level. A. Increasing concentration of CA-Akt construct was transfected in HEK293E cells, proteins were harvested after 24 hours of transfection. B. The mRNA level of NPC1 in empty plasmid, pCDNA3.1 (2μg), and CA-Akt (2μg) transfected HEK293E was measured by qRT-PCR. There was no significant change upon CA-Akt overexpression.

3.13 Increasing amount of P-Akt accelerated NPC1-mCherry degradation

P-Akt promotes endogenous NPC1 degradation and it is dependent on the level of Akt phosphorylation. To further confirm this effect, The NPC1-mCherry was co-transfected with different amount of constitutively active Akt constructs to see if increasing level of P-Akt would lead to lower NPC1-mCherry protein level in HeLa cells. As expected and similar to endogenous NPC1, the level of NPC1-mCherry degradation was depending on the amount of constitutively active Akt construct transfected (Figure 3.17).

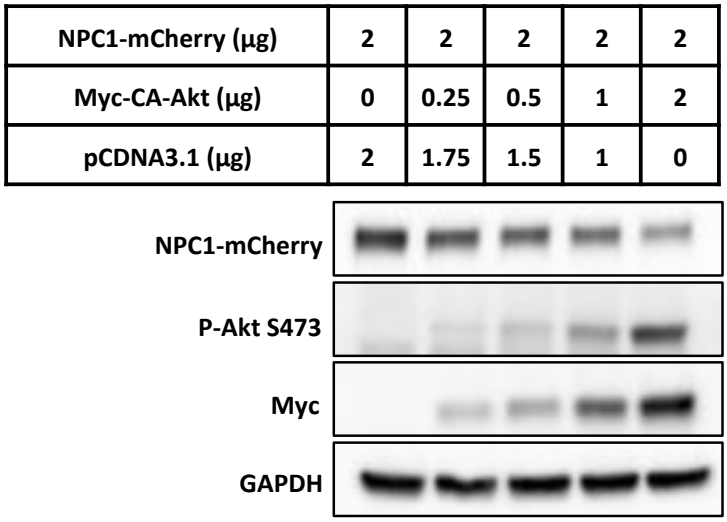

Figure 3.17 Overexpression of constitutively active Akt construct in HeLa cells degrades mCherry-NPC1 in a concentration dependent manner. HeLa cells were transfected with different concentrations of constitutively active Akt construct (Myc-CA-Akt) and 2µg of NPC1-mCherry for 24 hours. Increasing amount of phosphorylated Akt at serine 473 further decreased the level of mCherry-NPC1. pCDNA3.1, the backbone of the constitutively active Akt construct, was used to make up the amount of plasmid transfected to 4µg in total in all transfection mixture.

3.14 Inhibition of Akt phosphorylation reduced NPC1 ubiquitination

NPC1 can be ubiquitinated and undergo proteasomal degradation. Since inhibition of Akt phosphorylation by either MK2206 (Figure 3.12) or overexpression of dominant negative Akt construct (Figure 3.15) greatly rescued NPC1 from degradation, it is important to see if the inhibition of Akt phosphorylation could reduce the ubiquitination of NPC1. For this purpose, mCherry-NPC1 was pulled down from transfected HepG2 cells with RFP antibody conjugated dynabeads and ubiquitin was detected with ubiquitin antibody. In Lanes 1 and 2 of Figure 3.18, which was not treated with insulin or MK2206, the addition of MG132 inhibited the degradation of NPC1 and ubiquitinated NPC1 was detected in Lane 2. The addition of MK2206 greatly decreased the level of NPC1 ubiquitination. The insulin treatment did not further target NPC1 for ubiquitination, this might be due to low level of P-Akt. Importantly, this experiment showed a 50% decrease of NPC1 ubiquitination upon Akt inhibition.

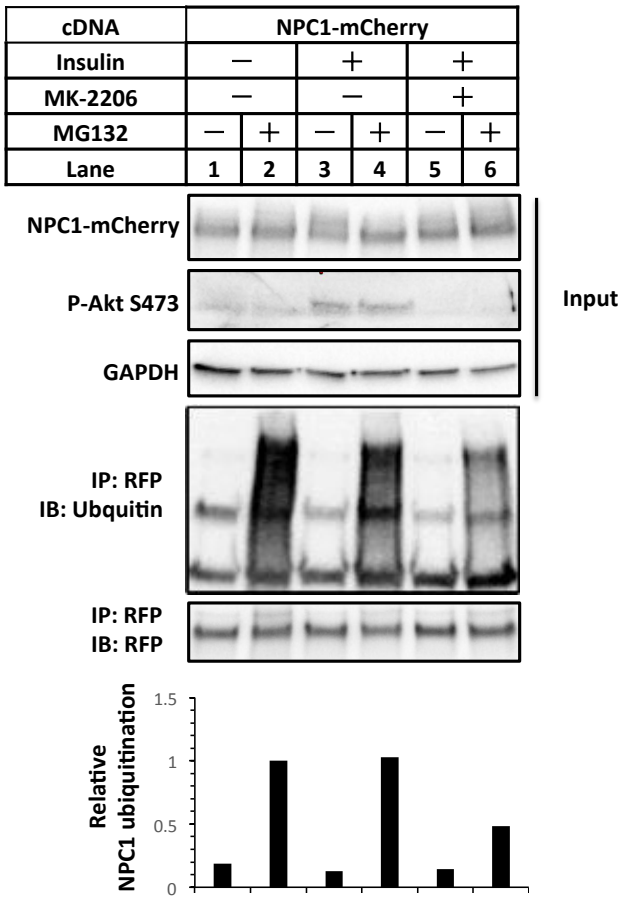

Figure 3.18 Akt inhibition reduced NPC1 ubiquitination. HepG2 cells were transfected with mCherry-NPC1 and the transfected cells were treated with DMSO, insulin or insulin with MK2206. mCherry-NPC1 was pulled down with RFP antibody and ubiquitin was detected. The inhibition of Akt phosphorylation clearly reduced the level of NPC1 ubiquitination.

3.15 Rapamycin treatment rescued NPC1 from degradation

The PI3K/Akt pathway has large numbers of downstream targets. One of the most studied Akt targets is the mechanistic target of rapamycin complex 1 (mTORC1). There are two mechanisms that Akt activates mTORC1. The first one is the direct phosphorylation of the heterodimer complex consisting of tuberous sclerosis 1 and 2 (TSC1/2). They function as the GTPase-activating protein (GAP) for the Ras homolog

enriched in brain (Rheb) GTPase. The phosphorylation of TSC1/2 complex by Akt allows the GTP-bound form of Rheb to activate mTORC1 by direct interaction. Secondly, Akt can activate mTORC1 in a TSC1/2 independent fashion by phosphorylating the raptor interacting protein proline-rich Akt substrate 40kDa (PRAS40)[86].

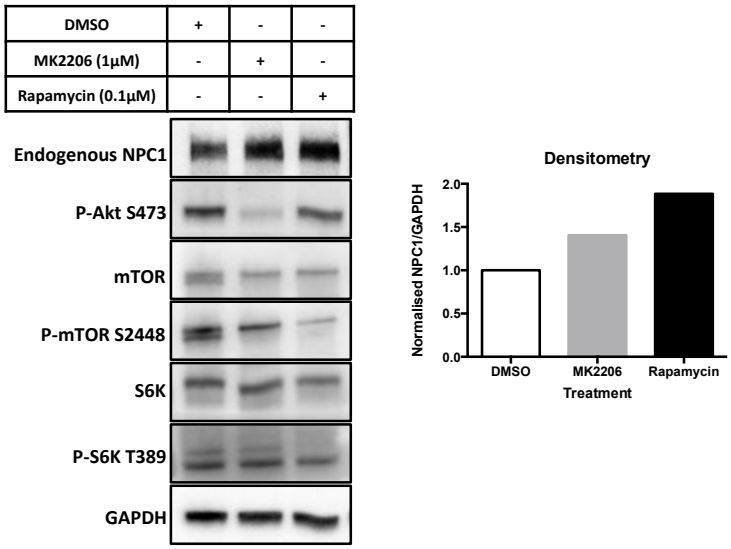

Figure 3.19 Inhibition of mTORC1 by rapamycin rescued NPC1 in C33A cells. The treatment of C33A cells with rapamycin greatly stablised NPC1 level in C33A cells. Densitometry study shows the NPC1 level in rapamycin treated cells was increased by about 80%, where MK2206 treated cells only increased by about 50%.

The degradation of NPC1 in the C33A cell might be triggered by direct phosphorylation of the protein by Akt and target it for degradation. Another possible mechanism was that Akt may activated one of its downstream pathways and indirectly target NPC1 for degradation. The first approach was to check if the downstream target mTORC1 was involved. Figure 3.19 shows the treatment of C33A cells with rapamycin greatly rescued NPC1 protein level. The recovery of NPC1 reached to almost 100% comparing to 50% by Akt inhibitor MK2206. The same treatment was also conducted in SiHa

cells, Akt inhibitor MK2206 and rapamycin greatly stablised NPC1 from degradation (Figure 3.20). One interesting finding here is the MK2206 treatment, in which the SiHa cells had almost no P-Akt. However, the P-mTOR level was decreased upon Akt inhibition and there were more NPC1 observed after the treatment. The Rapamycin treatment gave the same result but with higher degree of P-mTOR inhibition.

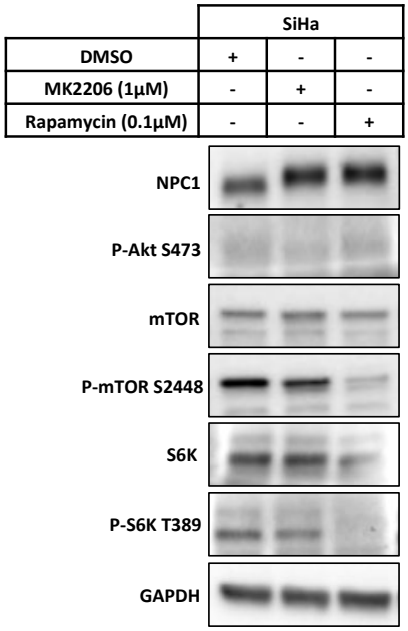

Figure 3.20 Inhibition of mTORC1 stablised NPC1 in SiHa cells. Rapamycin and MK2206 were added to SiHa cells for 14 hours and cell lysates were subjected to Western blot. MK2206 greatly inhibited phosphorylation of Akt at serine 473 and stablised NPC1 from degradation. mTORC1 was inhibited by rapamycin and NPC1 was rescued from degradation.

The important finding here was the Akt dependent activation of mTOC1 promotes NPC1 degradation, but this is not the only mechanism to trigger NPC1 degradation. The mTORC1 pathway integrates signals from growth factors, stress, energy status, oxygen and amino acid, so the degradation of NPC1 due to high level of P-Akt is just one of them. However, the rapamycin treatment helped us to narrow down the target to mTOR, which is a very important control centre in cells.

3.16 Raptor knockdown but not Rictor rescued NPC1

Rapamycin treatment rescued NPC1 from degradation in both C33A and SiHa cells. Although Rapamycin is more specific to mTORC1 inhibition, it has been shown that long-term treatment of rapamycin could inhibit the assembly of mTORC2 in some cell types as well[114, 140]. To find out the specific mTOR pathway that triggers the degradation of NPC1, small interference RNAs that targets either Raptor or Rictor, were used to silence gene expression. Raptor and Rictor are important component for mTORC1 and mTORC2 activation, respectively. Knockdown of raptor would inhibit mTORC1 activation, and this inhibition would prevent NPC1 degradation in C33A cells.

The knockdown experiment clearly showed the degradation of NPC1 was caused by mTORC1 not mTORC2. S6K is one of the downstream targets of mTORC1, the knockdown of Raptor completely abolished the phosphorylation of S6K which accompanied with dramatic increase of NPC1 level (Figure 3.21). However, the knockdown of Rictor did not have any effect on the NPC1 protein level. The knockdown efficiency of the Rictor siRNA was confirmed with the decreased phosphorylation of Akt at serine 473, because mTORC2 phosphorylates Akt at this site.

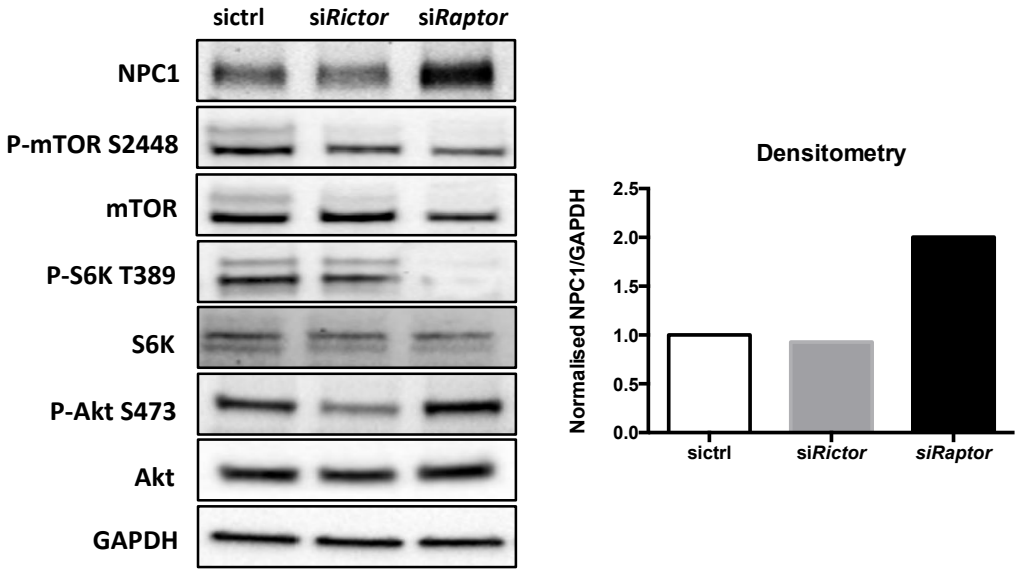

Figure 3.21 Knocking down of mTOR complex 1 (mTORC1) protein raptor but not rictor rescued NPC1 degradation. siRNA knockdown of raptor reduced phosphorylation of mTOR at serine 2448 and phosphorylation of S6K at T389. Reduced level of P-mTOR and P-S6K stablised NPC1 after 48 hours of siRNA transfection. However, knocking down of Rictor did not have any effect to the NPC1 protein level.

3.17. Activation of Akt through glucose infusion showed decreased of NPC1 in Rats

The treatment of HEK293E cells with insulin decreased NPC1 level *in vitro* (Figure 3.13), it is important to see if this regulation mechanism is conserved in real physiological condition. Liver tissues from rats infused with glucose for 0, 3, 5 and 8 hours were obtained and proteins were extracted from those tissues. Similar to HEK293E cells, stimulation of Akt phosphorylation via glucose infusion triggered NPC1 degradation (Figure 3.22). P-mTOR level was also increased after 3 hours of glucose infusion. After 8 hours of treatment, the level of NPC1 reduced to 30% of the original level. These data demonstrated that the degradation of NPC1 is correlated to Akt signalling *in vivo*.

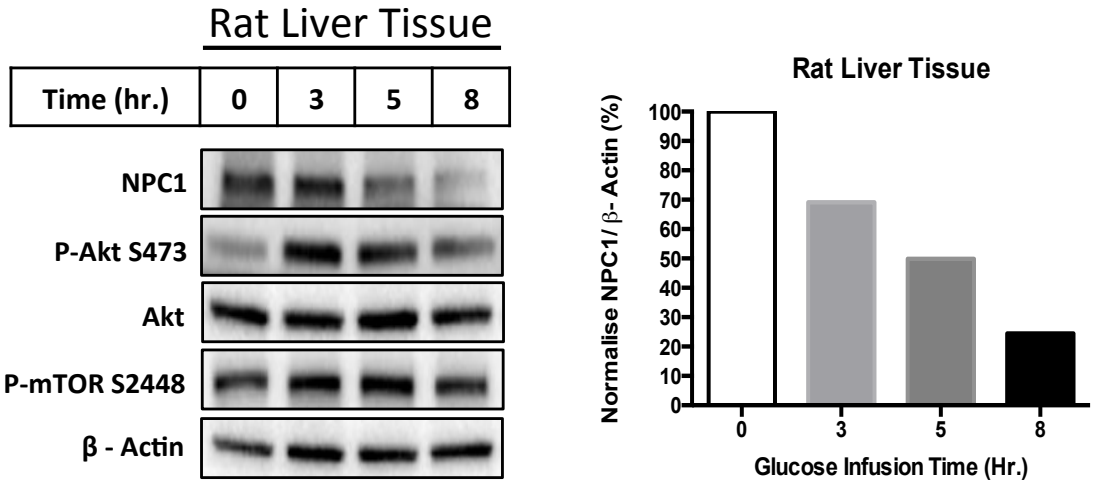

Figure 3.22 NPC1 degradation trigged by P-Akt was conserved in rat liver tissues. Rats were infused with glucose for 3, 5 and 8 hours. Rat liver tissues were homogenised and proteins were extracted and subjected to Western blot for NPC1 analysis. P-Akt S473 was greatly increased after 3 hours of glucose infusion and maintained at the same level after 5 hours of infusion then started to decrease after 8 hours of the treatment. The band intensities of NPC1 was normalised to β actin and the densitometry study shows that there was approximately 70% loss of the protein after 8 hours of glucose infusion.

3.18 Discussion

The finding of free cholesterol accumulation in human cervical cancer cell line C33A has lead to the discovery of a novel mechanism of how the degradation of NPC1, an important cholesterol trafficking protein, is regulated through the PI3K/Akt/mTORC1 pathway. As a late endosomal membrane protein, NPC1 works with NPC2 in tandem to make sure LDL-derived cholesterol is transported to the ER and other organelles. Mutations of NPC1, like the I1061T, lead to the misfolding of the protein and target it for degradation. It has been shown that NPC1 could undergo the ubiquitin proteasome degradation pathway[139], but it is still not clear about how this pathway is initiated. The ubiquitination of NPC1 is likely dependent on cellular cholesterol level and depletion of cholesterol facilitates NPC1 ubiquitination[141]. However, none of these

studies have given a possible mechanism of what triggers NPC1 for degradation. This study revealed a novel relationship between Akt activation and NPC1 degradation. It is not surprising that mTORC1 also plays a role in regulating the level of NPC1 due to its central role of cellular growth and metabolism.

Aberrant regulation of cholesterol homeostasis was observed in some cancer cells [142-147]. The enormous accumulation of free cholesterol in the C33A cells was due to not only the absence of NPC1, but also the upregulation of *HMG-CoAR* and *LDLR* and decreased expression of the cholesterol exporter *ABCA1* (Figure 3.6B). These phenotypes were also commonly observed in other cancer cells[148-153]. The endogenously synthesised cholesterol could be packaged into lipid droplets at the ER by ACAT, but the cholesterol accumulated in the LE/LY due to NPC1 deficiency might be toxic to cells. What are the benefits of accumulating huge amount of cholesterol in the C33A and LNCaP cells? Pharmacological approaches, like using cholesterol-lowering drug statin that inhibits HMG-CoAR, have been shown to reduce tumour growth[154-156]. However, mevastatin treatment did not enhance the effect of chemotherapeutic drugs on the C33A cell (data not shown). Statin might inhibit cholesterol biosynthesis, but it could not reduce the amount of cholesterol accumulated in the LE/LY compartments. It has been shown that the accumulation of cholesterol in lysosomes rescued human fibroblasts from lysosome-dependent cell death induced by chemotherapeutic drug cisplatin[157]. This study showed cholesterol accumulation in the lysosomes could increase lysosomal membrane stability and lead to the attenuation of apoptosis. Therefore, the cholesterol accumulated in the C33A cell protected the cells from apoptosis, which made the cell more aggressive than the HPV positive cervical cancer cells. The current HPV vaccination program is only effective for HPV positive

cervical cancer prevention; the percentage of HPV negative cervical cancer cases will increase due to no prevention method is currently available. The overexpression of Rab9 GTPase in *NPC1*$^{-/-}$ cells has been shown to reduce cholesterol storage and correct cholesterol trafficking[158, 159]. Furthermore, Rab9 transgenic mice displayed longer lifespan[160]. If NPC1 could be restored in HPV negative cervical cancer cells to lower cholesterol accumulation together with cholesterol biosynthesis inhibition, it might shed some light for treatment development.

The finding of ectopic free cholesterol accumulation in the C33A cell identified a new regulation node between insulin signalling and cholesterol metabolism. It is widely known that high level of P-Akt is activated in certain cancer cell types[94], the relationship of P-Akt level and NPC1 degradation may reveal a new regulation mechanism. PI3K activation through the binding of growth factors such as insulin to the insulin receptor on the surface of plasma membrane promotes the binding of adaptor molecule insulin receptor substrate (IRS) to the insulin receptor. This triggers activation of PI3K and leads to subsequent conversion of phosphatidylinositol (3,4)-bisphosphate (PIP_2) lipids to phosphatidylinositol (3,4,5)-trisphosphate (PIP_3). Akt then binds to PIP_3 and allowing PDK1 to phosphorylate Akt at the T308 site. This partial Akt activation is sufficient to activate mTORC1[161, 162]. PI3K also activate mTORC2 through a poorly defined mechanism, mTORC2 phosphorylates Akt at the S473 site and leads to the maximum activation of Akt[106]. In this study, high level of P-Akt has been shown to promote NPC1 degradation and high level of P-Akt in cancer cells may benefit cancer cell growth by activating the mTORC1 pathway through TSC2 and PRAS40 inhibition[163-165]. The inhibition of mTORC1 by rapamycin or the knockdown of raptor in the C33A cell dramatically increased NPC1 protein level. Interestingly, when

NPC1 was knocked down in HepG2 cells, there was an approximately 50% decreased in P-Akt S473 level after insulin treatment comparing to the control cells (Figure 3.23). However, the decreased P-Akt S473 level in the NPC2 knocked down cells was less obvious. It is known that insulin decreases cAMP level and leads to the activation of HMG-CoAR for cholesterol biosynthesis[166-168]. This rate-limiting enzyme senses the level of cholesterol through its sterol-sensing domain (SSD), when cholesterol level is high the binding of insig-1 to the SSD of HMG-CoAR accelerates its degradation and the cholesterol biosynthesis is eventually inhibited. To enhance the feedback inhibitory effect it may also be possible that mTORC1 targets NPC1 for degradation and fully shuts down cholesterol transport. When *NPC1* was knocked down in the HepG2 cell (Figure 3.24), low cholesterol level was sensed in the ER and biosynthesis of cholesterol was activated. It is known that mTORC1 phosphorylates growth factor receptor-bound protein 10 (Grb10), this mediates the binding of Grb10 to insulin receptor and inhibit the activation of the insulin pathway[124, 169]. In this case, prolong insulin treatment in the HepG2 cells might also trigger the inhibition of the insulin pathway and lead to the decreased P-Akt level as seen in Figure 3.24. The knockdown of *NPC2* also has the same cholesterol accumulation phenotype as the NPC1 cells, but the level of P-Akt was not significantly decreased.

This study shows the activation of the PI3K/Akt/mTORC1 pathway plays a novel role of regulating the level of NPC1 in cells. It is essential to test the downstream targets of mTORC1, such as S6K. The inhibition of the S6K protein might reveal more important aspects of this new mechanism. NPC1 not only plays an important role in cholesterol trafficking, but it is also important for the regulation of the insulin dependent mTORC1 pathway. In normal cells, this cholesterol imbalance affects the signalling pathway, but

this imbalance helps cancer cells to proliferate and develop resistance to chemotherapeutic drugs. This study showed a conserved mechanism in various cell types, such as liver cell, kidney cells, cervical cancer cells and prostate cancer cells. More importantly, it is conserved in real physiological condition.

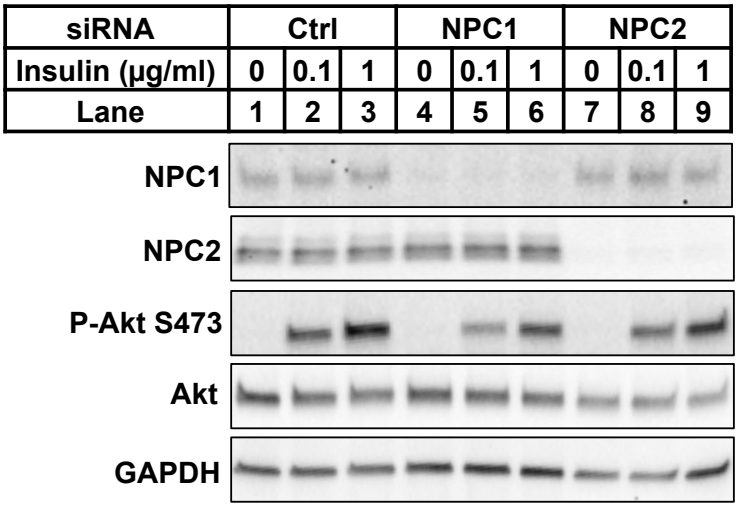

Figure 3.23 NPC1 and NPC2 knockdown interfered Akt phosphorylation in HepG2 cells. siRNA targets NPC1 and NPC2 was transfected into HepG2 cells, the absence of NPC1 and NPC2 after the knockdown confirmed the efficiency of the siRNAs. There was a clear decreased of P-Akt S473 level after insulin treatment in the NPC1 knocked down cells. The NPC2 knocked down cells had less effect.

3.19 Conclusion

This study has shown that the insulin dependent PI3K/Akt/mTORC1 pathway regulates the level of NPC1 in different cell types. The activation of P-Akt through the activation of receptor tyrosine kinase or the overexpression of constitutively active Akt had lead to the ubiquitination of NPC1 and its degradation via the proteasome degradation pathway. Pharmacological inhibition of the PI3K/Akt pathway greatly rescued NPC1 from

degradation and partially decreased the amount of free cholesterol accumulated in HPV negative C33A cervical cancer cells. The amount of NPC1 was also correlated with the level of P-Akt in cells. This study also revealed a new mechanism of how cholesterol trafficking and insulin signalling pathway is regulated. Overall, this study provides preliminary observation for the study of NPC1 degradation and it may provide important knowledge for the understanding of why certain cancer cells accumulate huge amount of free cholesterol. Importantly, it may help to develop new cancer treatment.

4. Chapter 4:PPARγ Regulates the Expression of Mouse *Seipin*

4.1 Background

Peroxisome proliferator-activated receptor γ (PPARγ) belongs to the members of the nuclear receptor superfamily of ligand-inducible transcription factors[56]. There are another two PPARs found in mammalian cells, PPARα and PPARδ (also known as PPARβ/δ). PPARs serve as lipid sensors and it can be activated by fatty acids and their derivatives. Importantly, the activation of the PPAR family greatly controls whole cell metabolism. PPARα is expressed predominantly in the liver, heart and brown adipose tissue. It was the first PPARs to be identified and it was found to be involved in the fatty acid oxidation pathway[67]. PPARβ/δ is ubiquitously expressed throughout the body and it is also involved in fatty acid oxidation like PPARα. The activation of PPARδ/β by pharmacological agonist has been shown to lower plasma triglyceride levels while high-density lipoprotein levels were increased in obese monkey[170]. PPARγ is known as the master regulator of adipogenesis, the activation of PPARγ in fibroblast leads to the differentiation of adipocytes[57]. It is highly expressed in white adipose tissue and brown adipose tissue. It is not only the master regulator of adipogenesis, but it also regulates lipid metabolism and insulin sensitivity[54]. The binding of insulin sensitisers Thiazolidinediones (TZDs) to PPARγ was found to have agonistic effect in adipose tissue; it improves the ability to store lipids and lower the lipotoxicity in muscle and liver. Overall, the activation of PPARs promotes their binding to PPAR-responsive regulatory elements (PPREs) and controls the expression of genes involved in adipogenesis, lipid metabolism and inflammation.

The binding of PPARγ to the PPREs requires the formation of PPARγ/RXRα heterodimer. However, some PPREs do not require the formation of the heterodimer and PPARγ may recruit other co-activators for transcription activation. Based on *in vitro* studies, this PPARγ/RXRα heterodimer binding sites contain a consensus sequence of AGGTCA N AGGTCA[171]. This direct repeat of AGGTCA element, also called DR1 element, is conserved to various degree. Lefterova and colleagues used ChIP followed by DNA hybridisation (ChIP-chip) identified 1370 PPARγ binding sites and 1347 (98.3%) of those sites also had binding for RXRα in 3T3-L1 adipocytes[172]. They also identified novel PPARγ binding sites and one of them is within the promoter region of mouse *Berardinelli-Seip congenital lipodystrophy 2* (*Bscl2*).

As mentioned in the introduction, the gene *Bscl2* produces a protein called Seipin in mammalian cells. The mutation or lack of *Bscl2* causes a rare autosomal recessive disease called congenital generalised lipodystrophy, which is characterised by a near total absence of adipose tissue[173]. It has been shown that Seipin is essential for adipogenesis and differentiation of *Bscl2*$^{-/-}$ MEFs to adipocytes was impaired[81, 174]. Lefterova *et. al.* identified a novel PPARγ binding site within the first 600 base pairs upstream of the transcription start site of mouse *Seipin* from their genome wild ChIP study[172, 175]. However, their study was not focused on *Seipin* and no confirmation study was followed. Because PPARγ regulates so many important lipid related genes, it is possible that it also regulates the expression of *Seipin*, an essential protein for adipogenesis.

The aim of this study was to confirm if PPARγ actually binds to the promoter of *Seipin*. Also, does the binding of PPARγ to the *Seipin* promoter lead to the expression of

Seipin? Finally, does the binding of PPARγ require RXRα to promote the expression of *Seipin*? All these questions would be answered using luciferase assay, gel shift assay and ChIP.

4.2 Potential PPARγ binding site in the mouse Seipin promoter region

Mouse *Seipin* has two transcript variants in which one of them has 1815 base pairs and the other has 1965 base pairs. The short transcript has an alternate 5' untranslated region (5'UTR) and this shorter isoform translates into the same protein as the long transcript variant. The finding of the potential PPARγ binding site upstream of the transcriptional start site (TSS) of *Seipin* came from the study conducted by Lefterova *et. al.* using mouse adipocytes[172, 175]. By comparing both ChIP raw data obtained from their studies, the PPARγ peaks identified from each of the studies showed exact localisation upstream of the mouse *Seipin* gene, which is approximately 500 base pairs upstream of the TSS. This drew the attention to that PPARγ may regulate the expression of *Seipin* in adipocytes. Figure 4.1 shows the schematic diagram of the two mouse *Seipin* transcript variants and labelled with the potential PPARγ binding site. With the aid of Matinspector, the software predicted a potential DR1 motif within this region, although there were some nucleotide variations. Figure 4.2 shows the sequence of the predicted DR1 site. Interestingly, the predicted PPARγ binding site is localised to the peak that was identified from Lefterova's study.

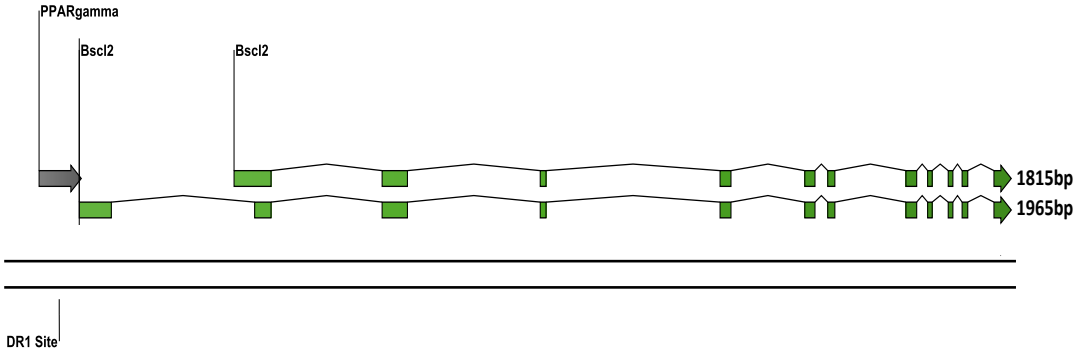

Figure 4.1 Mouse *Seipin* (*Bscl2*) transcript variants and potential PPARγ binding site. Mouse *Seipin* has two transcript variants, a short isoform which has about 1.8kb and a longer isoform which contains approximately 2kb. The two transcripts translate into the same protein Seipin. Potential PPARγ was identified from previous ChIP studies and it contains the DR1 consensus sequence within the binding site.

GATCCCACAGAGACCAAGGAACAGGGTGCTCCAAGATGGCCTGTTTAACACATTTGTGT
TATTACATACACCTCAAAGGGAACCTCTACTCAGGCGAGATTCTTATGCAAAACTCACTCT
GGGCTTCTTGGGTCCCAGTCCTAGTGACTGGTTGTTTTAAGTCAGGATTTCATTGTGTATT
GTGTGTCGTCGTGGCTGGCTTGGAACTCAGAGATCCATCTGCCTCTGTGTGTGTCCAACA
CCTCCGGAGTGTTGGTCACCACACTGAACTTAAGAACCCATGACTGCTTTAGGTGTCTCCC
CATCCCCACTCCCCGTGATTGGTCTCCAAAGCATGTCTAGTTCCAGATTCTATGGGACAGA
GAACCTGACTCTGACTTTGAGAGGGCAGGGGCAGCCATTTTAAGACCAGAGGATCGCAT
AAGGGATCGTTCCCTATTGGGAACGCTGGGGACCGCCATTTTAAGAGCACCCTCGGCGC
GTGCCTCCATGCGGGTACGAACAGGCAGCCGCCATCTTGGGCATTGGCTGCCGCGCCGA

Figure 4.2 500 base pair *seipin* promoter region. The predicted PPARγ/RXRα (DR1) motif is located approximately 200bp upstream of the first *Seipin* transcription start site. The DR1 motif is highlighted as red and the beginning of the *Seipin* gene is underlined.

It is known that PPARγ forms heterodimer with RXRα in order to recognise the DR1 motif of PPREs and initiate target gene expressions. Schematic diagram shown in Figure 4.3A illustrates the binding of PPARγ/RXRα heterodimer to the DR1 site of PPREs. Figure 4.3B shows the enrichment motif analysis of single PPARγ binding motif and the PPARγ/RXRα binding motif from the Lefterova's ChIP study. The

predicted PPARγ binding motif sequence showing in Figure 4.3C is quite different to the general PPARγ/RXRα motif sequence. However, it contains the PPARγ motif sequence AGTTCA reading in the 3' to 5' direction of the antisense strand and it is indicated in the red box. Thus, it is very likely that PPARγ may bind to this site and promote the expression of *Seipin*.

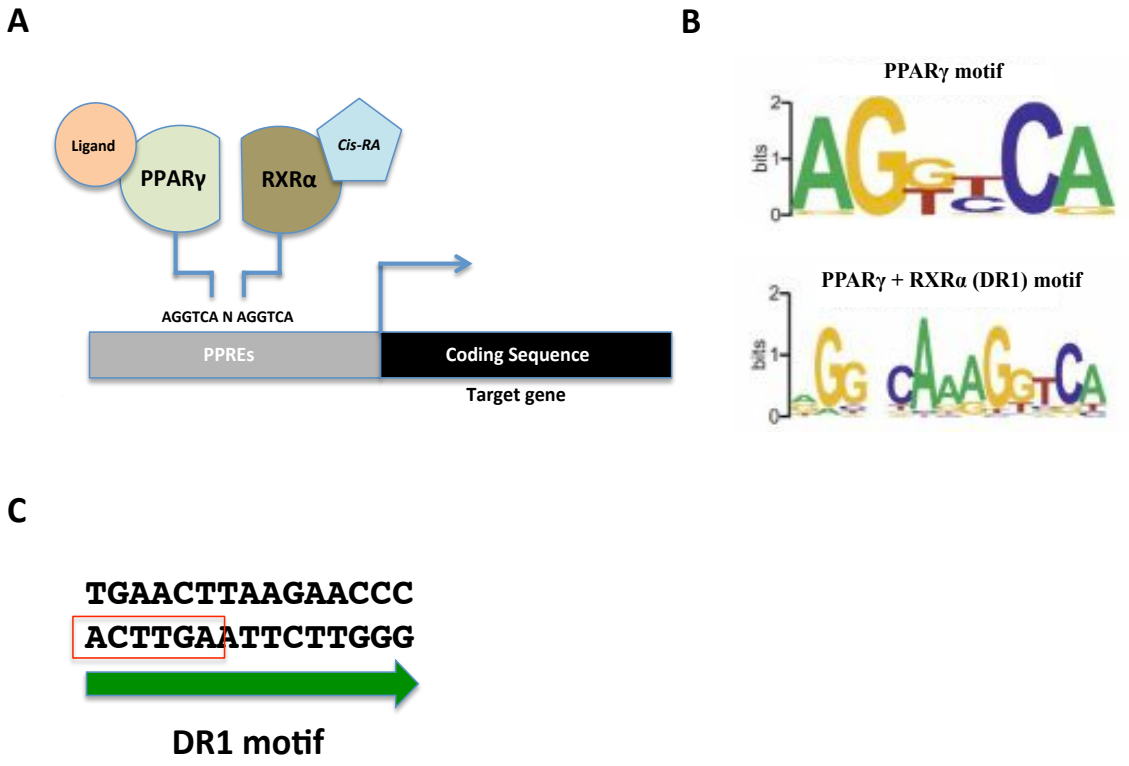

Figure 4.3 Schematic digram of PPARγ/RXRα heterodimer and their binding motif. A. PPARγ and RXRα form heterodimers and they recognise the DR1 motif AGGTCA N AGGTCA in the peroxisome proliferator response elements (PPREs) of PPARγ regulated promoters and promote target gene expression. The activation of PPARγ can be initiated by the binding of either endogenous ligand or pharmacological ligand like TZDs. Similar to PPARγ; retinoid X receptor α (RXR α) is activated by 9-*cis* retinoic acid (*Cis-RA*). B. Adopted from Lefterova *et. al., MCB* 2010. The consensus PPARγ and PPARγ/RXRα binding motif. C. The predicted DR1 motif of the novel PPARγ binding site in mouse *seipin* promoter. The novel DR1 motif contains only half of the PPARγ binding motif in the antisense strand and the second half of the motif is quite different to the general DR1 motif.

4.3 Expression of Seipin is enhanced when PPARγ is activated

Adipocyte differentiation of 3T3-L1 cells using traditional differentiation cocktail, which contained IBMX, dexamethasone and insulin, showed the *Seipin* expression started after 4 days of differentiation. The expression of *Seipin* increased dramatically after day 4 and reached to almost 80 folds in day 8 (Figure 4.4). The other marker genes like *cebpa and ap2* increased dramatically and the preadipocyte marker *pref1* decreased significantly indicating the cells were differentiated into adipocytes. The cell death marker *caspase3* showed the cells were healthy during differentiation. From the RT-PCR data, the expression of *Seipin* increased only after PPARγ level started to increase, although this was an assumption at the beginning of the experiment.

To test the assumption, PPARγ agonist rosiglitazone (1μM) was included in the differentiation cocktail. The preadipocytes were differentiated for 8 days just like the previous experiment shown in Figure 4.5 and the expression of *pparg*, *Seipin* and other marker genes were examined by RT-PCR. Differentiation of adipocytes with the addition of PPARγ agonist rosiglitazone greatly increased the expression of PPARγ after day 4. The expression level of differentiation mark genes like *cebpa and ap2* increased dramatically. More interestingly, the expression level of *Seipin* also increased significantly. This indicated *Seipin* expression may be controlled by PPARγ. However, one may argue that other transcription factors like *cebpa* could also regulate the expression of *Seipin*. To further test our hypothesis, luciferase assay was done to examine if PPARγ actually regulate the expression of *Seipin* through the binding to its promoter region.

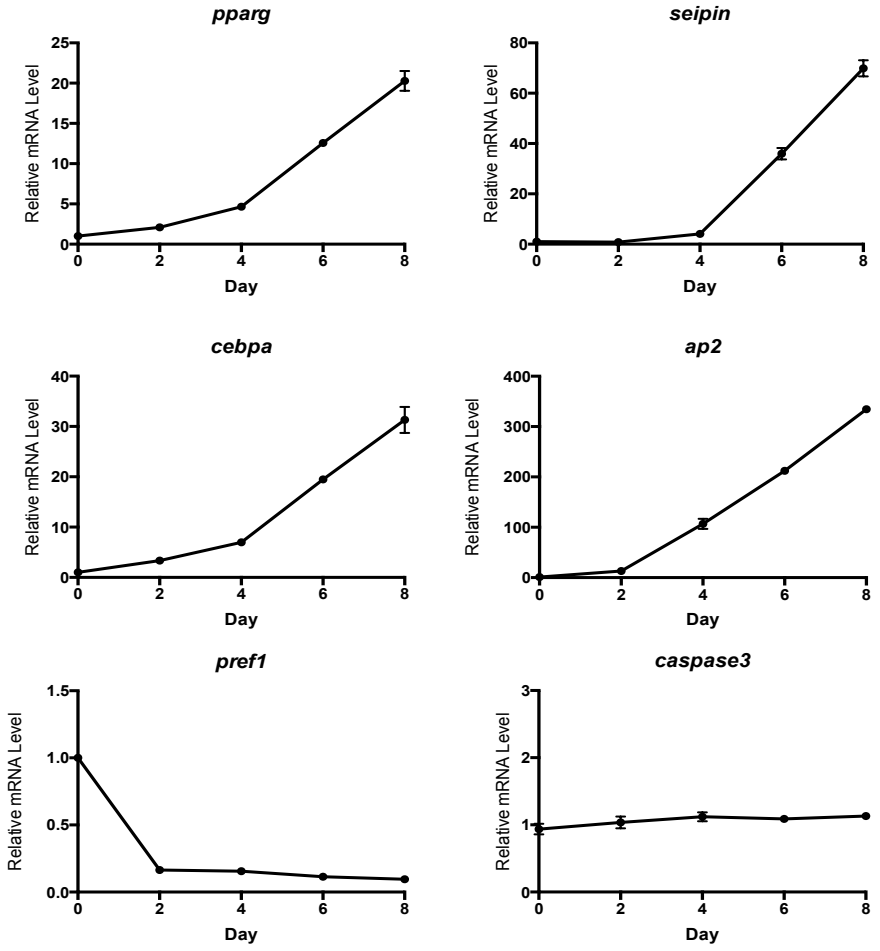

Figure 4.4 *pparg* and *seipin* expression during 3T3-L1 adipogenesis. 3T3-L1 preadipocytes were induced for differentiation using IBMX, dexamethasone and insulin. Total RNAs were extracted and the expression of *pparg* and *seipin* were checked. Other adipocyte differentiation markers, *cebpa, ap2, pref1* and *caspase3* were also checked. The expression of *seipin* started only after the expression level of PPARγ was high after 4 days of differentiation.

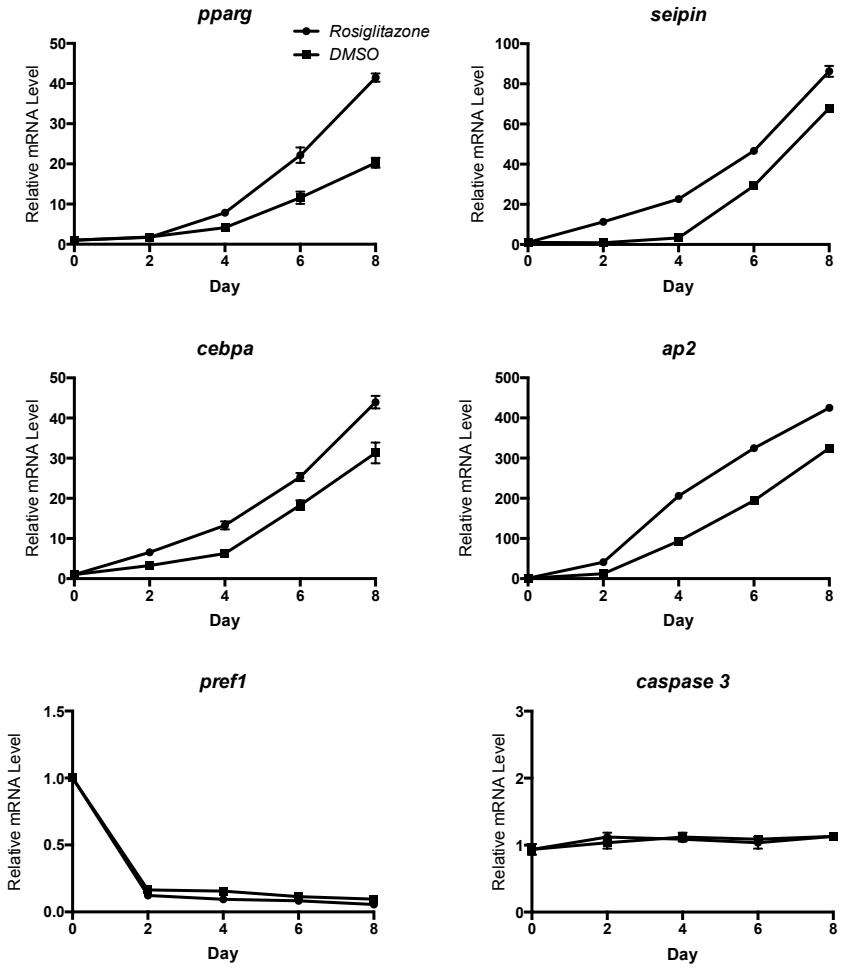

Figure 4.5 Expression of *Seipin* was accelerated when TZD rosiglitazone was included in the differentiation cocktail. 3T3-L1 preadipocytes were induced for differentiation using the differentiation cocktail with or without rosiglitazone. The expression of PPARγ was greatly increased while the expression of *Seipin* was accelerated comparing to the no rosiglitazone differentiated cells.

4.4 Luciferase assay showed PPARγ induced the expression of Seipin and the binding of PPARγ/RXRα further enhanced the expression

In order to find out if PPARγ regulates the expression of *Seipin*, the 500 base pair region upstream of the mouse *Seipin* TSS was cloned into luciferase reporter plasmid. This 500 base pair region contained the potential PPARγ binding site, the DR1 element. HeLa cells were used for this assay, although low level of PPARγ did present in this cell type. If PPARγ binds to this region and promote the expression of the luciferase gene, higher level of luciferase signal should be observed comparing to the background. Three sets of conditions were tested. First condition was transfected with the promoter region alone. Second condition was transfected with promoter region and PPARγ and the last one was transfected with promoter region, PPARγ and RXRα. Figure 4.6A shows the result of the luciferase assay and the read outs were normalised to the 500bp promoter alone. As the control, the transfection of luciferase empty plasmid and the combination of PPARγ or PPARγ + RXRα did not change the expression level of luciferase reporter gene. Interestingly, the expression of the 500bp promoter region and PPARγ significantly increased the expression of luciferase. Figure 4.6B shows that the expression of luciferase was enhanced with increasing amount of PPARγ overexpressed in the cells. The co-expression of PPARγ and RXRα dramatically increased the expression of luciferase (Figure 4.6A). To see if the binding of PPARγ was specific to the DR1 element within the promoter region to facilitate the expression of the luciferase gene, the DR1 motif within that region was mutated by site directed mutagenesis. The luciferase assay showed the mutation of the DR1 motif totally abolished the ability of PPARγ to induce the expression of the luciferase reporter gene. This experiment clearly

showed PPARγ could bind to the DR1 element of the 500bp promoter region and the binding induced the expression of luciferase reporter gene. More importantly, this positive effect was further enhanced when RXRα was co-expressed together with PPARγ.

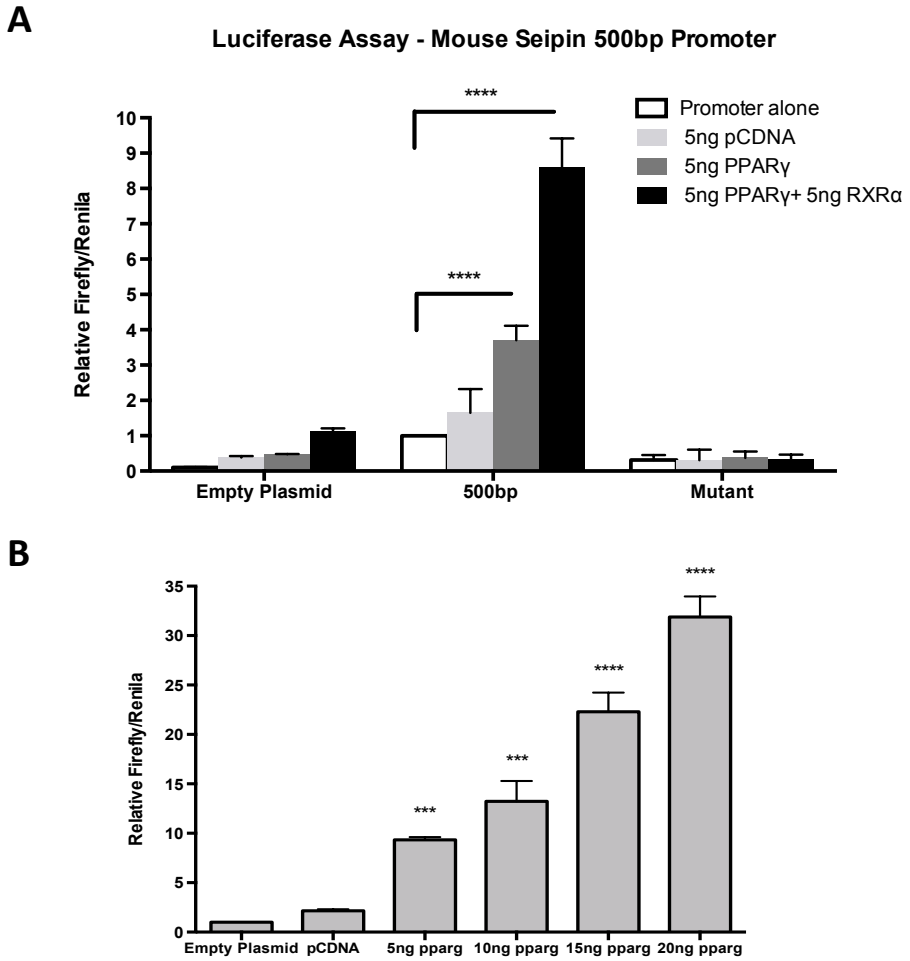

Figure 4.6 Luciferase assay of 500bp *seipin* promoter region. 500bp *seipin* promoter region was cloned into luciferase reporter plasmid. A. The reporter plasmid was co-expressed with PPARγ backbone plasmid pCDNA as the control. It was also co-expressed either with PPARγ alone or the combination of PPARγ/RXRα. The expression of PPARγ alone significantly increased the luciferase signal and the combination of both PPARγ/RXRα greatly enhanced the expression of the reporter gene. The mutation of the DR1 motif with the 500bp promoter region completely abolished the expression of the reporter gene. B. Different amount of PPARγ was co-expressed with the luciferase reporter plasmid. The expression of the reporter gene was dependent on the amount of PPARγ transfected indicating PPARγ could bind to the DR1 motif and induce expression. *** $p < 0.0001$, **** $P < 0.00001$, $n = 3$.

4.5 Gel shift assay confirmed the binding of PPARγ to the DR1 element of the mouse Seipin promoter region

Luciferase assay showed the positive regulatory effect of PPARγ on the expression of the luciferase reporter gene that was cloned downstream of the mouse *Seipin* promoter. The mutation of the DR1 element within that region completely abolished the expression. It was still be possible that PPARγ might bind to regions next to the DR1 element and recruited other co-activators to bind to the DR1 site. When the DR1 site was mutated, the binding of co-activators was inhibited and expression was lost. To eliminate this, gel shift assay was performed.

Two probes were designed for the gel shift assay. The first one contained the wild type DR1 element sequence of the mouse *Seipin* 500bp promoter region. The second one was the mutant in which the DR1 element sequence was changed. A transcription factor binding prediction was done to make sure the mutated sequence would not be bound by other transcription factors. Nuclear extracts were prepared from HeLa cells that were transfected with PPARγ construct or PPARγ and RXRα constructs. Nuclear extract from non-transfected HeLa cells was used as the control. Figure 4.7 shows the gel shift image. Due to the fact that there was PPARγ present in HeLa cells, the binding of PPARγ to the wild type probe was observed in lane 1. However, the incubation of the control nuclear extract with PPARγ antibody prior to the addition of the wild type probe decreased the band intensity indicating that band was the band of interest. Importantly, nuclear extract with overexpressed PPARγ greatly increased the PPARγ band intensity in lane 3 and the addition of PPARγ antibody to the nuclear extract in lane 4 inhibited the binding of PPARγ to the wild type probe. The overexpression of both PPARγ and

RXRα further enhanced the band intensity and the band observed in lane 5 travelled slightly slower than in lane 3 indicating a bigger complex of PPARγ/RXRα were formed. Strikingly, the binding of PPARγ was lost using the mutant probe. This confidently confirmed PPARγ binds to the DR1 element of the mouse *Seipin* promoter region to facilitate the expression of *Seipin*.

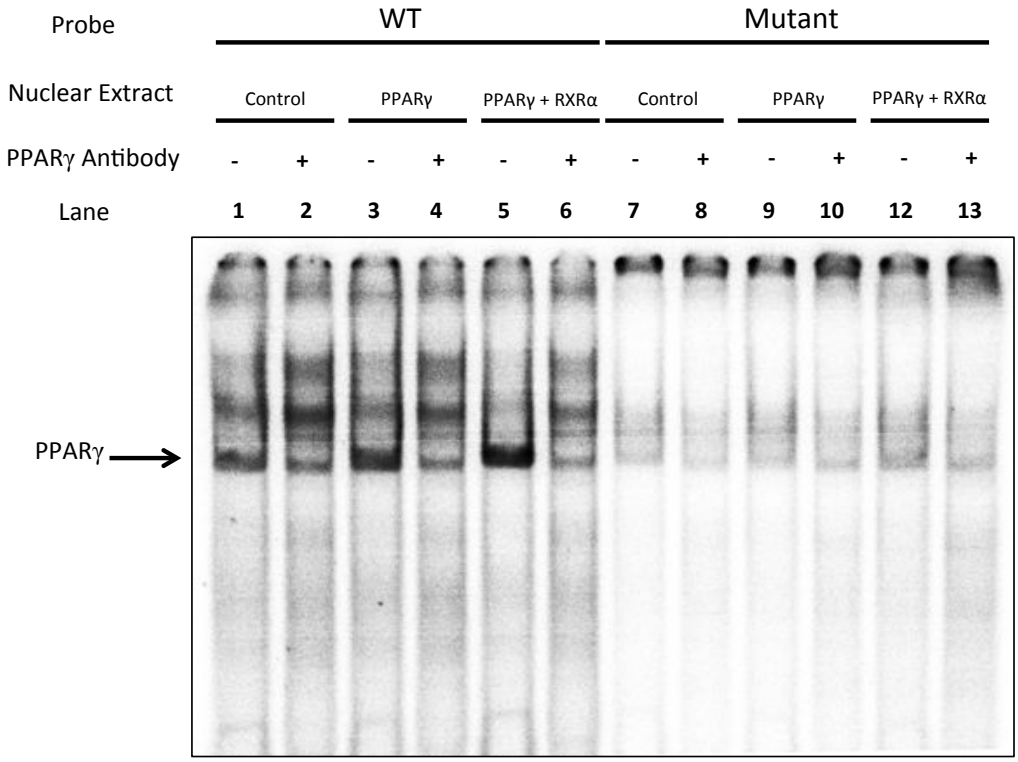

Figure 4.7 Electrophoretic mobility shift assay (Gel shift assay) showed PPARγ binds to the DR1 element. Nuclear extracts from control cells, cells transfected with PPARγ and cells transfected with PPARγ/RXRα were harvested. The presence of PPARγ greatly increased the PPARγ band intensity despite there was background in the control. The addition of RXRα further increased the band intensity and the band was slightly higher due to the larger size complex. The incubation of nuclear extracts with PPARγ antibody dramatically reduced the band intensity. The mutant probe which had mutation in the DR1 element totally abolished the binding of PPARγ indicating PPARγ could bind to this novel DR1 site.

4.6 ChIP qRT-PCR further confirmed the binding of PPARγ to the DR1 element

The overexpression of PPARγ enhanced the expression of *Seipin* and the mutation of the DR1 element abolished the binding of PPARγ to the promoter region. To confirm PPARγ binds to the novel DR1 element endogenously, ChIP was performed to pull down endogenous PPARγ that was bound to DNA. Mouse embryonic fibroblasts (MEFs) was used for this experiment and three different sets of qRT-PCR primers were designed. Both negative and positive primer sequences were obtained from published literature[176, 177]. The negative control primers bind to region where PPARγ does not bind and the positive control primers has been shown to bind to PPARγ positive region. The last set of primers was designed based on the novel DR1 element. Briefly, MEFs were induced for differentiation for 4 days, where the transcription of *Seipin* was induced. Nuclear extract was then prepared and PPARγ antibody was used to pull down PPARγ bound DNA fragment. DNA was then purified and subjected to qRT-PCR. The normalisation method used was the fold enrichment method where the ChIP signals were divided by the no-antibody signals. The output was represented as the fold increase in signal relative to the background signal. The final result was then normalised to the negative control signal. Figure 4.8 shows that the ChIP experiment successfully pulled down PPARγ bound region that was represented as approximately 4 fold increased using the positive control primers. Importantly, primers that detect the novel DR1 element had a 8 fold increased which suggested that endogenous PPARγ bound to the novel DR1 site. This further confirmed the luciferase and gel shift assays.

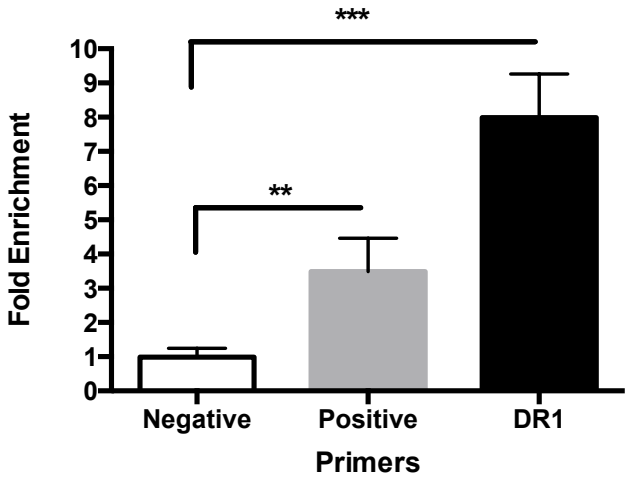

Figure 4.8 ChIP qRT-PCR proved endogenous PPARγ binds to the DR1 site of mouse *seipin*. Nuclear extract from 4 day differentiated MEFs was harvested and endogenous PPARγ DNA fragments were pulled down using PPARγ antibody conjugated dynabeads. qRT-PCR using primers that target the novel DR1 site showed positive binding of PPARγ. Negative primers target non-PPARγ target site. Positive primers detect PPARγ binding motif and the DR1 primers specifically recognise the novel DR1 site in the mouse *seipin* promoter. ** $p < 0.001$, *** $p < 0.0001$, $n = 3$.

4.7 Mouse Seipin DR1 element is not conserved in the human SEIPIN promoter

So far the binding of PPARγ to the mouse *Seipin* DR1 site was confirmed with luciferase and gel shift assays and the endogenous binding of PPARγ to this site was also proved with the ChIP qRT-PCR method. However, this DR1 site is not conserved in the human promoter region. Prediction suggested that PPARγ might bind to a region that is 2kb upstream of the human TSS. A 2.5kb promoter region upstream of the human *SEIPIN* TSS was cloned into the luciferase reporter plasmid, PPARγ or both PPARγ and RXRα were co-expressed in HeLa cells. Figure 4.9 shows that the co-expression of PPARγ alone could induce the expression of luciferase and the combination of PPARγ and RXRα further enhanced the luciferase expression. This

result was similar to the mouse *Seipin* promoter. However, more experiments are required to find out the exact location of the DR1 element within the human promoter. If time was allowed, ChIP-Seq would be able to map the potential PPARγ binding site and similar experiments performed in this chapter would be used to examine the human *SEIPIN* promoter.

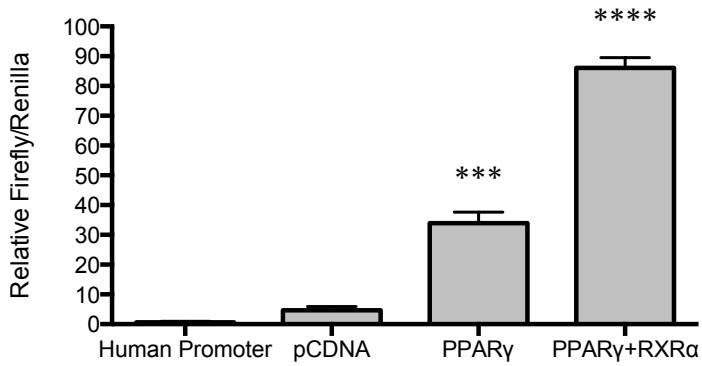

Figure 4.9 2.5kb promoter region of human *seipin* contains PPARγ binding site. Luciferase assay showed that a 2.5kb region upstream of the human *seipin* promoter contained PPARγ binding site and the co-expression of PPARγ and RXRα significantly enhanced the expression of the reporter gene. Human promoter = cells transfected only with the human promoter luciferase reporter plasmid. pCDN = human promoter with PPARγ backbone plasmid. PPARγ = human promoter with PPARγ. PPARγ + RXRa = human promoter with PPARγ/RXRα. *** $p < 0.0001$, **** $p < 0.00001$, $n = 3$.

4.8 Discussion

PPARγ as a transcription factor controls the expression of large number of lipid related genes. It is not surprised that the master regulator of adipogenesis also controls the expression of *seipin*, which is essential for adipocyte differentiation. The finding of potential PPARγ binding peaks from Lefterova's study has led to the finding of a novel PPARγ binding site in the mouse *seipin* promoter region. However, this DR1 site is not conserved at the same location in the human promoter region. This study clearly

showed that PPARγ bound to the DR1 element of the mouse *Seipin* promoter region and induced the expression of luciferase reporter gene. In contrast, the mutation of the DR1 element totally abolished the expression of the reporter gene. Gel shift assay confirmed the binding ability of PPARγ to the DR1 element and the withdrawal of overexpressed PPARγ using specific antibody inhibited the protein DNA complex formation. Furthermore, ChIP q-RT-PCR method showed the pulled down endogenous PPARγ was bound to the DR1 element. Therefore, PPARγ binds to the mouse *Seipin* promoter and regulates its expression.

The DR1 element of the mouse *seipin* consensus sequence is quite different to the general AGGTCA N AGGTCA DR1 motif. This variation might be useful for cells to regulate the expression of certain group of genes. It has been shown in this study that PPARγ alone could promote the expression of the *Seipin* gene and the presence of RXRα further enhanced the expression level. It would be better if the cell line used did not contained PPARγ and RXRα. However, the huge increased of luciferase signal indicated that the heterodimer could bind to the DR1 element of the *Seipin* promoter and induced the expression. Mouse *Seipin* contains two transcript variants and the shorter transcript has an alternate 5' UTR, although they translated into the same protein. PPARγ binds to the DR1 element upstream of the longer transcript; does PPARγ also regulate the expression of the shorter transcript or does it regulates both long and short isoforms? From published ChIP-Seq data on mouse adipocytes, there was no PPARγ binding site identified upstream of the short transcript. If the two transcripts translate into the same protein, is there any tissue specific distribution of the two transcripts? There was another potential transcriptional start site identified during the examination of the mouse *Seipin* gene. This potential shortest transcript is slightly

smaller than the short transcript, but it was not sure if it actually expressed. Three sets of qRT-PCR primers were designed to check the expression of the three transcripts during 3T3-L1 adipocyte differentiation (Figure 4.10). The qRT-PCR showed that the predicted transcript was not expressed during adipogenesis. Interestingly, the short transcript was highly expressed during adipogenesis. The longest transcript increased in day 4 and then decreased back to basal level. Therefore, there must be a transcriptional regulation mechanism to control the expression of the two transcripts. Depends on different tissues, PPARγ might recruit different co-activators or other transcription factors to the *Seipin* promoter and regulate the expression of different transcript variants. The longer isoform might be highly expressed in the brain or in the liver, but the short variant might be highly expressed in adipose tissue.

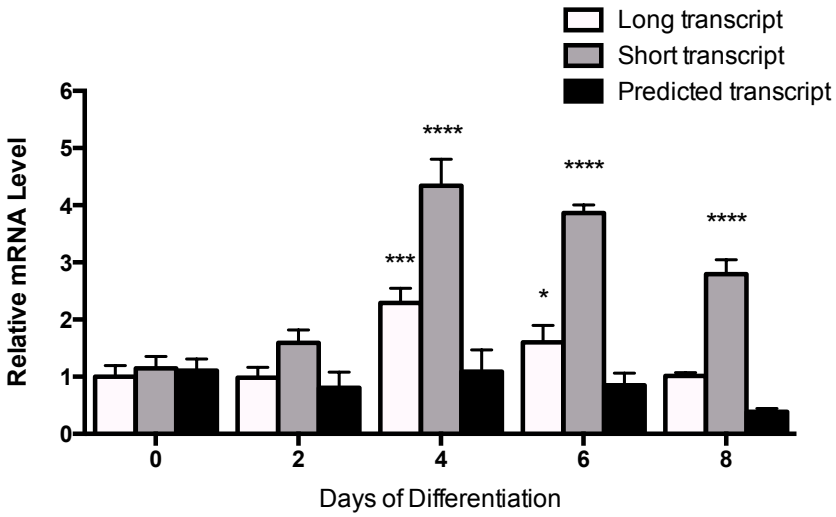

Figure 4.10 Expression of mouse *Seipin* transcripts during 3T3-L1 adipocyte differentiations. qRT-PCR was performed to check the expression of three mouse *Seipin* transcripts during adipogenesis. The predicted transcript was the shortest variant with an alternate 5' UTR. However, there was no significant change to the expression level of this transcript. The short transcript was the major variant that induced greatly during adipogenesis after 4 days of differentiation. The long transcript had the highest expression at day 4 and then decreased back to basal level after day 6. *** $p < 0.0001$, **** $p < 0.00001$, $n = 3$.

Seipin is essential in the differentiation of adipocytes in both human and mouse[35, 70, 72]. It has been shown that adipogenesis was inhibited when seipin was not functional. Also, the absence of *fld1*, the yeast orthologue of Seipin, led to increased in phosphatidic acid (PA) in yeast[25]. Studies also showed that lysophosphatidic acid acts as PPARγ agonist[178, 179]. Thus, the increased of PA may act as antagonist of PPARγ and inhibit adipogenesis. At the transcriptional level, there might be a regulation loop between Seipin and PPARγ. As the master regulator of adipogenesis, PPARγ binds to the promoter of *Seipin* and regulates its expression. It is an elegant mechanism and tiny changes in certain lipid level might influence the differentiation process. Seipin might be a transporter and itself can sense certain type of lipids, like PA. In a physiological point of view, adipogenesis is triggered after a high fat meal and cells try to package excess lipids into lipid droplets as triacylglycerol (TAG). PA is the precursor for TAG synthesis. In this case, PA is directed to TAG synthesis and leads to low PA level and Seipin may play a role in this pathway. Lipid mass spectrometry should be able to find out which PA species are increased in the Seipin deficient cells and ligand binding assay could be done to see if PA actually binds to PPARγ.

4.9 Conclusion

This chapter described the finding of a potential PPARγ binding site in the promoter region of mouse *Seipin.* Although this DR1 site is not conserved at the same location in the human SEIPIN promoter, luciferase assay showed there was a PPARγ binding site located within 2.5kb upstream of the human *SEIPIN* TSS. This study clearly showed PPARγ could regulate the expression of *Seipin* in both human and mouse and the formation of PPARγ/RXRα heterodimer further enhanced the expression of *Seipin*.

5. Chapter 5:Roles of Seipin in adipogenesis and Neuronal Growth

5.1 Background

Seipin is an ER membrane protein and its localisation to the ER was confirmed in several studies[30, 37, 70, 74]. Seipin has two transmembrane domains with both N and C termini facing the cytoplasm and a large luminal loop[75, 76]. However, it lacks any functional domains, which makes it hard to predict its function. The human *SEIPIN* encodes two isoforms, 398 and 462 amino acids in length, due to alternative translation initiation sites. The longer isoform has an additional of 64 amino acids at its N terminus. The central region of *SEIPIN* is well conserved in its orthologue in terms of secondary structure but both N and C termini are diverged. Yeast *fld1* has only 12 amino acids at its N terminus and 11 amino acids at the C terminus. Study showed the deletion of individual N terminus, the C terminus and the second transmembrane domain could result in ER localisation of the truncated Seipin indicating the first transmembrane domain is important for Seipin localisation[76]. More importantly, the full-length Seipin or mutant Seipin without the C terminus could rescue the supersized lipid droplet phenotype in yeast *fld1Δ* mutant suggesting an evolutionarily conserved function[30]. Furthermore, the C terminus of mammalian Seipin may have additional function that is not conserved in lower organisms.

It is known that Seipin is involved in adipogenesis; expression of transcription factors involved in this differentiation process was attenuated upon *SEIPIN* knockdown[35, 70]. There are two phases of adipogenesis. During the determination phase, mesenchymal stem cells are converted to preadipocytes. Then, genes required for the terminal differentiation are induced and preadipocytes are converted to adipocytes. In

our previous study in yeast *fld1Δ*, the level of microsomal PA was significantly increased. Our hypothesis is that PA may act as PPARγ antagonist and inhibit adipogenesis. Seipin knockout mouse showed significant reduction of major fat depots[72] and it represents the human lipodystrophy phenotype. Therefore, the understanding of the role of Seipin is not only beneficial for developing treatment for CGL, it is also important for the understanding of how adipogenesis is regulated.

As mentioned above, the gain of function mutation of *SEIPIN* could lead to mental retardation. It has been shown that the N88S and S90L mutants inhibited Seipin glycosylation results in an ER unfolded protein response and induces ER stress[74]. However, there is no study on lipid droplets in Seipin knockdown neuronal cells. In this chapter, the role of Seipin during adipogenesis and neuronal growth was explored and preliminary data showed the absence of Seipin during adipogenesis influenced PPARγ localisation to the nucleus. Also, the knockdown of *Seipin* in primary newborn mouse hippocampus neuronal cells inhibited neurite growth and supersized lipid droplets were observed in the knocked down cells.

5.2 Bscl2$^{-/-}$ MEFs accumulates supersized lipid droplets

We generated the first Seipin knockout mice using the Cre/loxP recombination system[72] with our collaborator overseas. The study showed complete loss of *Seipin* in multiple tissues, especially the adipose tissues. In order to study the role of Seipin during adipogenesis, mouse embryonic fibroblasts were used. However, due to the transportation issue with primary cells. The primary MEFs were immortalised using the SV40 T-antigen and the transfected MEFs were then passaged 10 times to select for the immortalised cells.

To confirm absence of *Seipin* in the knockout cells, qRT-PCR showed the Seipin gene *Bscl2* was absent (Figure 5.1). It is known that Seipin deficient fibroblasts accumulate lipid droplets[37]; fatty acid loading experiment was performed to confirm the phenotype. In order to observe the lipid droplets in the cells, BSA-coupled oleate was used to treat the MEFs for 6 hours and 14 hours. Figure 5.2 A shows *Bscl2*$^{-/-}$ accumulated large amount of small sized lipid droplets after 6 hours of oleate treatment. However, the wild type cells contained much less lipid droplets. After 14 hours of oleate treatment (Figure 5.2B), the Seipin knockout MEFs developed supersized lipid droplets and the largest lipid droplets observed were about 50 times the volume of the lipid droplets observed in the wild type cells. It has been shown in *C. elegans* that starvation would increase TAG to protein ratio result in increased lipid droplet size[180]. Prolong oleate treatment could lead to large sized lipid droplets formation even in the wild type cells. To further confirm the lack of *Seipin* would induce supersized lipid droplet formation. MEFs were starved for 8 hours and 24 hours to observe the lipid droplets. Figure 5.3A shows *Seipin* knockout MEFs accumulated more and larger size lipid droplets comparing to the wild type cells after 8 hours of starvation. After 24 hours of starvation, the *Seipin* knockout cells developed supersized lipid droplets and there were much less small sized lipid droplets observed in the wild type cells (Figure 5.3B). Therefore, the immortalisation process did not change the *Seipin* knockout fibroblast phenotype and these cells would be a good model system for our study.

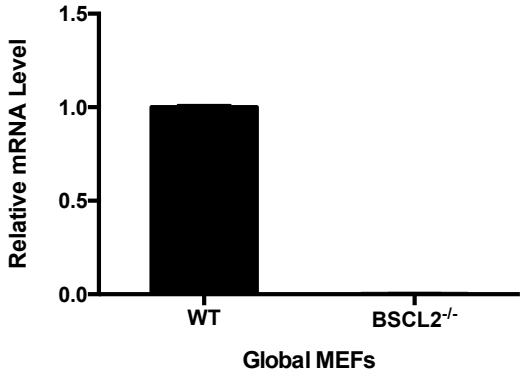

Figure 5.1 *Seipin* was absent in the *Bscl2*$^{-/-}$ MEFs. Total RNA from both wild type and *seipin* knockout MEFs were extracted for qRT-PCR analysis. qRT-PCR confirmed the *seipin* gene was abolished in the knockout MEFs.

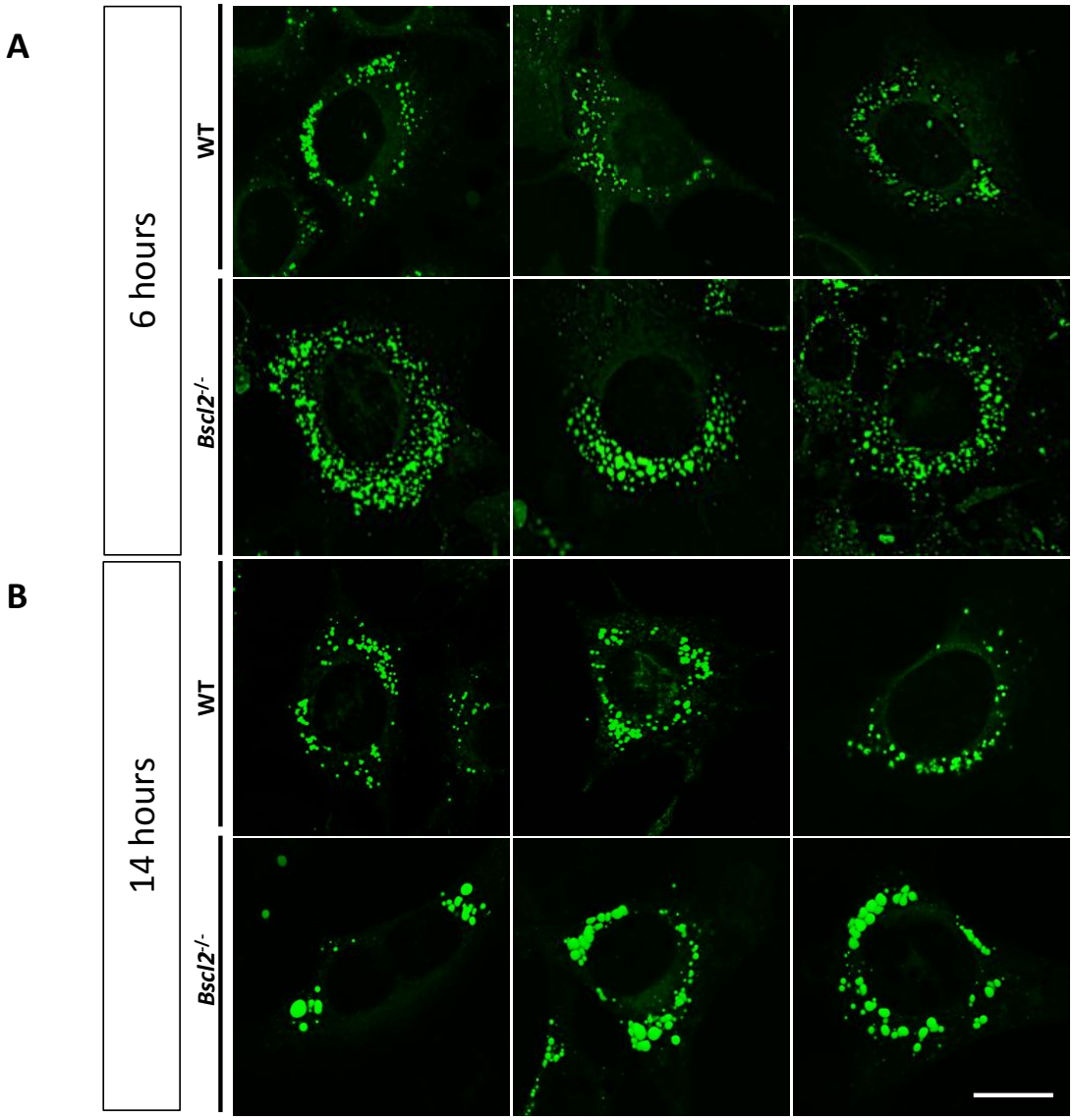

Figure 5.2 Oleate treatment of MEFs. Both wild type and *seipin* knockout MEFs were treated with 200μM BSA-coupled oleate for 6 hours and 14 hours. Lipid droplets were stained with BODIPY 493/503 and subjected to fluorescence microscopy. A. The wild type cells contained multiple small sized lipid droplets after 6 hours of treatment whereas the knockout cells had clusters of small sized lipid droplets. B. After 14 hours of oleate treatment, the knockout cells formed supersized lipid droplets and some of them were clustered together. In contrast, the lipid droplets of the wild type cells remained as small. Bar = 20μm.

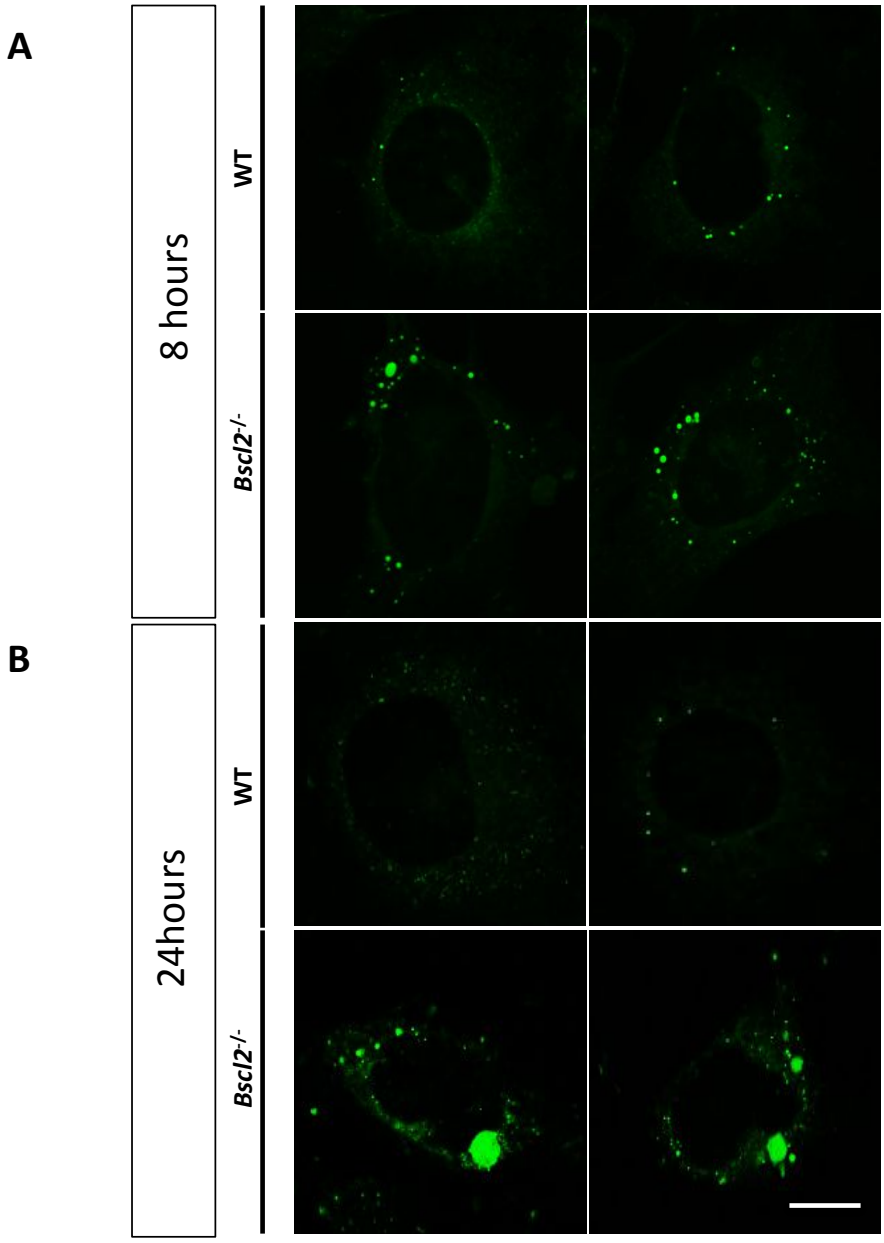

Figure 5.3 Starvation of *seipin* knockout MEFs accumulated supersized lipid droplets. Both wild type and *seipin* MEFs were cultured in starvation media for 8 hours and 24 hours. Lipid droplets were stained with BODIPY 493/503 and subjected to fluorescence microscopy. A. After 8 hours of starvation, the wild type cells contained tiny lipid droplets. In contrast, the knockout cells had larger sized lipid droplets comparing to the wild type cells. B. After 24 hours of starvation, the knockout cells contained supersized lipid droplets comparing to the tiny ones in the wild type cells. Bar = 20μm.

5.3 Seipin knockout MEFs failed to differentiate into adipocytes

It is well known that Seipin deficiency leads to impairment of adipogenesis in human and mouse. To see if the immortalised MEFs still have the ability to differentiate into adipocyte, differentiation cocktail was used to induce adipocyte differentiation. This was because the immortalisation process could lead to the loss of the differentiation ability of the cells. Both wild type and Seipin knockout MEFs were induced for differentiation using the 3T3-L1 differentiation protocol. The cells were differentiated for 8 days and their total RNAs were extracted for qRT-PCR analysis. Figure 5.4 shows the expression level of PPARγ and other adipogenic marker genes. The wild type cells were able to differentiate into mature adipocytes whereas the *Seipin* knockout MEFs showed no sign of differentiation. The qRT-PCR showed the PPARγ level increased in the first 2 days of adipogenesis in the *Seipin* knockout cells and then decreased back to the original level. This indicated the loss of Seipin would affect the activation of PPARγ and the expression of other adipogenic genes was also affected. The Oil Red O staining of the 8 day differentiated wild type cells and *Seipin* knockout cells confirmed the qRT-PCR results where the *Seipin* knockout cells were not able to differentiate into adipocytes. Therefore, the immortalisation process did not affect the ability of the MEFs to differentiate into adipocytes and the lack of *Seipin* totally inhibited adipogenesis.

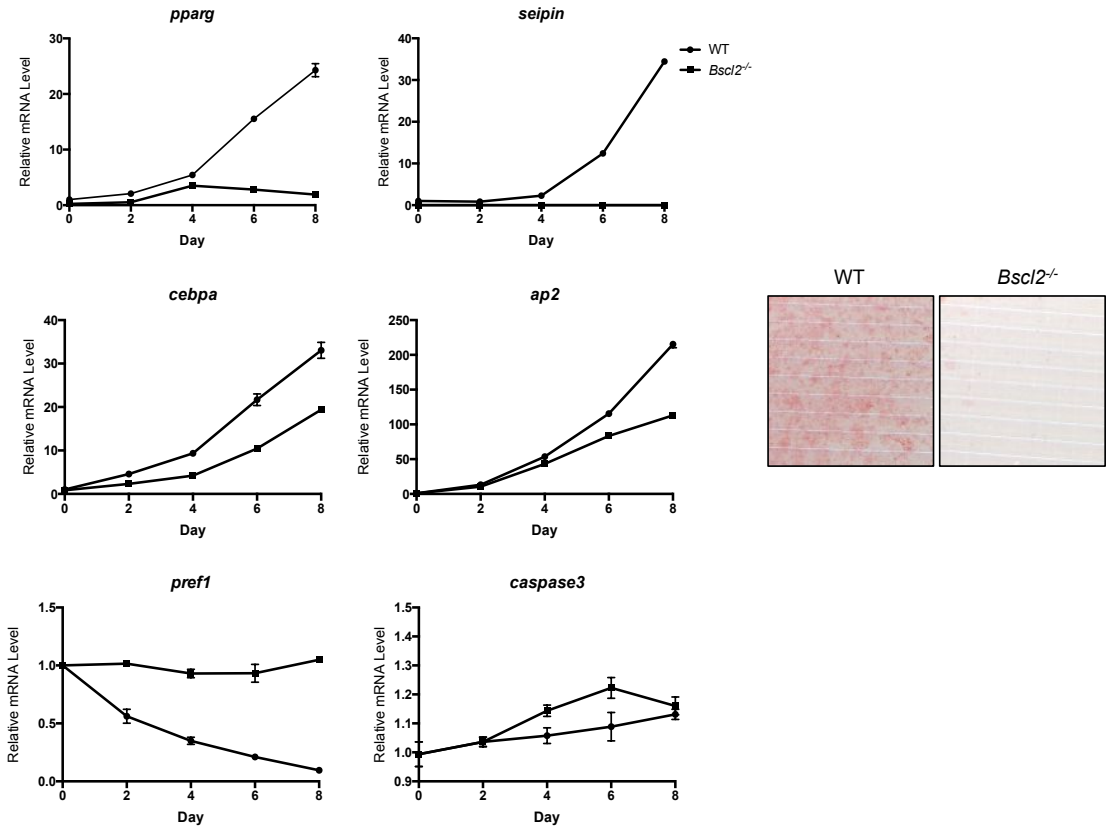

Figure 5.4 *Seipin* knockout MEFs were not be able to differentiate into adipocytes and PPARγ activation was inhibited. qRT-PCR showed the expression of *pparg* was attenuated and the expression of other adipogenic marker genes *cebpa* and *ap2* were also decreased in the *seipin* knockout MEFs. Oil Red O staining showed the *seipin* knockout MEFs were unable to differentiate into adipocytes comparing to the wild type cells.

5.4 Rosiglitazone rescued adipocyte differentiation defect of Seipin knockout MEFs

There was a controversy of the ability of PPARγ agonist TZD to rescue the adipogenic defect of Seipin knockout cells[81, 174]. One group claimed the treatment of Seipin knockout cells with Pioglitazone could not rescued the differentiation defect whereas the other group could partially restored the function of *Seipin* knockout adipocytes using the same drug. Rosiglitazone specifically binds to PPARγ and makes cells more sensitive to insulin. The differentiation of *Seipin* knockout MEFs with rosiglitazone

greatly improved the differentiation efficiency and rescued the differentiation defect of the cells. The total RNAs were extracted from 8 days differentiated MEFs (Figure 5.5), qRT-PCR showed the differentiation with rosiglitazone added throughout the experiment significantly increased the expression of adipogenic marker genes, especially PPARγ, the master regulator of adipogenesis. Although rosiglitazone did not fully rescued the *Seipin* knockout MEFs to the extent of the wild type cells, Oil Red O staining showed about 40% of the cells were differentiated into adipocytes.

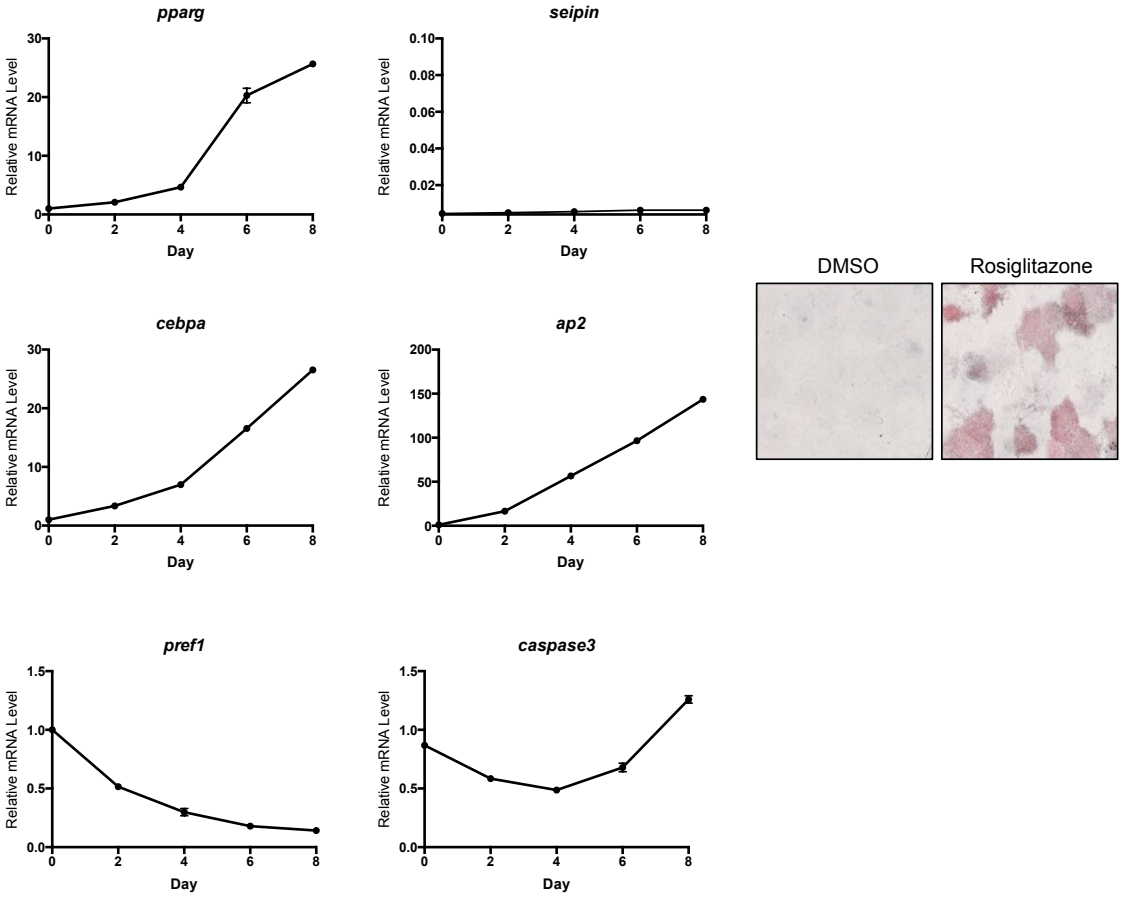

Figure 5.5 Rosiglitazone rescued the expression of *pparg* of *Seipin* knockout MEFs. 1μM of rosiglitazone was added to the media throughout 8 days of adipocyte differentiation. The expression of *pparg* was greatly increased in the presence of rosiglitazone and the knockout MEFs were differentiated (Oil Red O staining).

An interesting phenotype was observed in the differentiated Seipin knockout adipocytes. The size of the lipid droplets in the differentiated Seipin knockout adipocytes was much larger than the wild type cells. The differentiated wild type cells contained multiple large and small sized lipid droplets. However, the Seipin knockout adipocytes contained huge supersized lipid droplets, most of cells contained one supersized lipid droplet surrounding by multiple tiny lipid droplets (Figure 5.6). It is known that *fld1/seipin* deletion in yeast and *Drosophila* results in TAG accumulation[30, 38], the formation of extremely large sized lipid droplets in the Seipin knockout adipocytes may due to the accumulation of TAG. However, were these extremely large sized lipid droplets formed by local lipid synthesis or fusion of lipid droplets? Live cell imaging of 6-day differentiating Seipin knockout MEFs showed these extremely large sized lipid droplets were formed by fusion of neighbouring lipid droplets (Figure 5.7).

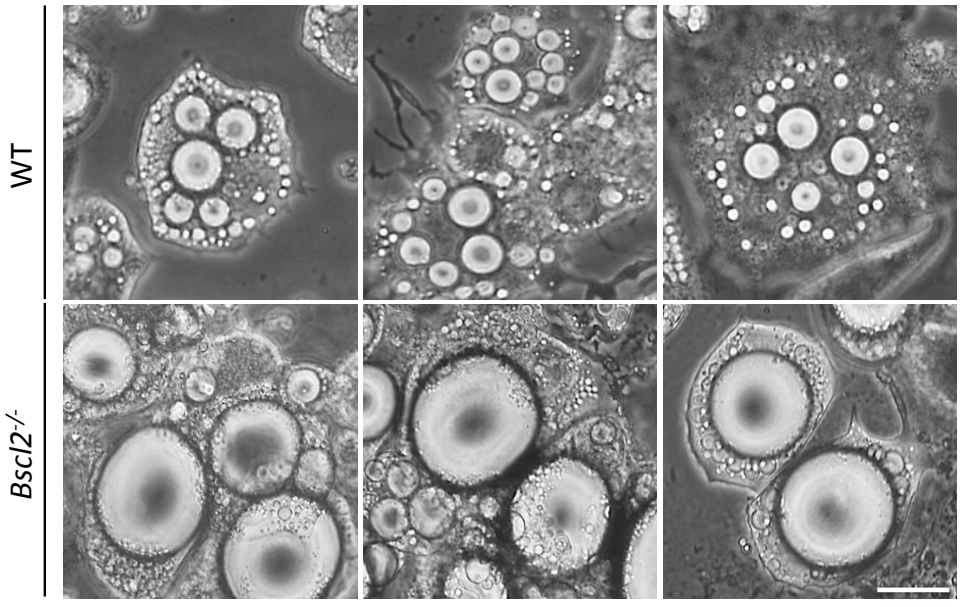

Figure 5.6 Differentiated *Seipin* knockout MEFs accumulated extremely large sized lipid droplets. Both MEFs were differentiated for 8 days in the presence of rosiglitazone. The differentiated *Seipin* knockout MEFs had one extremely large supersized lipid droplets surrounded by small sized lipid droplets. In contrast, the wild type adipocytes contained multiple large sized lipid droplets. Bar = 20μm.

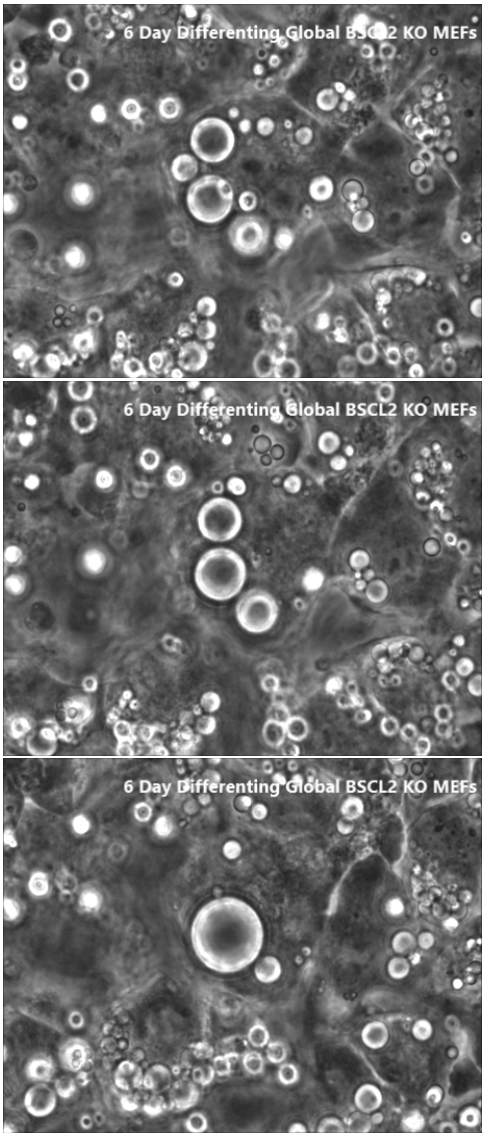

Figure 5.7 Live cell imaging showed the differentiating *Seipin* knockout MEFs. *Seipin* knockout MEFs were differentiated in the presence of rosiglitazone. The formation of the extremely supersized lipid droplets in the knockout cells was observed starting after 6 days of differentiation.

5.5 PPARγ loss nuclear localisation in the Seipin knockout MEFs during adipogenesis

The lack of Seipin impaired adipogenesis and the expression level PPARγ was greatly affected. It is not only the master regulator of adipogenesis, but it also regulates genes for fatty acid storage and glucose metabolism[181]. The localisation of PPARγ, as a transcription factor, to the nucleus is very important for the initiation of transcription.

The protein level of PPARγ during 8 days of adipogenesis was examined (Figure 5.8). In the wild type MEFs, PPARγ protein level increased dramatically from day 2 onward. However, there was no detectable PPARγ observed in the *Seipin* knockout MEFs. Phosphorylation of PPARγ at serine 112 has been shown to increased adipogenesis in mouse fibroblasts[182-184]. Western blotting showed that the phosphorylation of PPARγ at serine 112 was increased during adipogenesis in the wild type MEFs but not in the *Seipin* knockout cells.

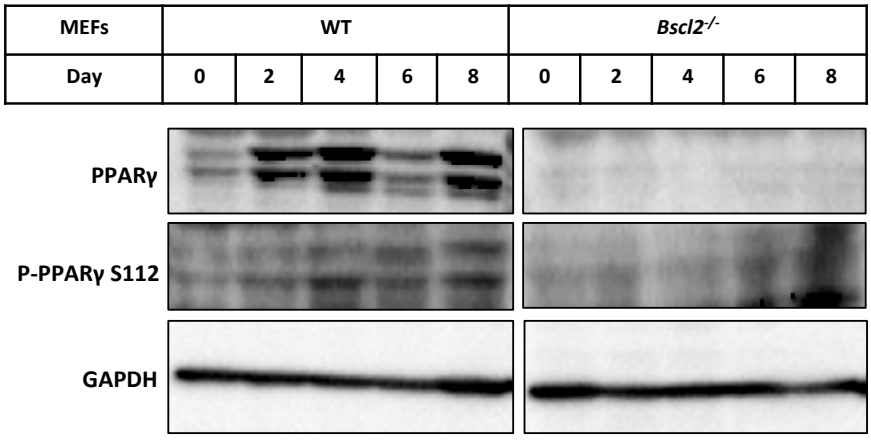

Figure 5.8 Western blot of PPARγ and phospho-PPARγ (P-PPARγ) S112 detected in wild type and *seipin* knockout MEFs. PPARγ and P-PPARγ S112 were detected in the wild type MEFs and the protein level was increased during 8 days of adipogenesis. In contrast no obvious PPARγ and P-PPARγ was detected in the *seipin* knockout MEFs.

The localisation of PPARγ was then examined by immunofluorescence study. Both wild type and *Seipin* knockout MEFs were differentiated with hormonal cocktail and cells were harvested on day 0, 2, 4, 6 and 8. PPARγ was then detected with primary antibody and labelled with green fluorescence secondary antibody. The DAPI staining represented the nucleus of the cells (Figure 5.9). From the immunofluorescence study, it clearly showed the enrichment of the PPARγ fluorescence signal was increasing from

day 2 and was highly enriched on day 8. In contrast, the localisation of the PPARγ fluorescence signal was loss in the *Seipin* knockout MEFs.

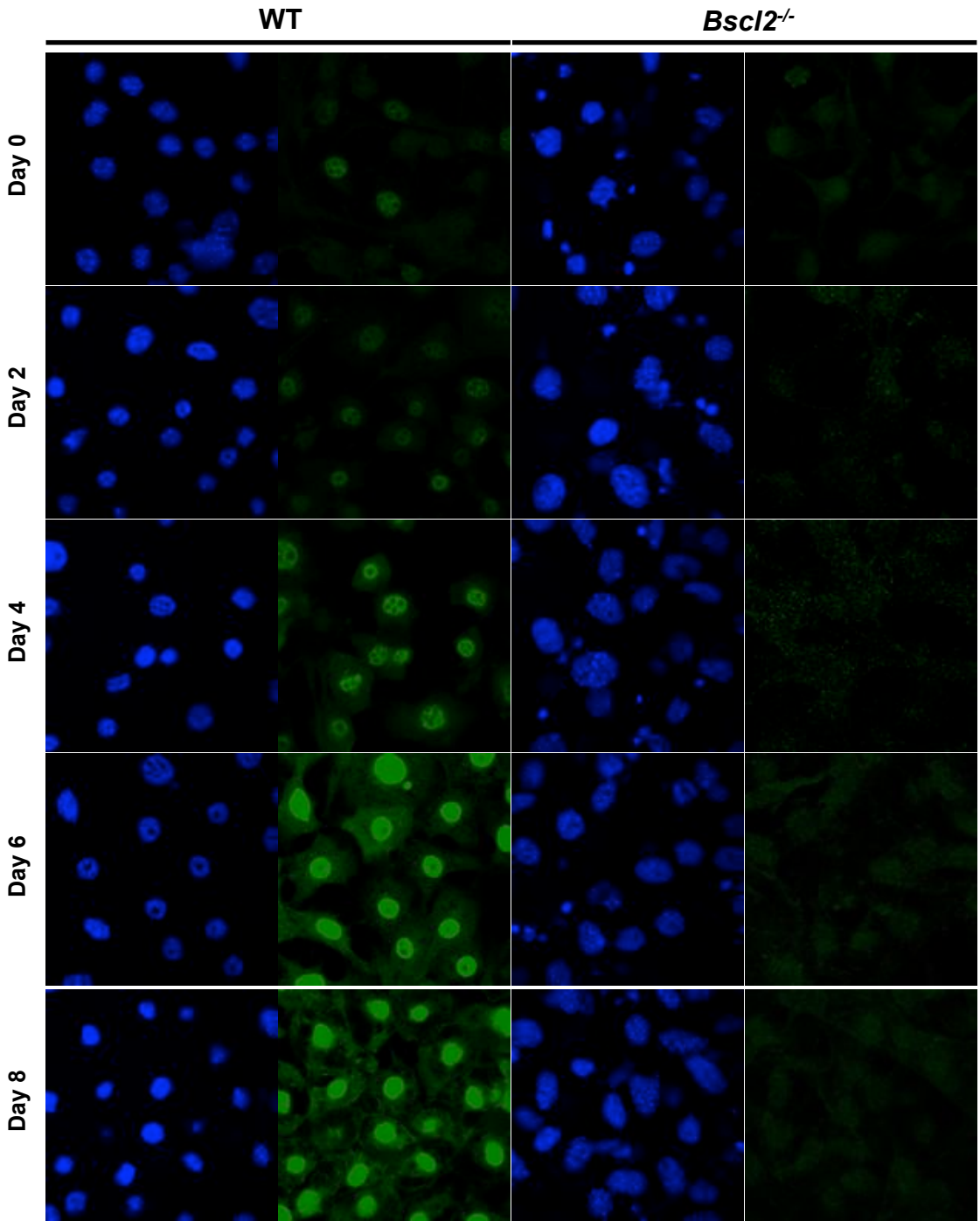

Figure 5.9 Immunofluorescence of PPARγ in wild type and *seipin* knockout MEFs during adipogenesis. Both wild type and *seipin* knockout MEFs were differentiated for 2, 4, 6 and 8 days. PPARγ was detected with specific antibody and it was labelled with Alexa 488 secondary antibody. The nucleus were stained with DAPI. Cells were then subjected to immunofluorescence microscopy. PPARγ was highly enriched in the wild type cells during differentiation. In contrast, no obvious PPARγ fluorescence signal was detected in the knockout cells.

The addition of rosiglitazone in the differentiation cocktail rescued the differentiation defect of *Seipin* knockout MEFs. It was interesting to see if the drug could restore the nuclear localisation of PPARγ in the Seipin deficient MEFs during adipogenesis. The *Seipin* knockout MEFs were differentiated using the same protocol, except rosiglitazone was included during the whole differentiation process. Figure 5.10 shows the *Seipin* knockout MEFs differentiated without rosiglitazone was not be able to differentiate into adipocytes. On the other hand, the addition of the drug clearly restored the nuclear localisation of PPARγ (green immunofluorescence signal) and the DIC microscopy showed the lipid droplets of the differentiated adipocytes. Therefore, the differentiation defect of the *Seipin* knockout cells was due to the lack of PPARγ in the nucleus and this defect was restored with rosiglitazone.

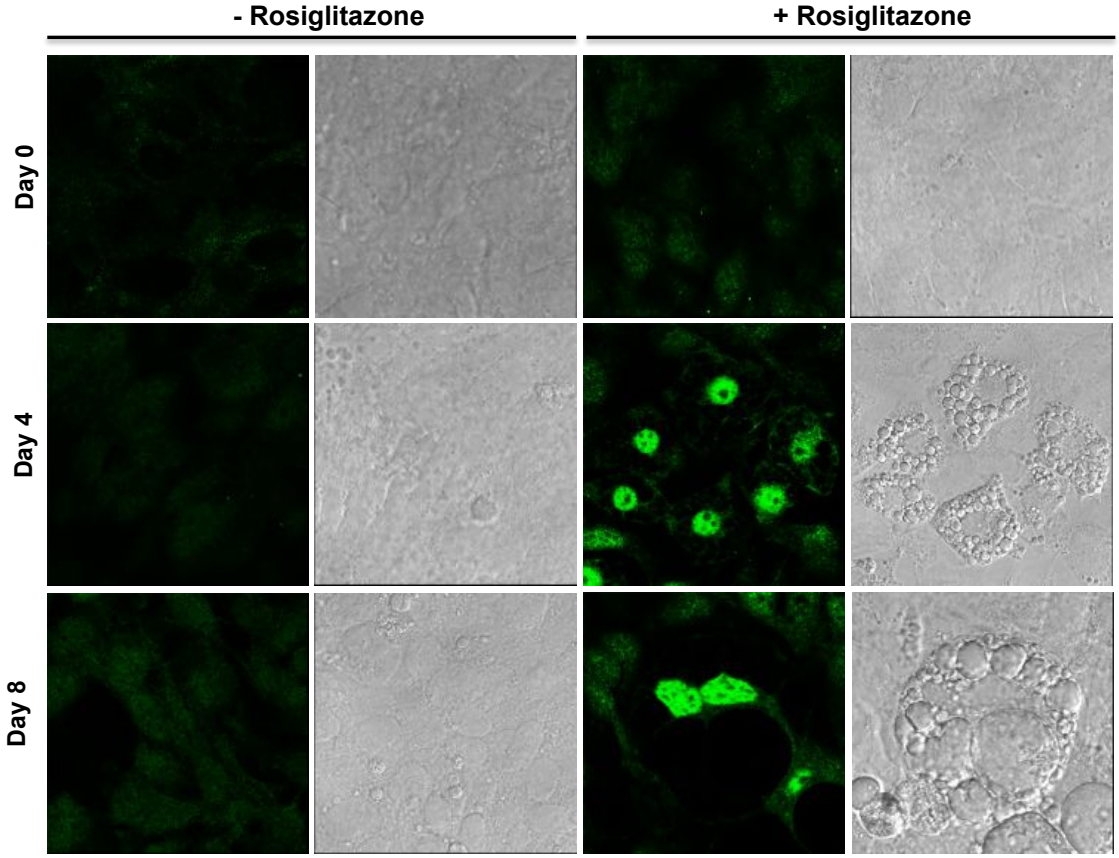

Figure 5.10 Rosiglitazone restored the PPARγ localisation in the nucleus of *Seipin* knockout adipocytes. *Seipin* knockout MEFs were subjected to adipocyte differentiation for 4 and 8 days in the presence of rosiglitazone. PPARγ was detected with specific antibody and it was labelled with Alexa 488 secondary antibody. The localisation of PPARγ was restored in the presence of rosigltason during adipocyte differentiation.

5.6 Increased PA level in the Seipin knockout MEFs

Previous study in yeast showed the phospholipid PA was significantly increased in the microsomes of *fld1* yeast mutant[25]. We hypothesised PA may act as PPARγ antagonist and inhibit adipogenesis. Also, this fusogenic phospholipid may promote the fusion of lipid droplets as shown in the differentiated Seipin knockout adipocytes (Figure 5.6). The infection of both wild type and *Seipin* knockout MEFs with lentiviral vector of RFP-PA sensor, which consisting of RFP fused to the phosphatidic acid binding domain of yeast Spo20p, clearly showed increased PA level in the knockout MEFs (Figure 5.11).

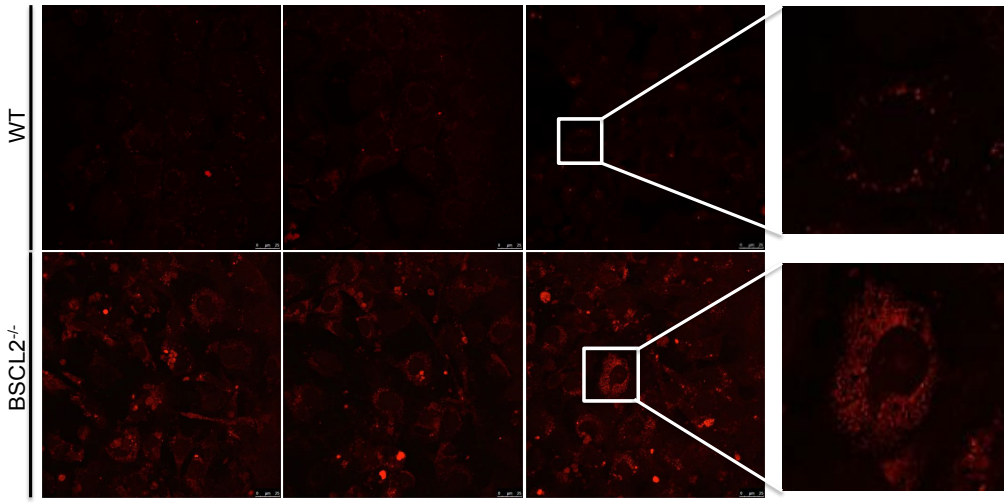

Figure 5.11 *Seipin* knockout MEFs accumulated high level of PA. Both wild type and *Seipin* knockout MEFs were infected with RFP-PA sensor lentiviral vector. Stable cell lines of both MEFs were obtained. Fluorescence microscopy revealed that the *seipin* knockout MEFs contained high level of PA, which is represented as red RFP fluorescence signal.

5.7 Knockdown of Seipin in primary newborn mouse hippocampus neurons promoted supersized lipid droplet formation and inhibited neurite growth

It is known that Seipin is highly expressed in the brain and the mutation of Seipin causes neuronal disorders. It is interesting to see if there is any phenotype when *Seipin* is knocked down in primary newborn mouse hippocampus neuronal cells. The

knockdown of *Seipin* in the primary cells was achieved with electroporation. BSA-coupled oleate was added to favour the formation of lipid droplets and lipid droplets were then detected using ADRP antibody. Figure 5.12A shows that the *Seipin* knocked down cells had supersized lipid droplets. However, the control cells had multiple lipid droplets and their sizes were small. Due to the limited supply of the primary cells, the knockdown efficiency of the siRNA was confirmed in NIH3T3 cells (Figure 5.12B).

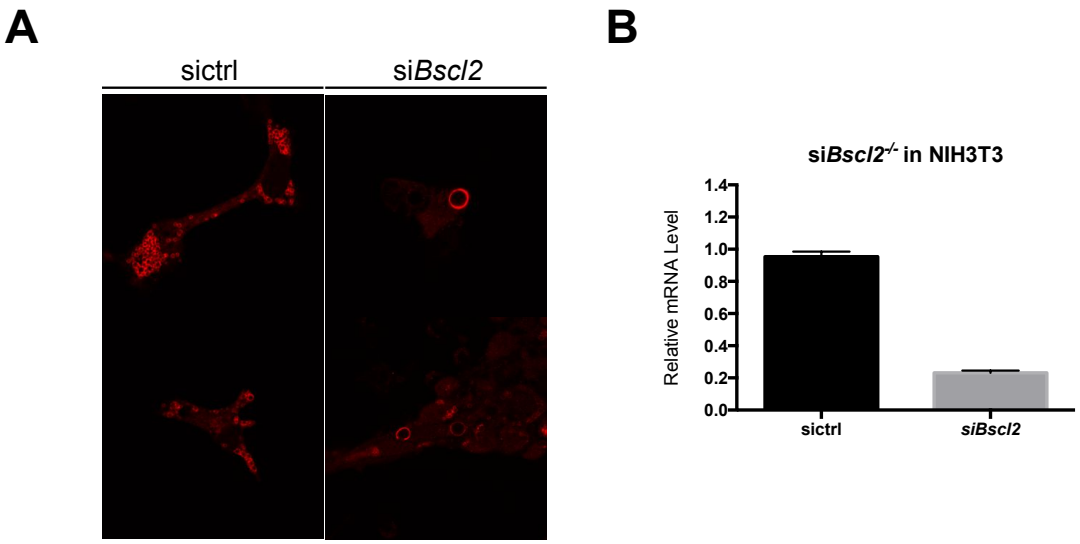

Figure 5.12 Knockdown of *Seipin* in primary newborn mouse hippocampus neurons promote supersized lipid droplet formation. A. *Seipin* was knockdown with siRNA for 24 hours and cells were treated with 200μM BSA-coupled oleate for 14 hours. Lipid droplets were detected with ADRP antibody and labelled with Alexa 568 secondary antibody. Supersized lipid droplets were observed only in the knockdown cells. B. The efficiency of the siRNA was confirmed with qRT-PCR. About 80% of *Seipin* was silent.

The knockdown of *Seipin* also inhibited neurite growth. The same transfection protocol was used but the cells were not treated with oleate due to the fact that fatty acid treatment may affect neurite growth. Empty GFP was co-transfected with the siRNA to confirm the transfected cells were knocked down. Figure 5.13 shows the transfection of Seipin siRNA inhibited neurite growth comparing to the control cells and the neurite length from 100 cells of each group was measured. The length of the neurites of the

Seipin knocked down cells was significantly decreased comparing to the control cells. Although this was a preliminary observation, it indicated the cause of neuronal diseases may be due to the inhibition of neuronal growth in patients with seipinopathy.

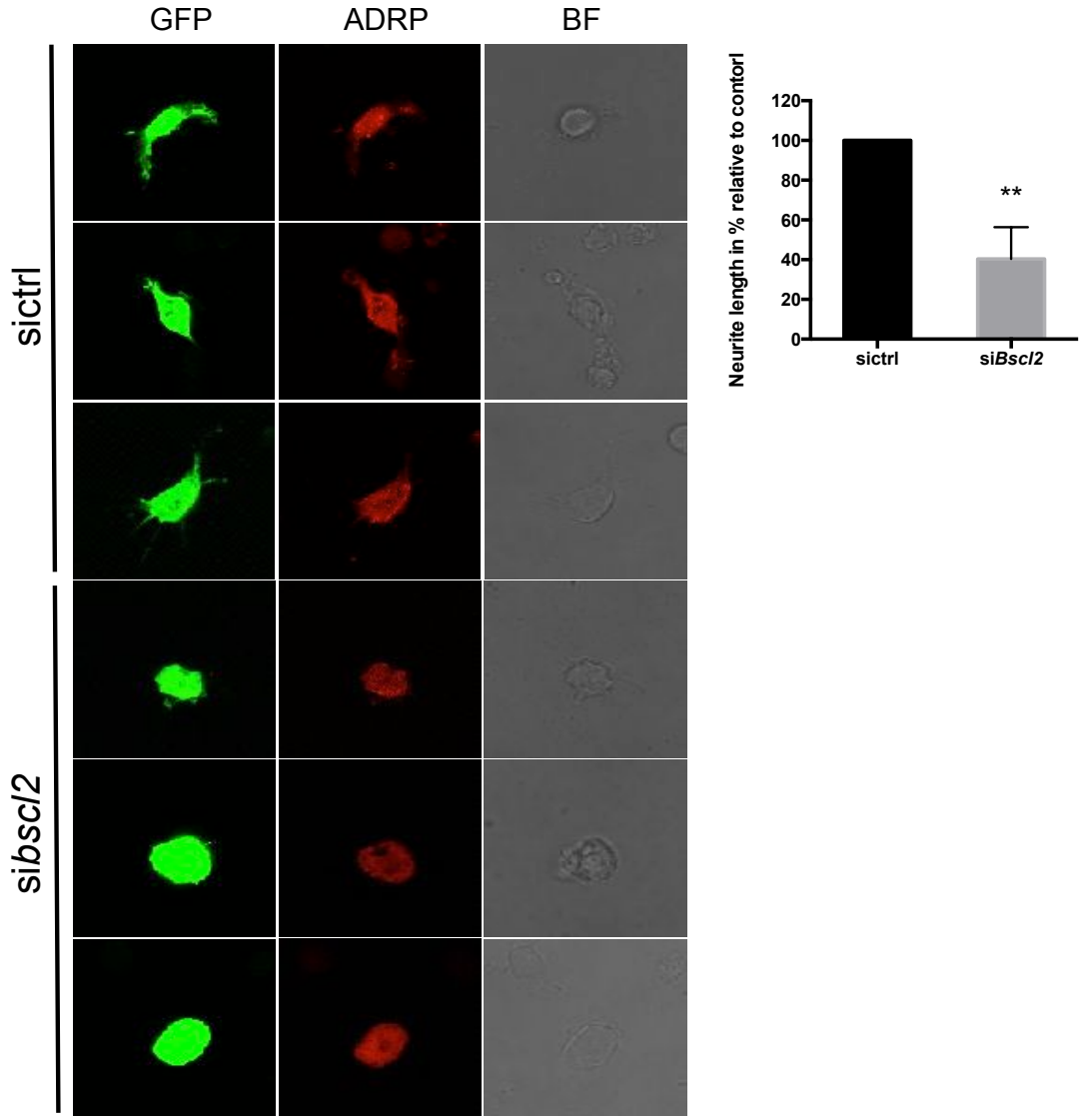

Figure 5.13 Knockdown of *Seipin* in primary newborn mouse hippocampus neuronal cells decreased neurite growth. *Seipin* was knocked down in primary hippocampus neuronal cells for 24 hours. GFP empty plasmid was co-transfected with siRNAs to confirm the cells observed were the knocked down cells. Lipid droplets were not observed without the treatment of oleate (ADRP). Neurite length of 100 cells from each group was measured and the length is represented in percentage relative to the control cells. ** $p < 0.001$, n=150.

5.8 Discussion

Seipin plays important roles at both cellular and systemic level. At the cellular level it helps to maintain lipid droplet size and at the systemic level, it involves in the differentiation of adipocytes. The increasing prevalence of obesity and diabetes attracted more attention on the understating of lipid storage and metabolism. Lack of Seipin increases TAG accumulation resulting in supersized lipid droplet formation in yeast, flies and mammalian cells. In yeast, the knockout of *fld1/seipin* increases microsomal PA level and leads to lipid droplet fusion due to its fusogenic characteristic. The increase of PA may also inhibit PPARγ activation through direct binding. Study showed lysophosphatidic acid could act as PPARγ agonist[178]. Thus, it is possible that PA may act as PPARγ antagonist and inhibit adipogenesis in the *Seipin* knockout cells.

The generation of *Seipin* knockout mice provided a great model to study its function. The accumulation of supersized lipid droplets in the *Seipin* knockout MEFs confirmed its role in the regulation of lipid droplet size. Studies showed that Seipin works closely to TAG synthesis[30, 37]. The localisation of Seipin may suggest its role in the packaging of TAG into lipid droplets. Importantly, the overexpression of the DGAT enzyme can rescue the lipid droplet phenotype in flies[38]. Studies in yeast and flies suggested the impairment of phospholipid synthesis would lead to supersized lipid droplet formation. In those studies, the knocking down of phosphocholine cytidylytransferase (*Cct1* or *Cct2*), the rate-limiting enzyme for phosphatidylcholine (PC) synthesis, increased the relative amount of phosphatidylentholamine (PE). PE is a cone shaped phospholipid that can increase membrane curvature and promote membrane fusion. The impairment of PC synthesis also increases TAG synthesis and lipid droplets may fuse to reduce surface-to-volume ratio due to increased ratio of TAG-

to-phospholipid[25, 31]. *In vitro* study showed small increased of PA in liposomes was sufficient to promote lipid droplet fusion[25]. The *Seipin* knockout MEFs accumulated high level of PA as shown in Figure 5.11. However, lipid mass spectrometry could be done to identify the specific PA species that were increased in the MEFs. This may help us to identify the actual PPARγ antagonist PA species.

The adipocyte differentiation defect of *Seipin* knockout MEFs was rescued with rosiglitazone. There was controversy that TZDs could not rescue the adipogenesis defect. However, this study confirmed with other group that rosiglitazone could rescue adipocyte differentiation in MEFs[81]. Western blotting showed the protein level of PPARγ was completely abolished in the *Seipin* knockout MEFs during adipogenesis. qRT-PCR also showed the expression level of *pparg* and *cebpa* were greatly affected, but the inclusion of rosiglitazone fully rescued their expression. Rosiglitazone also restored the nuclear localisation of PPARγ in the *Seipin* knockout MEFs during adipogenesis. This shows a potential treatment for patients with lipodystrophy. However, animal study is necessary to confirm the positive effect of rosiglitazone *in vivo*.

Extremely large sized lipid droplets were observed in the differentiated *Seipin* knockout MEFs. After 8 days of differentiation, wild type cells contained multiple, normally 3 or 4 large sized lipid droplets and some small lipid droplets. In contrast, the differentiated *Seipin* knockout adipocytes with the aid of rosiglitazone contained, usually just one extremely large supersized lipid droplet. Live cell imaging revealed that the extremely large sized lipid droplets were formed through fusion of contacting lipid droplets. The fusion of lipid droplets in the *Seipin* knockout adipocytes might be due to increase level

of PA. Extraction of the lipid droplets from the *Seipin* knockout adipocytes for lipid mass spectrometry analysis may help us to identify specific species of PA that promote lipid droplet fusion. It has been shown that FSP27 facilitates lipid transfer from small lipid droplets to larger lipid droplets under internal pressure during lipid droplet fusion[23]. However, this process usually takes quite a long time. The fusion event observed in the *Seipin* knockout adipocytes took about 30 minutes to 1 hour to complete. Therefore, Seipin may control the size of lipid droplets indirectly through the regulation of lipids, like PA and TAG.

This chapter also revealed a role of Seipin in neuronal growth. The knockdown of *Seipin* in primary newborn mouse hippocampus neurons significantly reduced neurite length. As a highly expressed protein in the brain, it was not surprised to see the knockdown of *Seipin* could affect neuronal growth. Interesting, oleate treatment on the *Seipin* knocked down neurons also promoted supersized lipid droplet formation. This suggested that Seipin is involved in both lipid metabolism and neuronal growth in the brain. Due to the limited supply of the cells, lipid analysis of the knocked down cells should tell us more about the lipid composition in these cells. The inhibition of neuronal growth may explain the neurological-related disease phenotype.

5.9 Conclusion

This chapter showed the differentiation defect of *Seipin* knockout MEFs might be due to high level of PA. We hypothesised that PA may act as PPARγ antagonist. The addition of rosiglitazone in the differentiation media greatly rescued the differentiation defect and restored PPARγ localisation in the nucleus of the *Seipin* knockout MEFs

during adipogenesis. This chapter also explored the phenotype of *Seipin* knocked down hippocampus neurons. The decreased Seipin level in neurons reduced neurite length and fatty acid medium promoted supersized lipid droplet formation in the *Seipin* knocked down neuronal cells.

6. Chapter 6: Final Conclusion and Future Direction

6.1 Involvement of the PI3K/Akt/mTORC1 Pathway in NPC1 Degradation

The observation of increased free cholesterol accumulation in the HPV negative C33A cervical cancer cells revealed a novel degradation pathway of the cholesterol trafficking protein NPC1. The same cholesterol accumulation phenotype was also observed in LNCaP prostate cancer cells. One major characteristic of the LNCaP cells is the frame-shift mutation of PTEN, a tumour suppressor protein that inhibits PI3 kinase dependent signalling[185]. The mutation of the PTEN leads to hyperactive Akt pathway. Similarly, the major characteristic observed in the C33A cells was high phospho-Akt (P-Akt) level. The finding of high Akt level in both cells lead to the hypothesis of Akt-dependent NPC1 degradation. The phosphorylation of Akt through either transfection of constitutively active Akt or insulin treatment promoted NPC1 degradation. Glucose infusion study in rats showed the same mechanism was also conserved *in vivo*. High proliferation is one of the characteristics of cancer cells due to highly active mTOR pathway, especially the mTORC1 pathway. The mTORC1 pathway is a complex and tightly regulated control centre of cells. The hyperactive Akt in the C33A cells leads to further hypothesis that mTORC1 may involve in the degradation of NPC1 and the rescuing of NPC1 when raptor was knocked down proved this speculation.

Raptor is an essential binding protein of mTORC1; the knock down of raptor inhibits mTORC1 activation. This study showed the knockdown of raptor dramatically rescued NPC1 from degradation. However, downstream targets of mTORC1 were not examined in this study. One of the potential targets for future study will be the S6 kinase 1 (S6K1). It has been shown that S6K1 targets the tumour suppressor programmed cell

death protein 4 (PDCD4) for ubiquitination via the ubiquitin ligase $SCF^{\beta TRCP}$[186]. Therefore, it is possible that S6K1 either directly or indirectly controls the ubiquitination of NPC1. S6K1 inhibitor treatment would be great to see if the inhibition of S6K1 would rescue NPC1 degradation. It has been shown that NPC1 could be ubiquitinated and it is important to see if the inhibition of S6K1 also decreased ubiquitination of NPC1. It is also necessary to activate mTORC1 in other cell lines to see this mechanism is not only conserved in cervical cancer cells, although the Akt-dependent degradation of NPC1 was confirmed in several cell lines in this study. The ultimate goal of finding the specific E3 ligase would be necessary to have a complete picture of this novel pathway. Several potential E3 ligases were knocked down, but none of them showed a clear reduction of NPC1 ubiquitination (data not shown). Immunoprecipitation together with protein mass spectrometry may help us to identify the E3 ligase.

This study also showed the knockdown of NPC1 in HepG2 cells or the absence of NPC1 in human fibroblasts led to decreased phosphorylation of Akt. It has been shown the hepatocyte insulin receptor function was significantly impaired in *Npc1*$^{-/-}$ mice[187]. This suggested a possible role of NPC1 in the insulin signaling pathway. The degradation of NPC1 via the mTORC1 pathway may help to regulate the insulin/PI3K pathway. When the PI3K pathway is activated upon insulin stimulation, prolong insulin stimulation leads to high mTORC1 level. In order to turn off the pathway, cells may target the insulin receptor for degradation. It is known that insulin receptor could be targeted for degradation via the binding of Grb10. It may also be possible that the degradation of NPC1 via the mTORC1 pathway would inhibit the insulin pathway with a yet identified mechanism.

The accumulation of free cholesterol in cancer cells has shown to improve the resistance of chemotherapeutic drugs. Although the treatment of mevastatin did not have any effect on the C33A cells (data not shown), methods to lower free cholesterol in C33A might improve the efficiency of chemotherapy. It has been shown in chapter 3 that the inhibition of Akt phosphorylation was able to rescue NPC1 from degradation. However, the restoration of NPC1 upon pharmacological treatment or transfection of dominant Akt did not completely cleared the free cholesterol accumulated in the cells. Because most of the drug treatments were done for a longest period of 16 hours, it would be good to see if prolong treatment could lead to the clearance of free cholesterol in C33A cells and improve the efficiency of chemotherapeutic drugs.

In summary, this study revealed a new regulation mechanism of the mTORC1 pathway on NPC1 degradation. Furthermore, it may provide important findings on the understanding of the role of mTORC1 on the insulin pathway. Also, it may help to develop treatment for chemotherapeutic drug resistant cancer cells.

6.2 PPARγ regulates the expression of mouse Seipin

PPARγ is the master regulator of adipogenesis. It regulates the expression of genes involved in lipid metabolism, inflammation and adipogenesis. In this study, a novel PPARγ binding site was discovered within the promoter region of the mouse *Seipin* gene. The binding of PPARγ to the newly identified DR1 element promoted *Seipin* expression and the co-expression of both PPARγ and RXRα further increased the expression level of *Seipin*. Gel shift assay showed the PPARγ band was intensified when PPARγ was overexpressed. More importantly, the mutation of the DR1 element

completely abolished the binding of PPARγ to the probe. Also, the incubation of the probe with PPARγ antibody abolished the binding. The overexpression of both PPARγ and RXRα showed slightly higher molecular weight band suggesting the heterodimer was bound to the probe. Similarly, the incubation of the probe with PPARγ antibody shifted the band and the mutation of the DR1 element abolished the binding of the heterodimer. The binding ability of PPARγ was then further confirmed with ChIP qRT-PCR. The pulled down PPARγ bound DNA was confirmed as the newly identified DR1 element within the mouse *Seipin* promoter. However, this novel DR1 site is not conserved at the same location in the human *SEIPIN* promoter region. Luciferase assay showed PPARγ enhanced the expression of the human *SEIPIN* gene, but the binding site of PPARγ to the human *SEIPIN* promoter is still not clear. Overall, this chapter showed PPARγ/RXRα heterodimer binds to the DR1 site within the mouse *Seipin* promoter and regulates its expression.

Both luciferase and gel shift assays used HeLa cells as the host for PPARγ and RXRα overexpression. HeLa cells contained low amount of both transcription factors, cell lines without both transcription factors would be a better choice for the experiments. However, the results showed a clear difference to the control suggesting the reliability of the assays. ChIP raw data from Lefterova's study also showed a second PPARγ peak in the middle of the mouse *Seipin* gene. Although it might not be able to induce the expression of *Seipin*, it might act as enhancer for the expression of *Seipin*. Also, it might be an enhancer for other lipid-related genes. Similar experiments like luciferase and gel shift assays could be done to see if PPARγ actually binds to this site and promotes the expression of the luciferase reporter gene. In chapter 4, only two transcription factors were studied. It is believed that there are more co-activators or other lipid-related

transcription factors may bind to the promoter region of *Seipin*. Immunoprecipitation study could be done to identify proteins that may bind to the PPARγ complex during adipogenesis. After the finding of potential candidates, ChIP assay could be followed to see if the proteins actually bind to the candidate sites.

Prediction showed the PPARγ binding site of the human *SEIPIN* gene was located approximately 2kb upstream of the TSS. Although luciferase assay showed positive result, the exact binding site is still unknown. Truncations of the promoter region could be cloned into luciferase reporter plasmid to find out the region that gives the positive reading. The binding site could then be narrowed down to certain region and the mutation of the site could be done to see if PPARγ binds. ChIP qRT-PCR could be used to confirm if the binding is conserved *in vivo*.

In summary, PPARγ forms heterodimer with RXRα and the binding of the heterodimer to the mouse *Seipin* promoter initiates transcription. Gel shift assay confirmed PPARγ binds to the novel DR1 site and ChIP qRT-PCR showed the endogenous PPARγ was bound to the same site during adipogenesis.

6.3 Role of Seipin in adipogenesis and neuronal growth

The lack of Seipin greatly impairs adipogenesis from preadipocytes and its absence in other cells would lead to lipid imbalance resulting in supersized lipid droplet formation. At the systemic level, the knockout of *Seipin* in MEFs inhibited adipocyte differentiation. The disruption of adipogenesis may be due to the increase of PA, although there was no direct evidence in this study showing PA was the antagonist of

PPARγ. Transfecting cells with PA sensor showed there were great amount of PA detected in the *Seipin*$^{-/-}$ MEFs. The differentiation of the *Seipin*$^{-/-}$ MEFs was rescued when TZD rosiglitazone was included in the differentiation cocktail. The loss of PPARγ nuclear localisation in the nucleus of the knockout cells may be the cause of the differentiation defect. During adipogenesis, the nuclear localisation of PPARγ was enriched after 2 days of differentiation and the expression of PPARγ was increased in the wild type MEFs. However, both nuclear localisation and expression of PPARγ were impaired in the knockout MEFs. The addition of rosiglitazone restored the nuclear localisation of PPARγ and rescued the differentiation defect, although Seipin was absent. This suggested the differentiation defect was not directly due to the lack of Seipin; it was due to the imbalance of lipid that influenced the process. At the cellular level, *Seipin*$^{-/-}$ MEFs accumulated supersized lipid droplets that were observed from either fatty acid overloading or starvation. Interestingly, the differentiated *Seipin* knockout adipocytes contained extremely large sized lipid droplets comparing to the wild type cells. Importantly, those extremely large sized lipid droplets were formed through fusion of neighbouring lipid droplets. Fusion event was also observed in the yeast *fld1*Δ cells and the knockout yeast cells had significantly increase microsomal PA[25]. The fusogenic phospholipid PA may cause the fusion of lipid droplets in the differentiated *Seipin* knockout adipocytes. The deletion of *cds1*, encodes CDP-diacylglcerol synthases, also has increased PA level and lipid droplet fusion was observed[25]. Cds1 is responsible for the synthesis of CDP-DAG, the deletion of Cds1 causes accumulation of PA and it was observed in our study that the knockdown of Cds1 also inhibited adipogenesis. It has been shown that lysophosphatidic acid is the PPARγ agonist[178], it is possible that PA may act as PPARγ antagonist

Lipid analysis of the *Seipin*$^{-/-}$ knockout MEFs should be done to confirm the PA sensor experiment. Lipid mass spectrometry provides a better picture of changes in lipid composition between the wild type and knockout cells. In yeast, the increase of PE to PC ratio causes lipid droplet fusion. Therefore, it is important to find out the total level of each lipid class. It is suspected that the cause of lipid droplet fusion in the knockout cells was due to increased PA. Another experiment to do is to extract the lipid droplets from the MEFs and do lipid analysis. Similar experiment should be done in the differentiated MEFs. Because the differentiated *Seipin* knockout MEFs contained extremely large lipid droplets, it is important to examine the changes of lipid composition in the lipid droplets of the differentiated knockout MEFs. TAG level may also increase and promote the formation of larger lipid droplets. It is known that the lack of Seipin causes increased TAG level[37]. Thus, it is possible that Seipin may interact with enzymes in the TAG synthesis pathway. Study has been shown that myc tagged Seipin can inducibly interact with lipin1[188]. Importantly, loss-function-mutation of *lipin1* in fatty liver dystrophic (fld) mice causes lipodystrophy and it is important for adipogenesis. Therefore, Seipin may regulate the level of PA through the interaction with enzymes involved in the TAG biosynthesis pathway.

The knockdown of *Seipin* in newborn mouse hippocampus neuronal cells was observed with reduced neurite growth and the knocked down cells had supersized lipid droplets upon fatty acid treatment. It is known that Seipin is highly expressed in brains and toxic gain-of-function mutation of *Seipin* causes neurological diseases[73]. Due to the limited supply of the primary cells in this study, using the *Seipin* knockout mice would be better to perform biochemical studies instead of using siRNA. In this study, only the lipid droplets and neuronal growth were examined. It is good to check the distribution of

Seipin in neurons with or without oleic acid treatment. Brains from Seipin knockout mice could be isolated for lipidomics analysis. Lipid metabolism in neurons is sensitive to change; minute changes in lipid composition might be toxic to neuronal cells. The changes may affect the lipid composition of the lipid rafts on plasma membrane. Thus, lipid raft markers could be used to examine difference between wild type and *Seipin* knockout neurons. Lastly, the overexpression of lipin1 and DGAT could be done to lower the PA level in *Seipin* knockout neurons to see if it can rescue the neuronal growth defect.

In summary, the differentiation defect of *Seipin* knockout MEFs may be due to high level of PA accumulation and PA may act as PPARγ antagonist. Rosiglitazone rescued the differentiation defect and restored nuclear localisation of PPARγ in the knockout cell. It is also the first time to observe neuronal growth defect in mouse newborn hippocampus neuronal cells upon *Seipin* knockdown.

In summary, this thesis reports a novel degradation mechanism of the PI3K/Akt/mTORC1 pathway on the cholesterol trafficking protein NPC1. Also, the role of Seipin during adipogenesis was examined and the loss of PPARγ in the nucleus of Seipin knockout MEFs was found to be the cause of the differentiation defect. Furthermore, Seipin deficiency affected neurite growth.

References

1. Ogawa, K., T. Hishiki, Y. Shimizu, K. Funami, K. Sugiyama, Y. Miyanari, and K. Shimotohno, *Hepatitis C virus utilizes lipid droplet for production of infectious virus.* Proc Jpn Acad Ser B Phys Biol Sci, 2009. **85**(7): p. 217-228.
2. Spandl, J., D. Lohmann, L. Kuerschner, C. Moessinger, and C. Thiele, *Ancient ubiquitous protein 1 (AUP1) localizes to lipid droplets and binds the E2 ubiquitin conjugase G2 (Ube2g2) via its G2 binding region.* J Biol Chem, 2011. **286**(7): p. 5599-5606.
3. Wang, X., T.J. Reape, X. Li, K. Rayner, C.L. Webb, K.G. Burnand, and P.G. Lysko, *Induced expression of adipophilin mRNA in human macrophages stimulated with oxidized low-density lipoprotein and in atherosclerotic lesions.* FEBS Lett, 1999. **462**(1-2): p. 145-150.
4. Fujimoto, T., H. Kogo, K. Ishiguro, K. Tauchi, and R. Nomura, *Caveolin-2 is targeted to lipid droplets, a new "membrane domain" in the cell.* J Cell Biol, 2001. **152**(5): p. 1079-1085.
5. Liu, P., Y. Ying, Y. Zhao, D.I. Mundy, M. Zhu, and R.G. Anderson, *Chinese hamster ovary K2 cell lipid droplets appear to be metabolic organelles involved in membrane traffic.* J Biol Chem, 2004. **279**(5): p. 3787-3792.
6. Umlauf, E., E. Csaszar, M. Moertelmaier, G.J. Schuetz, R.G. Parton, and R. Prohaska, *Association of stomatin with lipid bodies.* J Biol Chem, 2004. **279**(22): p. 23699-23709.
7. Scott, C. and Y.A. Ioannou, *The NPC1 protein: structure implies function.* Biochim Biophys Acta, 2004. **1685**(1-3): p. 8-13.

8. Murphy, D.J., *The biogenesis and functions of lipid bodies in animals, plants and microorganisms.* Prog Lipid Res, 2001. **40**(5): p. 325-438.

9. Thiele, C. and J. Spandl, *Cell biology of lipid droplets.* Curr Opin Cell Biol, 2008. **20**(4): p. 378-385.

10. Bartz, R., W.H. Li, B. Venables, J.K. Zehmer, M.R. Roth, R. Welti, R.G. Anderson, P. Liu, and K.D. Chapman, *Lipidomics reveals that adiposomes store ether lipids and mediate phospholipid traffic.* J Lipid Res, 2007. **48**(4): p. 837-847.

11. Fujimoto, T., Y. Ohsaki, J. Cheng, M. Suzuki, and Y. Shinohara, *Lipid droplets: a classic organelle with new outfits.* Histochem Cell Biol, 2008. **130**(2): p. 263-279.

12. Tauchi-Sato, K., S. Ozeki, T. Houjou, R. Taguchi, and T. Fujimoto, *The surface of lipid droplets is a phospholipid monolayer with a unique Fatty Acid composition.* J Biol Chem, 2002. **277**(46): p. 44507-44512.

13. Welte, M.A., *Proteins under new management: lipid droplets deliver.* Trends Cell Biol, 2007. **17**(8): p. 363-369.

14. Bickel, P.E., J.T. Tansey, and M.A. Welte, *PAT proteins, an ancient family of lipid droplet proteins that regulate cellular lipid stores.* Biochim Biophys Acta, 2009.

15. Martin, S. and R.G. Parton, *Lipid droplets: a unified view of a dynamic organelle.* Nat Rev Mol Cell Biol, 2006. **7**(5): p. 373-378.

16. Ducharme, N.A. and P.E. Bickel, *Lipid droplets in lipogenesis and lipolysis.* Endocrinology, 2008. **149**(3): p. 942-949.

17. Cermelli, S., Y. Guo, S.P. Gross, and M.A. Welte, *The lipid-droplet proteome reveals that droplets are a protein-storage depot.* Curr Biol, 2006. **16**(18): p. 1783-1795.

18. Ohsaki, Y., J. Cheng, M. Suzuki, Y. Shinohara, A. Fujita, and T. Fujimoto, *Biogenesis of cytoplasmic lipid droplets: From the lipid ester globule in the membrane to the visible structure.* Biochim Biophys Acta, 2008.

19. Zechner, R., J.G. Strauss, G. Haemmerle, A. Lass, and R. Zimmermann, *Lipolysis: pathway under construction.* Curr Opin Lipidol, 2005. **16**(3): p. 333-340.

20. Bezaire, V. and D. Langin, *Regulation of adipose tissue lipolysis revisited.* Proc Nutr Soc, 2009. **68**(4): p. 350-360.

21. Lafontan, M. and D. Langin, *Lipolysis and lipid mobilization in human adipose tissue.* Prog Lipid Res, 2009. **48**(5): p. 275-297.

22. Bostrom, P., L. Andersson, M. Rutberg, J. Perman, U. Lidberg, B.R. Johansson, J. Fernandez-Rodriguez, J. Ericson, T. Nilsson, J. Boren, and S.O. Olofsson, *SNARE proteins mediate fusion between cytosolic lipid droplets and are implicated in insulin sensitivity.* Nat Cell Biol, 2007. **9**(11): p. 1286-1293.

23. Gong, J., Z. Sun, L. Wu, W. Xu, N. Schieber, D. Xu, G. Shui, H. Yang, R.G. Parton, and P. Li, *Fsp27 promotes lipid droplet growth by lipid exchange and transfer at lipid droplet contact sites.* J Cell Biol, 2011. **195**(6): p. 953-963.

24. Ariotti, N., S. Murphy, N.A. Hamilton, L. Wu, K. Green, N.L. Schieber, P. Li, S. Martin, and R.G. Parton, *Postlipolytic insulin-dependent remodeling of micro lipid droplets in adipocytes.* Mol Biol Cell, 2012. **23**(10): p. 1826-1837.

25. Fei, W., G. Shui, Y. Zhang, N. Krahmer, C. Ferguson, T.S. Kapterian, R.C. Lin, I.W. Dawes, A.J. Brown, P. Li, X. Huang, R.G. Parton, M.R. Wenk, T.C.

Walther, and H. Yang, *A role for phosphatidic acid in the formation of "supersized" lipid droplets.* PLoS Genet, 2011. **7**(7): p. e1002201.

26. Kuerschner, L., C. Moessinger, and C. Thiele, *Imaging of lipid biosynthesis: how a neutral lipid enters lipid droplets.* Traffic, 2008. **9**(3): p. 338-352.

27. Stone, S.J., M.C. Levin, P. Zhou, J. Han, T.C. Walther, and R.V. Farese, Jr., *The endoplasmic reticulum enzyme DGAT2 is found in mitochondria-associated membranes and has a mitochondrial targeting signal that promotes its association with mitochondria.* J Biol Chem, 2009. **284**(8): p. 5352-5361.

28. Krahmer, N., Y. Guo, F. Wilfling, M. Hilger, S. Lingrell, K. Heger, H.W. Newman, M. Schmidt-Supprian, D.E. Vance, M. Mann, R.V. Farese, Jr., and T.C. Walther, *Phosphatidylcholine synthesis for lipid droplet expansion is mediated by localized activation of CTP:phosphocholine cytidylyltransferase.* Cell Metab, 2011. **14**(4): p. 504-515.

29. McFie, P.J., S.L. Banman, S. Kary, and S.J. Stone, *Murine diacylglycerol acyltransferase-2 (DGAT2) can catalyze triacylglycerol synthesis and promote lipid droplet formation independent of its localization to the endoplasmic reticulum.* J Biol Chem, 2011. **286**(32): p. 28235-28246.

30. Fei, W., G. Shui, B. Gaeta, X. Du, L. Kuerschner, P. Li, A.J. Brown, M.R. Wenk, R.G. Parton, and H. Yang, *Fld1p, a functional homologue of human seipin, regulates the size of lipid droplets in yeast.* J Cell Biol, 2008. **180**(3): p. 473-482.

31. Guo, Y., T.C. Walther, M. Rao, N. Stuurman, G. Goshima, K. Terayama, J.S. Wong, R.D. Vale, P. Walter, and R.V. Farese, *Functional genomic screen reveals genes involved in lipid-droplet formation and utilization.* Nature, 2008. **453**(7195): p. 657-661.

32. Tansey, J.T., C. Sztalryd, J. Gruia-Gray, D.L. Roush, J.V. Zee, O. Gavrilova, M.L. Reitman, C.X. Deng, C. Li, A.R. Kimmel, and C. Londos, *Perilipin ablation results in a lean mouse with aberrant adipocyte lipolysis, enhanced leptin production, and resistance to diet-induced obesity.* Proc Natl Acad Sci U S A, 2001. **98**(11): p. 6494-6499.

33. van Meer, G., D.R. Voelker, and G.W. Feigenson, *Membrane lipids: where they are and how they behave.* Nat Rev Mol Cell Biol, 2008. **9**(2): p. 112-124.

34. Agarwal, A.K. and A. Garg, *Seipin: a mysterious protein.* Trends Mol Med, 2004. **10**(9): p. 440-444.

35. Payne, V.A., N. Grimsey, A. Tuthill, S. Virtue, S.L. Gray, E. Dalla Nora, R.K. Semple, S. O'Rahilly, and J.J. Rochford, *The human lipodystrophy gene BSCL2/seipin may be essential for normal adipocyte differentiation.* Diabetes, 2008. **57**(8): p. 2055-2060.

36. Szymanski, K.M., D. Binns, R. Bartz, N.V. Grishin, W.P. Li, A.K. Agarwal, A. Garg, R.G. Anderson, and J.M. Goodman, *The lipodystrophy protein seipin is found at endoplasmic reticulum lipid droplet junctions and is important for droplet morphology.* Proc Natl Acad Sci U S A, 2007. **104**(52): p. 20890-20895.

37. Fei, W., H. Li, G. Shui, T.S. Kapterian, C. Bielby, X. Du, A.J. Brown, P. Li, M.R. Wenk, P. Liu, and H. Yang, *Molecular characterization of seipin and its mutants: implications for seipin in triacylglycerol synthesis.* J Lipid Res, 2011. **52**(12): p. 2136-2147.

38. Tian, Y., J. Bi, G. Shui, Z. Liu, Y. Xiang, Y. Liu, M.R. Wenk, H. Yang, and X. Huang, *Tissue-autonomous function of Drosophila seipin in preventing ectopic lipid droplet formation.* PLoS Genet, 2011. **7**(4): p. e1001364.

39. Cui, X., Y. Wang, L. Meng, W. Fei, J. Deng, G. Xu, X. Peng, S. Ju, L. Zhang, G. Liu, L. Zhao, and H. Yang, *Overexpression of a short human seipin/BSCL2 isoform in mouse adipose tissue results in mild lipodystrophy.* Am J Physiol Endocrinol Metab, 2012. **302**(6): p. E705-713.

40. Nishino, N., Y. Tamori, S. Tateya, T. Kawaguchi, T. Shibakusa, W. Mizunoya, K. Inoue, R. Kitazawa, S. Kitazawa, Y. Matsuki, R. Hiramatsu, S. Masubuchi, A. Omachi, K. Kimura, M. Saito, T. Amo, S. Ohta, T. Yamaguchi, T. Osumi, J. Cheng, T. Fujimoto, H. Nakao, K. Nakao, A. Aiba, H. Okamura, T. Fushiki, and M. Kasuga, *FSP27 contributes to efficient energy storage in murine white adipocytes by promoting the formation of unilocular lipid droplets.* J Clin Invest, 2008. **118**(8): p. 2808-2821.

41. Martin, S., K. Driessen, S.J. Nixon, M. Zerial, and R.G. Parton, *Regulated localization of Rab18 to lipid droplets: effects of lipolytic stimulation and inhibition of lipid droplet catabolism.* J Biol Chem, 2005. **280**(51): p. 42325-42335.

42. Miura, S., J.W. Gan, J. Brzostowski, M.J. Parisi, C.J. Schultz, C. Londos, B. Oliver, and A.R. Kimmel, *Functional conservation for lipid storage droplet association among Perilipin, ADRP, and TIP47 (PAT)-related proteins in mammals, Drosophila, and Dictyostelium.* J Biol Chem, 2002. **277**(35): p. 32253-32257.

43. Robenek, H., M.J. Robenek, I. Buers, S. Lorkowski, O. Hofnagel, D. Troyer, and N.J. Severs, *Lipid droplets gain PAT family proteins by interaction with specialized plasma membrane domains.* J Biol Chem, 2005. **280**(28): p. 26330-26338.

44. van Meer, G., *Caveolin, cholesterol, and lipid droplets?* J Cell Biol, 2001. **152**(5): p. F29-34.

45. Wolins, N.E., B. Rubin, and D.L. Brasaemle, *TIP47 associates with lipid droplets.* J Biol Chem, 2001. **276**(7): p. 5101-5108.

46. Bulankina, A.V., A. Deggerich, D. Wenzel, K. Mutenda, J.G. Wittmann, M.G. Rudolph, K.N. Burger, and S. Honing, *TIP47 functions in the biogenesis of lipid droplets.* J Cell Biol, 2009. **185**(4): p. 641-655.

47. Blouin, C.M., S. Le Lay, F. Lasnier, I. Dugail, and E. Hajduch, *Regulated association of caveolins to lipid droplets during differentiation of 3T3-L1 adipocytes.* Biochem Biophys Res Commun, 2008. **376**(2): p. 331-335.

48. Pol, A., R. Luetterforst, M. Lindsay, S. Heino, E. Ikonen, and R.G. Parton, *A caveolin dominant negative mutant associates with lipid bodies and induces intracellular cholesterol imbalance.* J Cell Biol, 2001. **152**(5): p. 1057-1070.

49. Salloum, S., H. Wang, C. Ferguson, R.G. Parton, and A.W. Tai, *Rab18 binds to hepatitis C virus NS5A and promotes interaction between sites of viral replication and lipid droplets.* PLoS Pathog, 2013. **9**(8): p. e1003513.

50. Vance, J.E., *Phosphatidylserine and phosphatidylethanolamine in mammalian cells: two metabolically related aminophospholipids.* J Lipid Res, 2008. **49**(7): p. 1377-1387.

51. Chernomordik, L.V. and M.M. Kozlov, *Mechanics of membrane fusion.* Nat Struct Mol Biol, 2008. **15**(7): p. 675-683.

52. Lin, C.S., Z.C. Xin, C.H. Deng, H. Ning, G. Lin, and T.F. Lue, *Defining adipose tissue-derived stem cells in tissue and in culture.* Histol Histopathol, 2010. **25**(6): p. 807-815.

53. Tang, Q.Q. and M.D. Lane, *Activation and centromeric localization of CCAAT/enhancer-binding proteins during the mitotic clonal expansion of adipocyte differentiation.* Genes Dev, 1999. **13**(17): p. 2231-2241.

54. Tontonoz, P. and B.M. Spiegelman, *Fat and beyond: the diverse biology of PPARgamma.* Annu Rev Biochem, 2008. **77**: p. 289-312.

55. Kim, J.B. and B.M. Spiegelman, *ADD1/SREBP1 promotes adipocyte differentiation and gene expression linked to fatty acid metabolism.* Genes Dev, 1996. **10**(9): p. 1096-1107.

56. Evans, R.M., G.D. Barish, and Y.X. Wang, *PPARs and the complex journey to obesity.* Nat Med, 2004. **10**(4): p. 355-361.

57. Tontonoz, P., E. Hu, and B.M. Spiegelman, *Stimulation of adipogenesis in fibroblasts by PPAR gamma 2, a lipid-activated transcription factor.* Cell, 1994. **79**(7): p. 1147-1156.

58. Pittas, A.G. and A.S. Greenberg, *Thiazolidinediones in the treatment of type 2 diabetes.* Expert Opin Pharmacother, 2002. **3**(5): p. 529-540.

59. Barish, G.D., V.A. Narkar, and R.M. Evans, *PPAR delta: a dagger in the heart of the metabolic syndrome.* J Clin Invest, 2006. **116**(3): p. 590-597.

60. Hofmann, C., K. Lorenz, S.S. Braithwaite, J.R. Colca, B.J. Palazuk, G.S. Hotamisligil, and B.M. Spiegelman, *Altered gene expression for tumor necrosis factor-alpha and its receptors during drug and dietary modulation of insulin resistance.* Endocrinology, 1994. **134**(1): p. 264-270.

61. Hollenberg, A.N., V.S. Susulic, J.P. Madura, B. Zhang, D.E. Moller, P. Tontonoz, P. Sarraf, B.M. Spiegelman, and B.B. Lowell, *Functional antagonism between CCAAT/Enhancer binding protein-alpha and peroxisome proliferator-*

activated receptor-gamma on the leptin promoter. J Biol Chem, 1997. **272**(8): p. 5283-5290.

62. Iwaki, M., M. Matsuda, N. Maeda, T. Funahashi, Y. Matsuzawa, M. Makishima, and I. Shimomura, *Induction of adiponectin, a fat-derived antidiabetic and antiatherogenic factor, by nuclear receptors.* Diabetes, 2003. **52**(7): p. 1655-1663.

63. Tomaru, T., D.J. Steger, M.I. Lefterova, M. Schupp, and M.A. Lazar, *Adipocyte-specific expression of murine resistin is mediated by synergism between peroxisome proliferator-activated receptor gamma and CCAAT/enhancer-binding proteins.* J Biol Chem, 2009. **284**(10): p. 6116-6125.

64. Forman, B.M., P. Tontonoz, J. Chen, R.P. Brun, B.M. Spiegelman, and R.M. Evans, *15-Deoxy-delta 12, 14-prostaglandin J2 is a ligand for the adipocyte determination factor PPAR gamma.* Cell, 1995. **83**(5): p. 803-812.

65. Forman, B.M., J. Chen, and R.M. Evans, *The peroxisome proliferator-activated receptors: ligands and activators.* Ann N Y Acad Sci, 1996. **804**: p. 266-275.

66. Forman, B.M., J. Chen, and R.M. Evans, *Hypolipidemic drugs, polyunsaturated fatty acids, and eicosanoids are ligands for peroxisome proliferator-activated receptors alpha and delta.* Proc Natl Acad Sci U S A, 1997. **94**(9): p. 4312-4317.

67. Poulsen, L., M. Siersbaek, and S. Mandrup, *PPARs: fatty acid sensors controlling metabolism.* Semin Cell Dev Biol, 2012. **23**(6): p. 631-639.

68. Hegele, R.A., *Lessons from human mutations in PPARgamma.* Int J Obes (Lond), 2005. **29 Suppl 1**: p. S31-35.

69. Magre, J., M. Delepine, E. Khallouf, T. Gedde-Dahl, Jr., L. Van Maldergem, E. Sobel, J. Papp, M. Meier, A. Megarbane, A. Bachy, A. Verloes, F.H. d'Abronzo,

E. Seemanova, R. Assan, N. Baudic, C. Bourut, P. Czernichow, F. Huet, F. Grigorescu, M. de Kerdanet, D. Lacombe, P. Labrune, M. Lanza, H. Loret, F. Matsuda, J. Navarro, A. Nivelon-Chevalier, M. Polak, J.J. Robert, P. Tric, N. Tubiana-Rufi, C. Vigouroux, J. Weissenbach, S. Savasta, J.A. Maassen, O. Trygstad, P. Bogalho, P. Freitas, J.L. Medina, F. Bonnicci, B.I. Joffe, G. Loyson, V.R. Panz, F.J. Raal, S. O'Rahilly, T. Stephenson, C.R. Kahn, M. Lathrop, J. Capeau, and B.W. Group, *Identification of the gene altered in Berardinelli-Seip congenital lipodystrophy on chromosome 11q13.* Nat Genet, 2001. **28**(4): p. 365-370.

70. Chen, W., V.K. Yechoor, B.H. Chang, M.V. Li, K.L. March, and L. Chan, *The human lipodystrophy gene product Berardinelli-Seip congenital lipodystrophy 2/seipin plays a key role in adipocyte differentiation.* Endocrinology, 2009. **150**(10): p. 4552-4561.

71. Boutet, E., H. El Mourabit, M. Prot, M. Nemani, E. Khallouf, O. Colard, M. Maurice, A.M. Durand-Schneider, Y. Chretien, S. Gres, C. Wolf, J.S. Saulnier-Blache, J. Capeau, and J. Magre, *Seipin deficiency alters fatty acid Delta9 desaturation and lipid droplet formation in Berardinelli-Seip congenital lipodystrophy.* Biochimie, 2009. **91**(6): p. 796-803.

72. Cui, X., Y. Wang, Y. Tang, Y. Liu, L. Zhao, J. Deng, G. Xu, X. Peng, S. Ju, G. Liu, and H. Yang, *Seipin ablation in mice results in severe generalized lipodystrophy.* Hum Mol Genet, 2011. **20**(15): p. 3022-3030.

73. Ito, D. and N. Suzuki, *Seipinopathy: a novel endoplasmic reticulum stress-associated disease.* Brain, 2009. **132**(Pt 1): p. 8-15.

74. Windpassinger, C., M. Auer-Grumbach, J. Irobi, H. Patel, E. Petek, G. Horl, R. Malli, J.A. Reed, I. Dierick, N. Verpoorten, T.T. Warner, C. Proukakis, P. Van

den Bergh, C. Verellen, L. Van Maldergem, L. Merlini, P. De Jonghe, V. Timmerman, A.H. Crosby, and K. Wagner, *Heterozygous missense mutations in BSCL2 are associated with distal hereditary motor neuropathy and Silver syndrome.* Nat Genet, 2004. **36**(3): p. 271-276.

75. Lundin, C., R. Nordstrom, K. Wagner, C. Windpassinger, H. Andersson, G. von Heijne, and I. Nilsson, *Membrane topology of the human seipin protein.* FEBS Lett, 2006. **580**(9): p. 2281-2284.

76. Ito, D., T. Fujisawa, H. Iida, and N. Suzuki, *Characterization of seipin/BSCL2, a protein associated with spastic paraplegia 17.* Neurobiol Dis, 2008. **31**(2): p. 266-277.

77. Wang, C.W., Y.H. Miao, and Y.S. Chang, *Size control of lipid droplets in budding yeast requires a collaboration of Fld1 and Ldb16.* J Cell Sci, 2014. **127**(6): p. 1214-28.

78. Kim, C.A., M. Delepine, E. Boutet, H. El Mourabit, S. Le Lay, M. Meier, M. Nemani, E. Bridel, C.C. Leite, D.R. Bertola, R.K. Semple, S. O'Rahilly, I. Dugail, J. Capeau, M. Lathrop, and J. Magre, *Association of a homozygous nonsense caveolin-1 mutation with Berardinelli-Seip congenital lipodystrophy.* J Clin Endocrinol Metab, 2008. **93**(4): p. 1129-1134.

79. Liu, L., D. Brown, M. McKee, N.K. Lebrasseur, D. Yang, K.H. Albrecht, K. Ravid, and P.F. Pilch, *Deletion of Cavin/PTRF causes global loss of caveolae, dyslipidemia, and glucose intolerance.* Cell Metab, 2008. **8**(4): p. 310-317.

80. Cartwright, B.R. and J.M. Goodman, *Seipin: from human disease to molecular mechanism.* J Lipid Res, 2012. **53**(6): p. 1042-1055.

81. Prieur, X., L. Dollet, M. Takahashi, M. Nemani, B. Pillot, C. Le May, C. Mounier, H. Takigawa-Imamura, D. Zelenika, F. Matsuda, B. Feve, J. Capeau,

M. Lathrop, P. Costet, B. Cariou, and J. Magre, *Thiazolidinediones partially reverse the metabolic disturbances observed in Bscl2/seipin-deficient mice.* Diabetologia, 2013. **56**(8): p. 1813-1825.

82. Peterfy, M., J. Phan, P. Xu, and K. Reue, *Lipodystrophy in the fld mouse results from mutation of a new gene encoding a nuclear protein, lipin.* Nat Genet, 2001. **27**(1): p. 121-124.

83. Han, G.S., W.I. Wu, and G.M. Carman, *The Saccharomyces cerevisiae Lipin homolog is a Mg2+-dependent phosphatidate phosphatase enzyme.* J Biol Chem, 2006. **281**(14): p. 9210-9218.

84. Tsukahara, T., R. Tsukahara, Y. Fujiwara, J. Yue, Y. Cheng, H. Guo, A. Bolen, C. Zhang, L. Balazs, F. Re, G. Du, M.A. Frohman, D.L. Baker, A.L. Parrill, A. Uchiyama, T. Kobayashi, K. Murakami-Murofushi, and G. Tigyi, *Phospholipase D2-dependent inhibition of the nuclear hormone receptor PPARgamma by cyclic phosphatidic acid.* Mol Cell, 2010. **39**(3): p. 421-432.

85. Binns, D., S. Lee, C.L. Hilton, Q.X. Jiang, and J.M. Goodman, *Seipin is a discrete homooligomer.* Biochemistry, 2010. **49**(50): p. 10747-10755.

86. Laplante, M. and D.M. Sabatini, *mTOR signaling in growth control and disease.* Cell, 2012. **149**(2): p. 274-293.

87. Bellacosa, A., D. de Feo, A.K. Godwin, D.W. Bell, J.Q. Cheng, D.A. Altomare, M. Wan, L. Dubeau, G. Scambia, V. Masciullo, G. Ferrandina, P. Benedetti Panici, S. Mancuso, G. Neri, and J.R. Testa, *Molecular alterations of the AKT2 oncogene in ovarian and breast carcinomas.* Int J Cancer, 1995. **64**(4): p. 280-285.

88. Wang, S.I., J. Puc, J. Li, J.N. Bruce, P. Cairns, D. Sidransky, and R. Parsons, *Somatic mutations of PTEN in glioblastoma multiforme.* Cancer Res, 1997. **57**(19): p. 4183-4186.

89. Forgacs, E., E.J. Biesterveld, Y. Sekido, K. Fong, S. Muneer, Wistuba, II, S. Milchgrub, R. Brezinschek, A. Virmani, A.F. Gazdar, and J.D. Minna, *Mutation analysis of the PTEN/MMAC1 gene in lung cancer.* Oncogene, 1998. **17**(12): p. 1557-1565.

90. Alimov, A., C. Li, R. Gizatullin, V. Fredriksson, B. Sundelin, G. Klein, E. Zabarovsky, and U. Bergerheim, *Somatic mutation and homozygous deletion of PTEN/MMAC1 gene of 10q23 in renal cell carcinoma.* Anticancer Res, 1999. **19**(5B): p. 3841-3846.

91. Chang, J.G., Y.J. Chen, L.I. Perng, N.M. Wang, M.C. Kao, T.Y. Yang, C.P. Chang, and C.H. Tsai, *Mutation analysis of the PTEN/MMAC1 gene in cancers of the digestive tract.* Eur J Cancer, 1999. **35**(4): p. 647-651.

92. Kawamura, N., H. Nagai, K. Bando, M. Koyama, S. Matsumoto, T. Tajiri, M. Onda, J. Fujimoto, T. Ueki, N. Konishi, T. Shiba, and M. Emi, *PTEN/MMAC1 mutations in hepatocellular carcinomas: somatic inactivation of both alleles in tumors.* Jpn J Cancer Res, 1999. **90**(4): p. 413-418.

93. Celebi, J.T., I. Shendrik, D.N. Silvers, and M. Peacocke, *Identification of PTEN mutations in metastatic melanoma specimens.* J Med Genet, 2000. **37**(9): p. 653-657.

94. Page, C., M. Huang, X. Jin, K. Cho, J. Lilja, R.K. Reynolds, and J. Lin, *Elevated phosphorylation of AKT and Stat3 in prostate, breast, and cervical cancer cells.* Int J Oncol, 2000. **17**(1): p. 23-28.

95. Yokoyama, Y., X. Wan, A. Shinohara, S. Takahashi, Y. Takahashi, K. Niwa, and T. Tamaya, *Expression of PTEN and PTEN pseudogene in endometrial carcinoma.* Int J Mol Med, 2000. **6**(1): p. 47-50.

96. Sun, M., G. Wang, J.E. Paciga, R.I. Feldman, Z.Q. Yuan, X.L. Ma, S.A. Shelley, R. Jove, P.N. Tsichlis, S.V. Nicosia, and J.Q. Cheng, *AKT1/PKBalpha kinase is frequently elevated in human cancers and its constitutive activation is required for oncogenic transformation in NIH3T3 cells.* Am J Pathol, 2001. **159**(2): p. 431-437.

97. Braccini, L., E. Ciraolo, M. Martini, T. Pirali, G. Germena, K. Rolfo, and E. Hirsch, *PI3K keeps the balance between metabolism and cancer.* Adv Biol Regul, 2012. **52**(3): p. 389-405.

98. Osaki, M., M. Oshimura, and H. Ito, *PI3K-Akt pathway: its functions and alterations in human cancer.* Apoptosis, 2004. **9**(6): p. 667-676.

99. Di Cristofano, A., B. Pesce, C. Cordon-Cardo, and P.P. Pandolfi, *Pten is essential for embryonic development and tumour suppression.* Nat Genet, 1998. **19**(4): p. 348-355.

100. Stambolic, V., M.S. Tsao, D. Macpherson, A. Suzuki, W.B. Chapman, and T.W. Mak, *High incidence of breast and endometrial neoplasia resembling human Cowden syndrome in pten+/- mice.* Cancer Res, 2000. **60**(13): p. 3605-3611.

101. Chen, W.S., P.Z. Xu, K. Gottlob, M.L. Chen, K. Sokol, T. Shiyanova, I. Roninson, W. Weng, R. Suzuki, K. Tobe, T. Kadowaki, and N. Hay, *Growth retardation and increased apoptosis in mice with homozygous disruption of the Akt1 gene.* Genes Dev, 2001. **15**(17): p. 2203-2208.

102. Cho, H., J.L. Thorvaldsen, Q. Chu, F. Feng, and M.J. Birnbaum, *Akt1/PKBalpha is required for normal growth but dispensable for maintenance of glucose homeostasis in mice.* J Biol Chem, 2001. **276**(42): p. 38349-38352.

103. Garofalo, R.S., S.J. Orena, K. Rafidi, A.J. Torchia, J.L. Stock, A.L. Hildebrandt, T. Coskran, S.C. Black, D.J. Brees, J.R. Wicks, J.D. McNeish, and K.G. Coleman, *Severe diabetes, age-dependent loss of adipose tissue, and mild growth deficiency in mice lacking Akt2/PKB beta.* J Clin Invest, 2003. **112**(2): p. 197-208.

104. Tschopp, O., Z.Z. Yang, D. Brodbeck, B.A. Dummler, M. Hemmings-Mieszczak, T. Watanabe, T. Michaelis, J. Frahm, and B.A. Hemmings, *Essential role of protein kinase B gamma (PKB gamma/Akt3) in postnatal brain development but not in glucose homeostasis.* Development, 2005. **132**(13): p. 2943-2954.

105. Stokoe, D., L.R. Stephens, T. Copeland, P.R. Gaffney, C.B. Reese, G.F. Painter, A.B. Holmes, F. McCormick, and P.T. Hawkins, *Dual role of phosphatidylinositol-3,4,5-trisphosphate in the activation of protein kinase B.* Science, 1997. **277**(5325): p. 567-570.

106. Sarbassov, D.D., D.A. Guertin, S.M. Ali, and D.M. Sabatini, *Phosphorylation and regulation of Akt/PKB by the rictor-mTOR complex.* Science, 2005. **307**(5712): p. 1098-1101.

107. Kim, D.H., D.D. Sarbassov, S.M. Ali, R.R. Latek, K.V. Guntur, H. Erdjument-Bromage, P. Tempst, and D.M. Sabatini, *GbetaL, a positive regulator of the rapamycin-sensitive pathway required for the nutrient-sensitive interaction between raptor and mTOR.* Mol Cell, 2003. **11**(4): p. 895-904.

108. Jacinto, E., R. Loewith, A. Schmidt, S. Lin, M.A. Ruegg, A. Hall, and M.N. Hall, *Mammalian TOR complex 2 controls the actin cytoskeleton and is rapamycin insensitive.* Nat Cell Biol, 2004. **6**(11): p. 1122-1128.

109. Hara, K., Y. Maruki, X. Long, K. Yoshino, N. Oshiro, S. Hidayat, C. Tokunaga, J. Avruch, and K. Yonezawa, *Raptor, a binding partner of target of rapamycin (TOR), mediates TOR action.* Cell, 2002. **110**(2): p. 177-189.

110. Sancak, Y., C.C. Thoreen, T.R. Peterson, R.A. Lindquist, S.A. Kang, E. Spooner, S.A. Carr, and D.M. Sabatini, *PRAS40 is an insulin-regulated inhibitor of the mTORC1 protein kinase.* Mol Cell, 2007. **25**(6): p. 903-915.

111. Peterson, T.R., M. Laplante, C.C. Thoreen, Y. Sancak, S.A. Kang, W.M. Kuehl, N.S. Gray, and D.M. Sabatini, *DEPTOR is an mTOR inhibitor frequently overexpressed in multiple myeloma cells and required for their survival.* Cell, 2009. **137**(5): p. 873-886.

112. Jacinto, E., V. Facchinetti, D. Liu, N. Soto, S. Wei, S.Y. Jung, Q. Huang, J. Qin, and B. Su, *SIN1/MIP1 maintains rictor-mTOR complex integrity and regulates Akt phosphorylation and substrate specificity.* Cell, 2006. **127**(1): p. 125-137.

113. Pearce, L.R., X. Huang, J. Boudeau, R. Pawlowski, S. Wullschleger, M. Deak, A.F. Ibrahim, R. Gourlay, M.A. Magnuson, and D.R. Alessi, *Identification of Protor as a novel Rictor-binding component of mTOR complex-2.* Biochem J, 2007. **405**(3): p. 513-522.

114. Sarbassov, D.D., S.M. Ali, S. Sengupta, J.H. Sheen, P.P. Hsu, A.F. Bagley, A.L. Markhard, and D.M. Sabatini, *Prolonged rapamycin treatment inhibits mTORC2 assembly and Akt/PKB.* Mol Cell, 2006. **22**(2): p. 159-168.

115. Farmer, S.R., *The forkhead transcription factor Foxo1: a possible link between obesity and insulin resistance.* Mol Cell, 2003. **11**(1): p. 6-8.

116. Daitoku, H. and A. Fukamizu, *FOXO transcription factors in the regulatory networks of longevity.* J Biochem, 2007. **141**(6): p. 769-774.

117. Hay, N. and N. Sonenberg, *Upstream and downstream of mTOR.* Genes Dev, 2004. **18**(16): p. 1926-1945.

118. Martin, K.A. and J. Blenis, *Coordinate regulation of translation by the PI 3-kinase and mTOR pathways.* Adv Cancer Res, 2002. **86**: p. 1-39.

119. Jastrzebski, K., K.M. Hannan, E.B. Tchoubrieva, R.D. Hannan, and R.B. Pearson, *Coordinate regulation of ribosome biogenesis and function by the ribosomal protein S6 kinase, a key mediator of mTOR function.* Growth Factors, 2007. **25**(4): p. 209-226.

120. Gingras, A.C., B. Raught, and N. Sonenberg, *Regulation of translation initiation by FRAP/mTOR.* Genes Dev, 2001. **15**(7): p. 807-826.

121. Wang, B.T., G.S. Ducker, A.J. Barczak, R. Barbeau, D.J. Erle, and K.M. Shokat, *The mammalian target of rapamycin regulates cholesterol biosynthetic gene expression and exhibits a rapamycin-resistant transcriptional profile.* Proc Natl Acad Sci U S A, 2011. **108**(37): p. 15201-15206.

122. Goldstein, J.L., R.A. DeBose-Boyd, and M.S. Brown, *Protein sensors for membrane sterols.* Cell, 2006. **124**(1): p. 35-46.

123. Osborne, T.F. and P.J. Espenshade, *Evolutionary conservation and adaptation in the mechanism that regulates SREBP action: what a long, strange tRIP it's been.* Genes Dev, 2009. **23**(22): p. 2578-2591.

124. Wick, K.R., E.D. Werner, P. Langlais, F.J. Ramos, L.Q. Dong, S.E. Shoelson, and F. Liu, *Grb10 inhibits insulin-stimulated insulin receptor substrate (IRS)-phosphatidylinositol 3-kinase/Akt signaling pathway by disrupting the*

association of IRS-1/IRS-2 with the insulin receptor. J Biol Chem, 2003. **278**(10): p. 8460-8467.

125. Zhang, J., Z. Gao, J. Yin, M.J. Quon, and J. Ye, *S6K directly phosphorylates IRS-1 on Ser-270 to promote insulin resistance in response to TNF-(alpha) signaling through IKK2.* J Biol Chem, 2008. **283**(51): p. 35375-35382.

126. Rosenbaum, A.I. and F.R. Maxfield, *Niemann-Pick type C disease: molecular mechanisms and potential therapeutic approaches.* J Neurochem, 2011. **116**(5): p. 789-795.

127. Carstea, E.D., J.A. Morris, K.G. Coleman, S.K. Loftus, D. Zhang, C. Cummings, J. Gu, M.A. Rosenfeld, W.J. Pavan, D.B. Krizman, J. Nagle, M.H. Polymeropoulos, S.L. Sturley, Y.A. Ioannou, M.E. Higgins, M. Comly, A. Cooney, A. Brown, C.R. Kaneski, E.J. Blanchette-Mackie, N.K. Dwyer, E.B. Neufeld, T.Y. Chang, L. Liscum, J.F. Strauss, 3rd, K. Ohno, M. Zeigler, R. Carmi, J. Sokol, D. Markie, R.R. O'Neill, O.P. van Diggelen, M. Elleder, M.C. Patterson, R.O. Brady, M.T. Vanier, P.G. Pentchev, and D.A. Tagle, *Niemann-Pick C1 disease gene: homology to mediators of cholesterol homeostasis.* Science, 1997. **277**(5323): p. 228-231.

128. Naureckiene, S., D.E. Sleat, H. Lackland, A. Fensom, M.T. Vanier, R. Wattiaux, M. Jadot, and P. Lobel, *Identification of HE1 as the second gene of Niemann-Pick C disease.* Science, 2000. **290**(5500): p. 2298-2301.

129. Chang, T.Y., C.C. Chang, N. Ohgami, and Y. Yamauchi, *Cholesterol sensing, trafficking, and esterification.* Annu Rev Cell Dev Biol, 2006. **22**: p. 129-157.

130. Davies, J.P. and Y.A. Ioannou, *Topological analysis of Niemann-Pick C1 protein reveals that the membrane orientation of the putative sterol-sensing domain is identical to those of 3-hydroxy-3-methylglutaryl-CoA reductase and*

sterol regulatory element binding protein cleavage-activating protein. J Biol Chem, 2000. **275**(32): p. 24367-24374.

131. Griffin, L.D., W. Gong, L. Verot, and S.H. Mellon, *Niemann-Pick type C disease involves disrupted neurosteroidogenesis and responds to allopregnanolone.* Nat Med, 2004. **10**(7): p. 704-711.

132. Choudhury, A., D.K. Sharma, D.L. Marks, and R.E. Pagano, *Elevated endosomal cholesterol levels in Niemann-Pick cells inhibit rab4 and perturb membrane recycling.* Mol Biol Cell, 2004. **15**(10): p. 4500-4511.

133. Pipalia, N.H., M. Hao, S. Mukherjee, and F.R. Maxfield, *Sterol, protein and lipid trafficking in Chinese hamster ovary cells with Niemann-Pick type C1 defect.* Traffic, 2007. **8**(2): p. 130-141.

134. Garver, W.S., G.A. Francis, D. Jelinek, G. Shepherd, J. Flynn, G. Castro, C. Walsh Vockley, D.L. Coppock, K.M. Pettit, R.A. Heidenreich, and F.J. Meaney, *The National Niemann-Pick C1 disease database: report of clinical features and health problems.* Am J Med Genet A, 2007. **143A**(11): p. 1204-1211.

135. Imrie, J., S. Dasgupta, G.T. Besley, C. Harris, L. Heptinstall, S. Knight, M.T. Vanier, A.H. Fensom, C. Ward, E. Jacklin, C. Whitehouse, and J.E. Wraith, *The natural history of Niemann-Pick disease type C in the UK.* J Inherit Metab Dis, 2007. **30**(1): p. 51-59.

136. Peake, K.B. and J.E. Vance, *Defective cholesterol trafficking in Niemann-Pick C-deficient cells.* FEBS Lett, 2010. **584**(13): p. 2731-2739.

137. Sleat, D.E., J.A. Wiseman, M. El-Banna, S.M. Price, L. Verot, M.M. Shen, G.S. Tint, M.T. Vanier, S.U. Walkley, and P. Lobel, *Genetic evidence for nonredundant functional cooperativity between NPC1 and NPC2 in lipid transport.* Proc Natl Acad Sci U S A, 2004. **101**(16): p. 5886-5891.

138. Infante, R.E., M.L. Wang, A. Radhakrishnan, H.J. Kwon, M.S. Brown, and J.L. Goldstein, *NPC2 facilitates bidirectional transfer of cholesterol between NPC1 and lipid bilayers, a step in cholesterol egress from lysosomes.* Proc Natl Acad Sci U S A, 2008. **105**(40): p. 15287-15292.

139. Gelsthorpe, M.E., N. Baumann, E. Millard, S.E. Gale, S.J. Langmade, J.E. Schaffer, and D.S. Ory, *Niemann-Pick type C1 I1061T mutant encodes a functional protein that is selected for endoplasmic reticulum-associated degradation due to protein misfolding.* J Biol Chem, 2008. **283**(13): p. 8229-8236.

140. Phung, T.L., K. Ziv, D. Dabydeen, G. Eyiah-Mensah, M. Riveros, C. Perruzzi, J. Sun, R.A. Monahan-Earley, I. Shiojima, J.A. Nagy, M.I. Lin, K. Walsh, A.M. Dvorak, D.M. Briscoe, M. Neeman, W.C. Sessa, H.F. Dvorak, and L.E. Benjamin, *Pathological angiogenesis is induced by sustained Akt signaling and inhibited by rapamycin.* Cancer Cell, 2006. **10**(2): p. 159-170.

141. Vance, J.E. and K.B. Peake, *Function of the Niemann-Pick type C proteins and their bypass by cyclodextrin.* Curr Opin Lipidol, 2011. **22**(3): p. 204-209.

142. Schaffner, C.P., *Prostatic cholesterol metabolism: regulation and alteration.* Prog Clin Biol Res, 1981. **75A**: p. 279-324.

143. Dessi, S., B. Batetta, C. Anchisi, P. Pani, P. Costelli, L. Tessitore, and F.M. Baccino, *Cholesterol metabolism during the growth of a rat ascites hepatoma (Yoshida AH-130).* Br J Cancer, 1992. **66**(5): p. 787-793.

144. Dessi, S., B. Batetta, D. Pulisci, O. Spano, C. Anchisi, L. Tessitore, P. Costelli, F.M. Baccino, E. Aroasio, and P. Pani, *Cholesterol content in tumor tissues is inversely associated with high-density lipoprotein cholesterol in serum in patients with gastrointestinal cancer.* Cancer, 1994. **73**(2): p. 253-258.

145. Rudling, M. and V.P. Collins, *Low density lipoprotein receptor and 3-hydroxy-3-methylglutaryl coenzyme A reductase mRNA levels are coordinately reduced in human renal cell carcinoma.* Biochim Biophys Acta, 1996. **1299**(1): p. 75-79.

146. Yoshioka, Y., J. Sasaki, M. Yamamoto, K. Saitoh, S. Nakaya, and M. Kubokawa, *Quantitation by (1)H-NMR of dolichol, cholesterol and choline-containing lipids in extracts of normal and phathological thyroid tissue.* NMR Biomed, 2000. **13**(7): p. 377-383.

147. Kolanjiappan, K., C.R. Ramachandran, and S. Manoharan, *Biochemical changes in tumor tissues of oral cancer patients.* Clin Biochem, 2003. **36**(1): p. 61-65.

148. Caruso, M.G., M. Notarnicola, M. Santillo, A. Cavallini, and A. Di Leo, *Enhanced 3-hydroxy-3-methyl-glutaryl coenzyme A reductase activity in human colorectal cancer not expressing low density lipoprotein receptor.* Anticancer Res, 1999. **19**(1A): p. 451-454.

149. Caruso, M.G., M. Notarnicola, A. Cavallini, and A. Di Leo, *3-Hydroxy-3-methylglutaryl coenzyme A reductase activity and low-density lipoprotein receptor expression in diffuse-type and intestinal-type human gastric cancer.* J Gastroenterol, 2002. **37**(7): p. 504-508.

150. Graziani, S.R., F.A. Igreja, R. Hegg, C. Meneghetti, L.I. Brandizzi, R. Barboza, R.F. Amancio, J.A. Pinotti, and R.C. Maranhao, *Uptake of a cholesterol-rich emulsion by breast cancer.* Gynecol Oncol, 2002. **85**(3): p. 493-497.

151. Tatidis, L., M. Masquelier, and S. Vitols, *Elevated uptake of low density lipoprotein by drug resistant human leukemic cell lines.* Biochem Pharmacol, 2002. **63**(12): p. 2169-2180.

152. Notarnicola, M., C. Messa, M. Pricci, V. Guerra, D.F. Altomare, S. Montemurro, and M.G. Caruso, *Up-regulation of 3-hydroxy-3-methylglutaryl*

coenzyme A reductase activity in left-sided human colon cancer. Anticancer Res, 2004. **24**(6): p. 3837-3842.

153. Schimanski, S., P.J. Wild, O. Treeck, F. Horn, A. Sigruener, C. Rudolph, H. Blaszyk, M. Klinkhammer-Schalke, O. Ortmann, A. Hartmann, and G. Schmitz, *Expression of the lipid transporters ABCA3 and ABCA1 is diminished in human breast cancer tissue.* Horm Metab Res, 2010. **42**(2): p. 102-109.

154. Gao, J., W.D. Jia, J.S. Li, W. Wang, G.L. Xu, J.L. Ma, Y.S. Ge, J.H. Yu, W.H. Ren, W.B. Liu, and C.H. Zhang, *Combined inhibitory effects of celecoxib and fluvastatin on the growth of human hepatocellular carcinoma xenografts in nude mice.* J Int Med Res, 2010. **38**(4): p. 1413-1427.

155. Huang, E.H., L.A. Johnson, K. Eaton, M.J. Hynes, J.E. Carpentino, and P.D. Higgins, *Atorvastatin induces apoptosis in vitro and slows growth of tumor xenografts but not polyp formation in MIN mice.* Dig Dis Sci, 2010. **55**(11): p. 3086-3094.

156. Kochuparambil, S.T., B. Al-Husein, A. Goc, S. Soliman, and P.R. Somanath, *Anticancer efficacy of simvastatin on prostate cancer cells and tumor xenografts is associated with inhibition of Akt and reduced prostate-specific antigen expression.* J Pharmacol Exp Ther, 2011. **336**(2): p. 496-505.

157. Appelqvist, H., C. Nilsson, B. Garner, A.J. Brown, K. Kagedal, and K. Ollinger, *Attenuation of the lysosomal death pathway by lysosomal cholesterol accumulation.* Am J Pathol, 2011. **178**(2): p. 629-639.

158. Choudhury, A., M. Dominguez, V. Puri, D.K. Sharma, K. Narita, C.L. Wheatley, D.L. Marks, and R.E. Pagano, *Rab proteins mediate Golgi transport of caveola-internalized glycosphingolipids and correct lipid trafficking in Niemann-Pick C cells.* J Clin Invest, 2002. **109**(12): p. 1541-1550.

159. Narita, K., A. Choudhury, K. Dobrenis, D.K. Sharma, E.L. Holicky, D.L. Marks, S.U. Walkley, and R.E. Pagano, *Protein transduction of Rab9 in Niemann-Pick C cells reduces cholesterol storage.* FASEB J, 2005. **19**(11): p. 1558-1560.

160. Kaptzan, T., S.A. West, E.L. Holicky, C.L. Wheatley, D.L. Marks, T. Wang, K.B. Peake, J. Vance, S.U. Walkley, and R.E. Pagano, *Development of a Rab9 transgenic mouse and its ability to increase the lifespan of a murine model of Niemann-Pick type C disease.* Am J Pathol, 2009. **174**(1): p. 14-20.

161. Alessi, D.R., S.R. James, C.P. Downes, A.B. Holmes, P.R. Gaffney, C.B. Reese, and P. Cohen, *Characterization of a 3-phosphoinositide-dependent protein kinase which phosphorylates and activates protein kinase Balpha.* Curr Biol, 1997. **7**(4): p. 261-269.

162. Vander Haar, E., S.I. Lee, S. Bandhakavi, T.J. Griffin, and D.H. Kim, *Insulin signalling to mTOR mediated by the Akt/PKB substrate PRAS40.* Nat Cell Biol, 2007. **9**(3): p. 316-323.

163. Hannan, K.M., E. Sanij, N. Hein, R.D. Hannan, and R.B. Pearson, *Signaling to the ribosome in cancer--It is more than just mTORC1.* IUBMB Life, 2011. **63**(2): p. 79-85.

164. Engelman, J.A., J. Luo, and L.C. Cantley, *The evolution of phosphatidylinositol 3-kinases as regulators of growth and metabolism.* Nat Rev Genet, 2006. **7**(8): p. 606-619.

165. Chan, J.C., K.M. Hannan, K. Riddell, P.Y. Ng, A. Peck, R.S. Lee, S. Hung, M.V. Astle, M. Bywater, M. Wall, G. Poortinga, K. Jastrzebski, K.E. Sheppard, B.A. Hemmings, M.N. Hall, R.W. Johnstone, G.A. McArthur, R.D. Hannan, and

R.B. Pearson, *AKT promotes rRNA synthesis and cooperates with c-MYC to stimulate ribosome biogenesis in cancer.* Sci Signal, 2011. **4**(188): p. ra56.

166. Zhang, S.R., Q.H. Shi, and R.J. Ho, *Cyclic AMP-lowering mediator of insulin.* J Biol Chem, 1983. **258**(10): p. 6471-6476.

167. Minokoshi, Y., T. Alquier, N. Furukawa, Y.B. Kim, A. Lee, B. Xue, J. Mu, F. Foufelle, P. Ferre, M.J. Birnbaum, B.J. Stuck, and B.B. Kahn, *AMP-kinase regulates food intake by responding to hormonal and nutrient signals in the hypothalamus.* Nature, 2004. **428**(6982): p. 569-574.

168. Lim, C.T., B. Kola, and M. Korbonits, *AMPK as a mediator of hormonal signalling.* J Mol Endocrinol, 2010. **44**(2): p. 87-97.

169. Yu, Y., S.O. Yoon, G. Poulogiannis, Q. Yang, X.M. Ma, J. Villen, N. Kubica, G.R. Hoffman, L.C. Cantley, S.P. Gygi, and J. Blenis, *Phosphoproteomic analysis identifies Grb10 as an mTORC1 substrate that negatively regulates insulin signaling.* Science, 2011. **332**(6035): p. 1322-1326.

170. Oliver, W.R., Jr., J.L. Shenk, M.R. Snaith, C.S. Russell, K.D. Plunket, N.L. Bodkin, M.C. Lewis, D.A. Winegar, M.L. Sznaidman, M.H. Lambert, H.E. Xu, D.D. Sternbach, S.A. Kliewer, B.C. Hansen, and T.M. Willson, *A selective peroxisome proliferator-activated receptor delta agonist promotes reverse cholesterol transport.* Proc Natl Acad Sci U S A, 2001. **98**(9): p. 5306-5311.

171. Gearing, K.L., M. Gottlicher, M. Teboul, E. Widmark, and J.A. Gustafsson, *Interaction of the peroxisome-proliferator-activated receptor and retinoid X receptor.* Proc Natl Acad Sci U S A, 1993. **90**(4): p. 1440-1444.

172. Lefterova, M.I., Y. Zhang, D.J. Steger, M. Schupp, J. Schug, A. Cristancho, D. Feng, D. Zhuo, C.J. Stoeckert, Jr., X.S. Liu, and M.A. Lazar, *PPARgamma and*

C/EBP factors orchestrate adipocyte biology via adjacent binding on a genome-wide scale. Genes Dev, 2008. **22**(21): p. 2941-2952.

173. Capeau, J., J. Magre, M. Caron-Debarle, C. Lagathu, B. Antoine, V. Bereziat, O. Lascols, J.P. Bastard, and C. Vigouroux, *Human lipodystrophies: genetic and acquired diseases of adipose tissue.* Endocr Dev, 2010. **19**: p. 1-20.

174. Chen, W., B. Chang, P. Saha, S.M. Hartig, L. Li, V.T. Reddy, Y. Yang, V. Yechoor, M.A. Mancini, and L. Chan, *Berardinelli-seip congenital lipodystrophy 2/seipin is a cell-autonomous regulator of lipolysis essential for adipocyte differentiation.* Mol Cell Biol, 2012. **32**(6): p. 1099-1111.

175. Lefterova, M.I., D.J. Steger, D. Zhuo, M. Qatanani, S.E. Mullican, G. Tuteja, E. Manduchi, G.R. Grant, and M.A. Lazar, *Cell-specific determinants of peroxisome proliferator-activated receptor gamma function in adipocytes and macrophages.* Mol Cell Biol, 2010. **30**(9): p. 2078-2089.

176. Wu, L., G. Wang, P. Qu, C. Yan, and H. Du, *Overexpression of dominant negative peroxisome proliferator-activated receptor-gamma (PPARgamma) in alveolar type II epithelial cells causes inflammation and T-cell suppression in the lung.* Am J Pathol, 2011. **178**(5): p. 2191-2204.

177. Renga, B., A. Mencarelli, C. D'Amore, S. Cipriani, F. Baldelli, A. Zampella, E. Distrutti, and S. Fiorucci, *Glucocorticoid receptor mediates the gluconeogenic activity of the farnesoid X receptor in the fasting condition.* FASEB J, 2012. **26**(7): p. 3021-3031.

178. McIntyre, T.M., A.V. Pontsler, A.R. Silva, A. St Hilaire, Y. Xu, J.C. Hinshaw, G.A. Zimmerman, K. Hama, J. Aoki, H. Arai, and G.D. Prestwich, *Identification of an intracellular receptor for lysophosphatidic acid (LPA): LPA is a*

transcellular PPARgamma agonist. Proc Natl Acad Sci U S A, 2003. **100**(1): p. 131-136.

179. Tsukahara, T., R. Tsukahara, S. Yasuda, N. Makarova, W.J. Valentine, P. Allison, H. Yuan, D.L. Baker, Z. Li, R. Bittman, A. Parrill, and G. Tigyi, *Different residues mediate recognition of 1-O-oleyllysophosphatidic acid and rosiglitazone in the ligand binding domain of peroxisome proliferator-activated receptor gamma.* J Biol Chem, 2006. **281**(6): p. 3398-3407.

180. Palgunow, D., M. Klapper, and F. Doring, *Dietary restriction during development enlarges intestinal and hypodermal lipid droplets in Caenorhabditis elegans.* PLoS One, 2012. **7**(11): p. e46198.

181. Jones, J.R., C. Barrick, K.A. Kim, J. Lindner, B. Blondeau, Y. Fujimoto, M. Shiota, R.A. Kesterson, B.B. Kahn, and M.A. Magnuson, *Deletion of PPARgamma in adipose tissues of mice protects against high fat diet-induced obesity and insulin resistance.* Proc Natl Acad Sci U S A, 2005. **102**(17): p. 6207-6212.

182. Hu, E., J.B. Kim, P. Sarraf, and B.M. Spiegelman, *Inhibition of adipogenesis through MAP kinase-mediated phosphorylation of PPARgamma.* Science, 1996. **274**(5295): p. 2100-2103.

183. Adams, M., M.J. Reginato, D. Shao, M.A. Lazar, and V.K. Chatterjee, *Transcriptional activation by peroxisome proliferator-activated receptor gamma is inhibited by phosphorylation at a consensus mitogen-activated protein kinase site.* J Biol Chem, 1997. **272**(8): p. 5128-5132.

184. Camp, H.S. and S.R. Tafuri, *Regulation of peroxisome proliferator-activated receptor gamma activity by mitogen-activated protein kinase.* J Biol Chem, 1997. **272**(16): p. 10811-10816.

185. Reiss, K., J.Y. Wang, G. Romano, F.B. Furnari, W.K. Cavenee, A. Morrione, X. Tu, and R. Baserga, *IGF-I receptor signaling in a prostatic cancer cell line with a PTEN mutation.* Oncogene, 2000. **19**(22): p. 2687-2694.

186. Dorrello, N.V., A. Peschiaroli, D. Guardavaccaro, N.H. Colburn, N.E. Sherman, and M. Pagano, *S6K1- and betaTRCP-mediated degradation of PDCD4 promotes protein translation and cell growth.* Science, 2006. **314**(5798): p. 467-471.

187. Vainio, S., I. Bykov, M. Hermansson, E. Jokitalo, P. Somerharju, and E. Ikonen, *Defective insulin receptor activation and altered lipid rafts in Niemann-Pick type C disease hepatocytes.* Biochem J, 2005. **391**(Pt 3): p. 465-472.

188. Sim, M.F., R.J. Dennis, E.M. Aubry, N. Ramanathan, H. Sembongi, V. Saudek, D. Ito, S. O'Rahilly, S. Siniossoglou, and J.J. Rochford, *The human lipodystrophy protein seipin is an ER membrane adaptor for the adipogenic PA phosphatase lipin 1.* Mol Metab, 2012. **2**(1): p. 38-46.